SVSOLID

2D/3D FINITE ELEMENT
STRESS DEFORMATION MODELING

Verification Manual

Written by:
The Bentley Systems Team

Last Updated: Wednesday, August 28, 2019

Bentley Systems Incorporated

COPYRIGHT NOTICE

TRADEMARK NOTICE

1 INTRODUCTION

The word “Verification”, when used in connection with computer software can be defined as “the ability of the computer code to provide a solution consistent with the physics defined by the governing partial differential equation, PDE”. There are also other factors such as initial conditions, boundary conditions, and control variables that affect the accuracy of the code to perform as stated.

“Verification” is generally achieved by solving a series of so-called “benchmark” problems. “Benchmark” problems are problems for which there is a closed-form solution or for which the solution has become “reasonably certain” as a result of long-hand calculations that have been performed. Publication of the “benchmark” solutions in research journals or textbooks also lends credibility to the solution. There are also example problems that have been solved and published in User Manual documentation associated with other comparable software packages. While these are valuables checks to perform, it must be realized that it is possible that errors can be transferred from one software solution to another. Consequently, care must be taken in performing the “verification” process on a particular software package. It must also be remembered there is never such a thing as complete software verification for “all” possible problems. Rather, “Verification” is an ongoing process that establishes credibility with time.

Bentley Systems takes the process of “verification” most seriously and has undertaken a wide range of steps to ensure that the SVSOLID software will perform as intended by the theory of stress/deformation.

The following models represent comparisons made to textbook solutions, hand calculations, and other software packages. We at Bentley Systems, are dedicated to providing our clients with reliable and tested software. While the following list of example models is comprehensive, it does not reflect the entirety of models which may be posed to the SVSOLID software. It is our recommendation that longhand calculation checking be performed on all model runs prior to presentation of results. It is also our recommendation that the modeling process move from simple model representations to complex models with simpler models being verified through the use of longhand calculations or simple spreadsheet calculations.

2 2D PLANE STRAIN

SVSOLID is used to simulate various stress-strain problems in 2D plane strain analysis. SVSOLID uses the finite element method to solve several 2D plane strain solid (or continuum) problems. The material properties used in these verification problems varies from linear, non-linear elastic to elastic-plastic soil models.

2.1 TUNNEL IN AN INFINITE ELASTIC MEDIUM

Reference: Brady and Brown (2004)

Project: Tunnels
Model: Tunnels_Elastic_GT

Main Factors Considered:

- Comparison to the closed-form solution against the SVSOLID solver for linear elastic material under 2D plane strain conditions in polar coordinates.

2.1.1 Model Description

A tunnel of 1 m diameter constructed in an infinite linear elastic medium is considered. The medium is under a uniform compressive stress of 30 MPa (in-situ stress field). The tunnel construction causes stress and deformation changes around the tunnel. The effect of the tunnel can be modeled as a 2D plane strain problem since the diameter of the tunnel is small compared to its length. The numerical results of this problem using SVSOLID are compared against a closed-form solution.

2.1.2 Geometry and boundary conditions

Figure 1 shows the geometry and boundary conditions used in this model. A two-stage setting was set for this problem. Stage 1 includes the original soil without the hole for the tunnel. Stage 2 has the tunnel excavated. The initial stresses are equal to 30 MPa in all directions. A finer mesh was created in the vicinity of the tunnel. The domain was extended to 21 times tunnel radius to eliminate any boundary effect.

2.1.3 Material Properties

A summary of the material properties using a linear elastic model is provided in Table 1.

Table 1. Input material properties

Parameter	Value
Young's modulus (E)	10,000 MPa
Poisson's ratio (ν)	0.2
In-situ stress (p)	30,000 kPa

2.1.4 Results

The analytical solution of the problem can be determined using the classical Kirsch equations with the assumption of plane strain. The radial, tangential, shear stress as well as radial and tangential displacements can be defined via the following equations in polar coordinates (r, θ) (Brady and Brown, 2004):

$$\begin{aligned}
\sigma_{rr} &= \frac{p}{2}\left[(1+K)\left(1-\frac{a^2}{r^2}\right)-(1-K)\left(1-4\frac{a^2}{r^2}+3\frac{a^4}{r^4}\right)cos\,2\,\theta\right] \\
\sigma_{\theta\theta} &= \frac{p}{2}\left[(1+K)\left(1+\frac{a^2}{r^2}\right)+(1-K)\left(1+3\frac{a^4}{r^4}\right)cos\,2\,\theta\right] \\
\sigma_{r\theta} &= \frac{p}{2}\left[(1-K)\left(1-2\frac{a^2}{r^2}-3\frac{a^4}{r^4}\right)sin\,2\,\theta\right] \\
u_r &= -\frac{pa^2}{4Gr}\left[(1+K)-(1-K)\left(4(1-\nu)-\frac{a^2}{r^2}\right)cos\,2\,\theta\right]
\end{aligned} \qquad [\,1\,]$$

where: σ_{rr}, $\sigma_{\theta\theta}$ and $\sigma_{r\theta}$ are the radial, tangential and shear stresses, respectively, and u_r and u_θ are the radial and tangential displacements, respectively. G is the shear modulus (equation [2]), a is the tunnel's radius, r is the distance to the point examined. K is the ratio between the horizontal to vertical initial stresses (Figure 2), which is 1 for this problem.

$$G = \frac{E}{2(1+\nu)} \qquad [\,2\,]$$

A comparison between the SVSOLID solution and the analytical theory for tangential, radial stresses and total displacement along a line between two points (1, 0) and (5, 0) is shown in Figure 3, Figure 4 and Figure 5. These figures show the results of the SVSOLID solver are similar to those of the closed-form solutions. Table 2 shows the difference between the SVSOLID solution and the closed-form results.

Table 2. Error between SVSOLID and the closed-form solution

Parameters	Differences (%)
Tangential stress	0.5
Radial stress	0.3
Displacement	2.0

Figure 6, Figure 7 and Figure 8 show contour plots of principal stresses and total displacements around the tunnel.

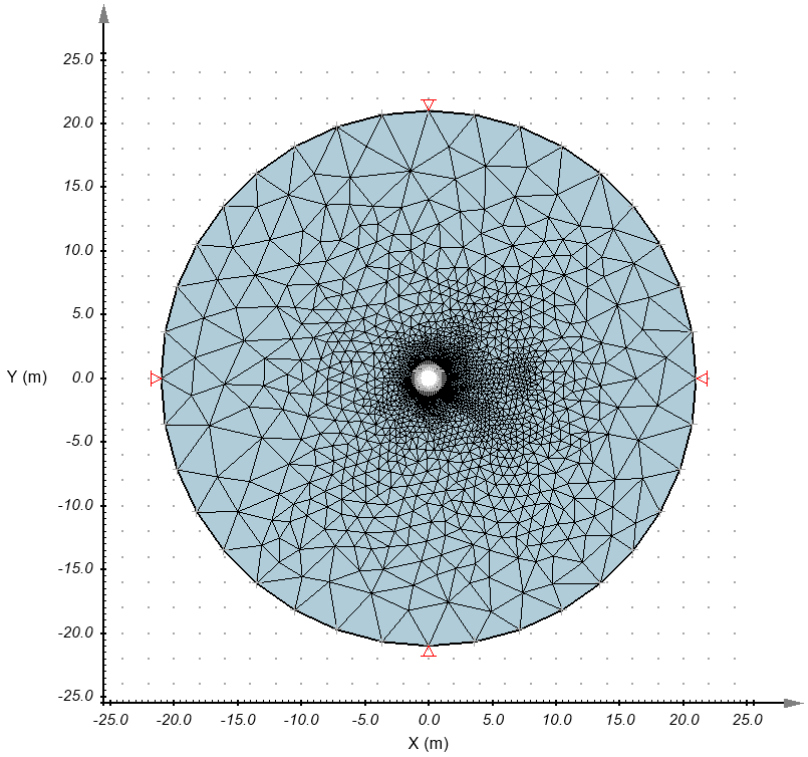

Figure 1. Geometry with mesh and boundary conditions

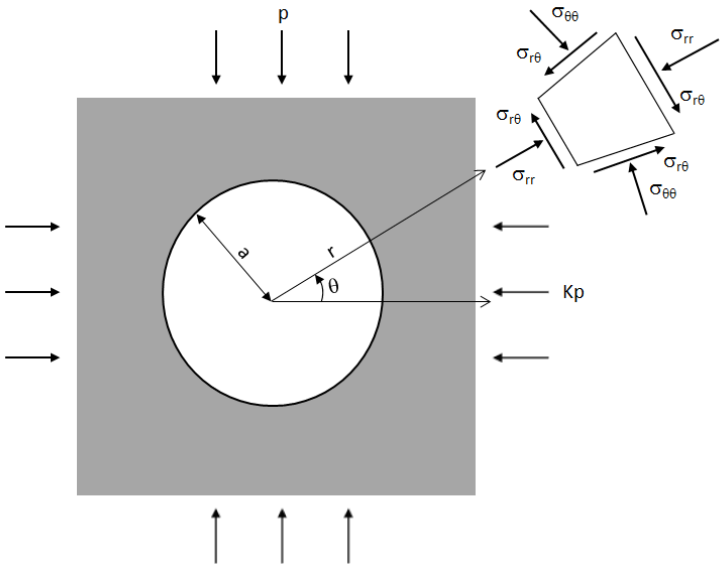

Figure 2. Classical Kirsch schematic

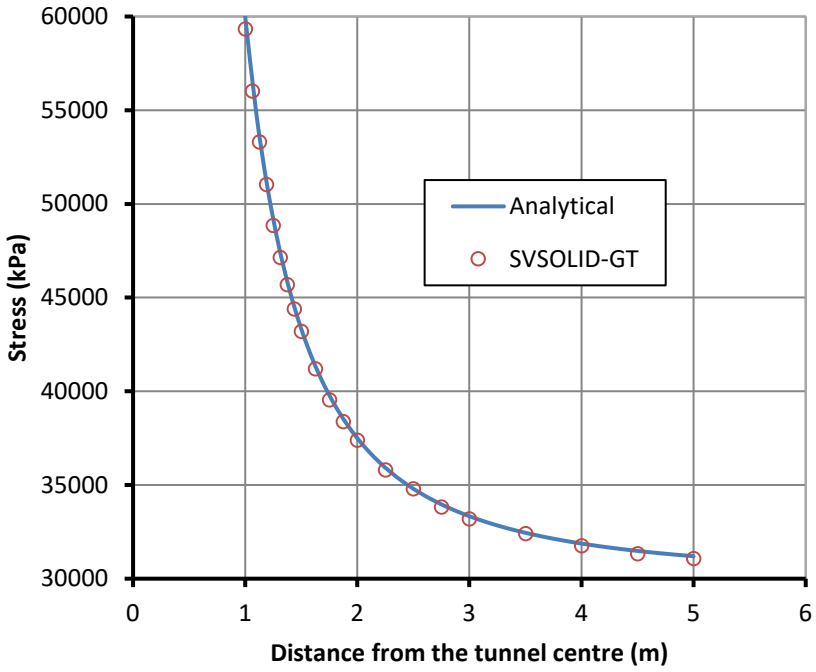

Figure 3. Comparison of tangential stresses along the selected line

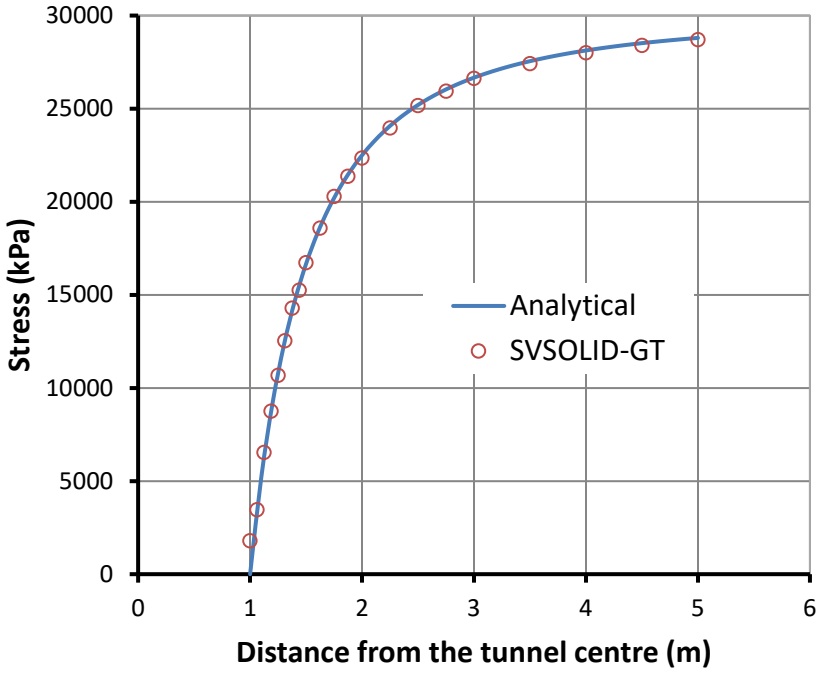

Figure 4. Comparison of radial stresses along the selected line

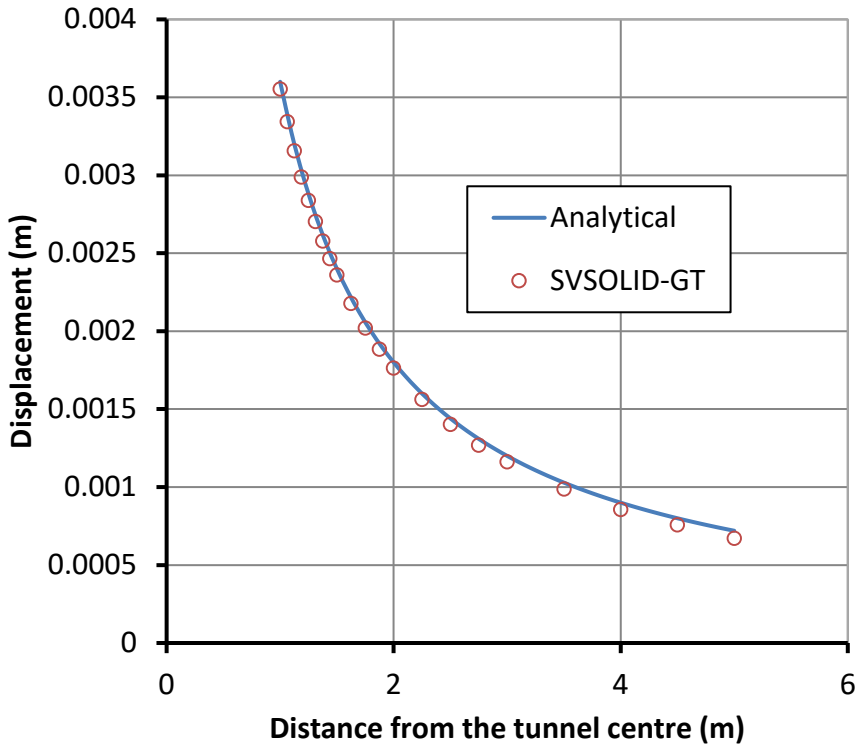

Figure 5. Comparison of total displacements along the selected line

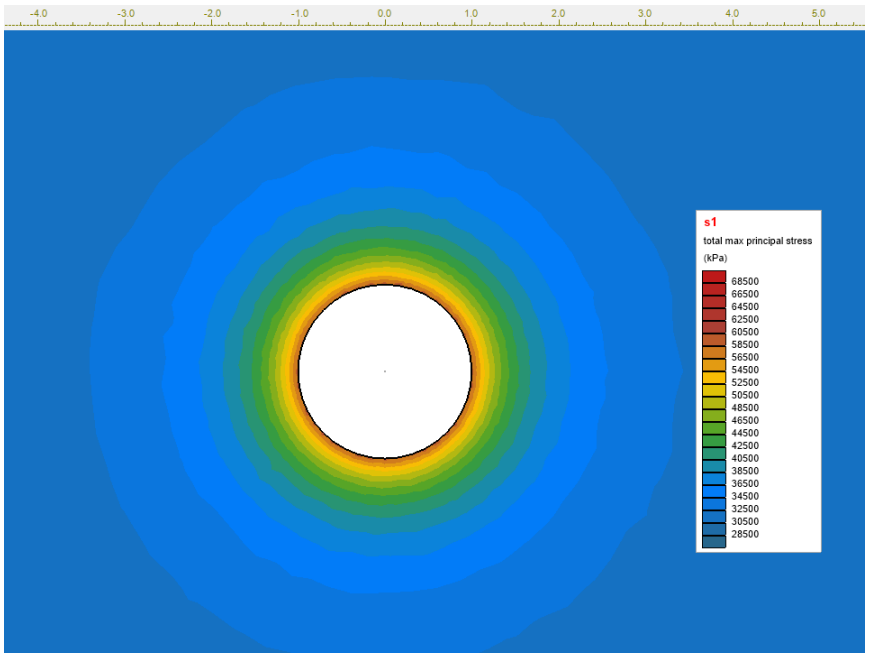

Figure 6. Contour plot of tangential stresses calculated in SVSOLID

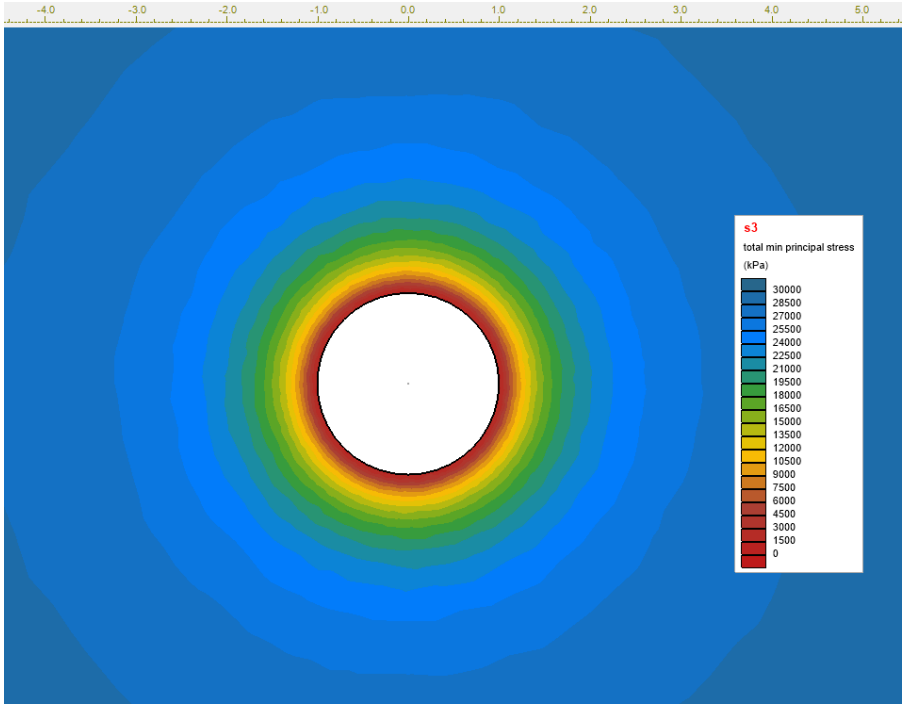

Figure 7. Contour plot of radial stresses calculated in SVSOLID

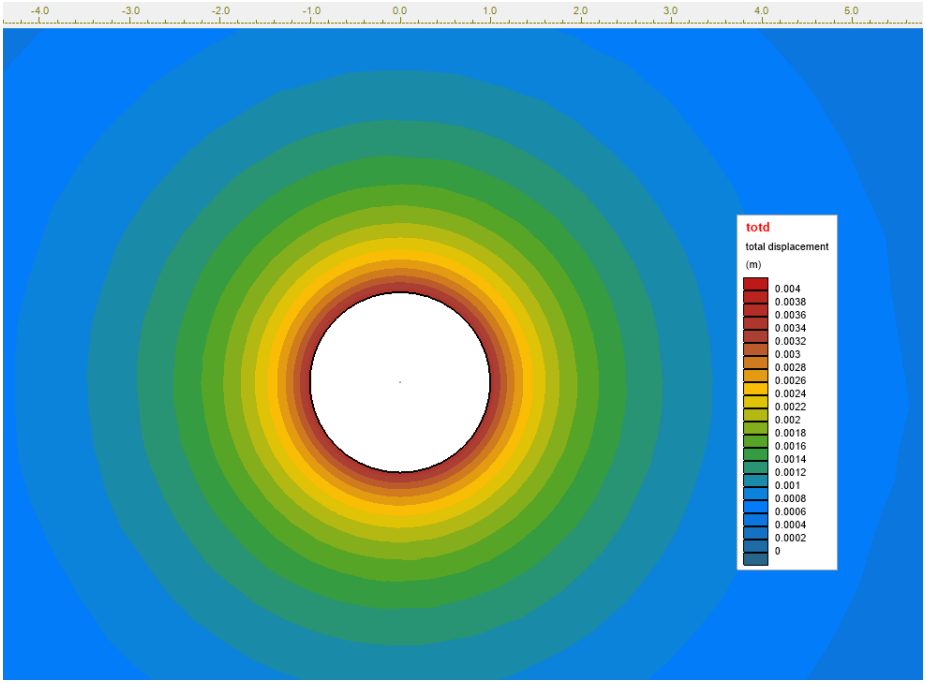

Figure 8. Contour plot of total displacements calculated in SVSOLID

2.2 Tunnel in Mohr-Coulomb Medium

Reference: Salencon (1969)

Project: Tunnels
Model: Tunnels_ElasticPlastic_Case1_GT and Tunnels_ElasticPlastic_Case2_GT

Main Factors Considered:

- Comparison to the closed-form solution against the SVSOLID solver when using a Mohr-Coulomb soil model under 2D plane strain conditions.

2.2.1 Model Description

A tunnel of 1 m in diameter, constructed in a linear elastic perfectly plastic medium, is considered. The medium is initially under a uniform compressive stress of 30 MPa (in-situ field stress). The yielding of the medium is assumed to the Mohr-Coulomb criterion. This problem is simulated under 2D plane strain conditions since the tunnel diameter is small in comparison to its length.

2.2.2 Geometry and boundary conditions

Figure 9 shows the geometry and boundary conditions used in this model. Two-stage loading conditions were used for this problem. Stage 1 includes the original soil in the tunnel. Stage 2 has the tunnel excavated. The initial stress state in Stage 1 has 30 MPa acting in all directions. A finer mesh was created around the tunnel. The domain was extended to 21 times tunnel radius to eliminate any boundary effect.

2.2.3 Material Properties

A summary of the material properties is provided in Table 3. Two cases are considered: Case 1: with a dilation angle = 30° (associative flow rule) and Case 2: with a dilation angle = 0° (non-associative flow rule).

Table 3. Input material properties

Parameter	Value
Young's modulus (E)	10,000 MPa
Poisson's ratio (ν)	0.2
In-situ stress (p)	30 MPa
Cohesion, (c)	3.45 MPa
Friction angle (ϕ)	30°
Tunnel radius (a)	1 m
Shear modulus (G)	4,166.7 MPa
Dilation angle (ψ)	0° (Case 1), 30° (Case 2)

2.2.4 Results

The analytical solution was developed by Salencon (1969), in which a uniform in-situ stress, p_o, was applied around the tunnel radius of a. Using polar coordinates (r, θ), the following equations are obtained:

$$R_o = a\left[\frac{2}{K_p+1}\frac{p_o+\frac{q}{K_p-1}}{p_i+\frac{q}{K_p-1}}\right]^{\frac{1}{K_p-1}} \quad [3]$$

$$\text{where: } K_p = \frac{1+\sin\varphi}{1-\sin\varphi}$$

$$q = 2c\tan\left(45+\frac{\varphi}{2}\right)$$

where: p_i = internal pressure, which is 0 kPa for this verification.

The radial stress at the elastic-plastic interface is:

$$\sigma_{rr}^{e} = \frac{1}{K_p+1}(2p_o - q) \quad [4]$$

Stresses and displacements in the elastic zone around the tunnel are as follows

$$\sigma_{rr} = p_o - (p_o - \sigma_{rr}^e)\left(\frac{R_o}{r}\right)^2$$
$$\sigma_{\theta\theta} = p_o + (p_o - \sigma_{rr}^e)\left(\frac{R_o}{r}\right)^2 \qquad [5]$$
$$u_{rr} = \frac{R_o^2}{2G}\left(p_o - \frac{2p_o - q}{K_p + 1}\right)\frac{1}{r}$$

Stresses and displacements in the plastic zone around the tunnel are as follows

$$\sigma_{rr} = -\frac{q}{K_p - 1} + \left(p_i + \frac{q}{K_p - 1}\right)\left(\frac{r}{a}\right)^{(K_p - 1)}$$
$$\sigma_{\theta\theta} = -\frac{q}{K_p - 1} + K_p\left(p_i + \frac{q}{K_p - 1}\right)\left(\frac{r}{a}\right)^{(K_p - 1)}$$
$$u_{rr} = \frac{r}{2G}\left[(2\nu - 1)\left(p_o + \frac{q}{K_p - 1}\right) + \frac{(1-\nu)(K_p^2 - 1)}{K_p + K_{ps}}\left(p_i + \frac{q}{K_p - 1}\right)\right] \qquad [6]$$
$$\left(\frac{R_o}{a}\right)^{(K_p - 1)}\left(\frac{R_o}{a}\right)^{(K_{ps} - 1)}$$
$$+\left(\frac{(1-\nu)(K_p K_{ps} - 1)}{K_p + K_{ps}} - \nu\right)\left(p_i + \frac{q}{K_p - 1}\right)\left(\frac{r}{a}\right)^{(K_p - 1)}$$

where, K_{ps} is defined using the dilation angle, ψ, as: $K_{ps} = \frac{1+\sin\psi}{1-\sin\psi}$

A comparison between numerical and the closed-form solution is presented in Figure 10 to Figure 15. These figures show close agreement for dilation angles of 0° and 30°. Contour plots of the stresses, displacement and yield zone are shown from Figure 6 to Figure 19. The radius of yield zone is 1.73 m form the tunnel center by the closed-form solution and this zone is clearly indicated in Figure 19.

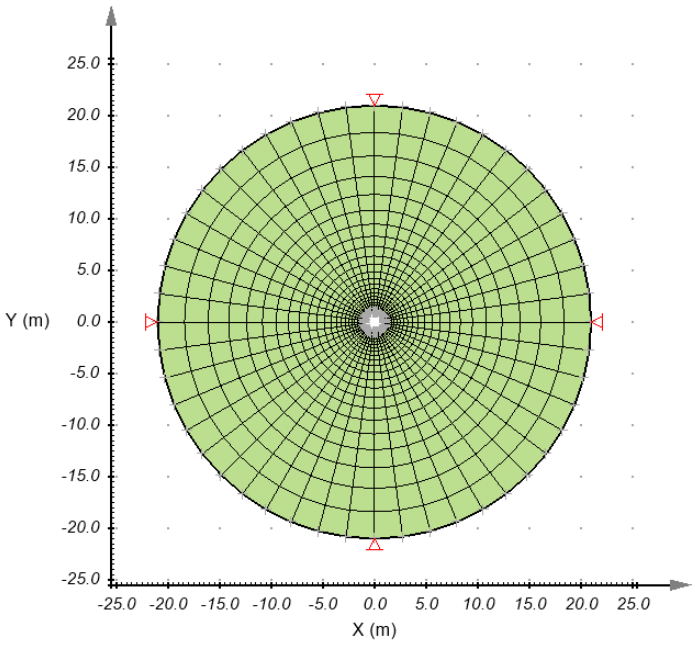

Figure 9. Geometry, mesh and boundary conditions

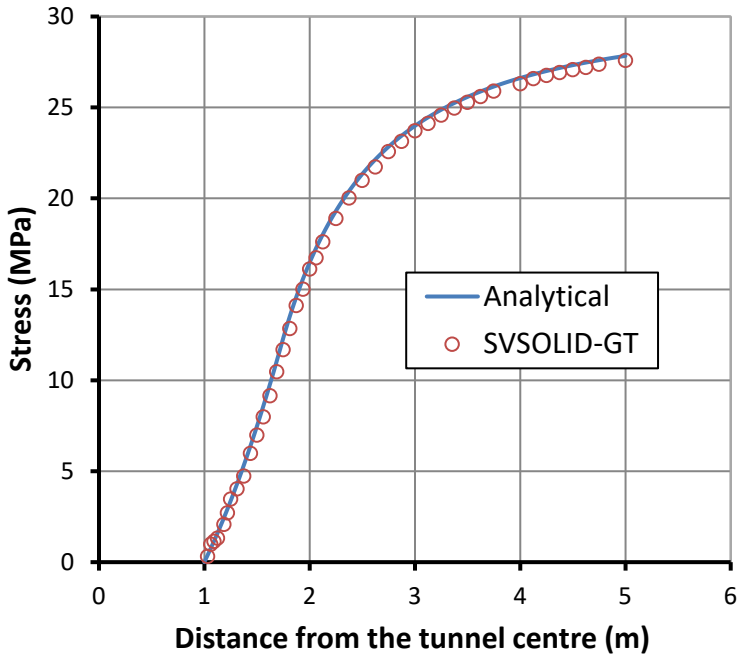

Figure 10. Comparison of the radial stress, $\psi=0°$ (non-associative flow rule)

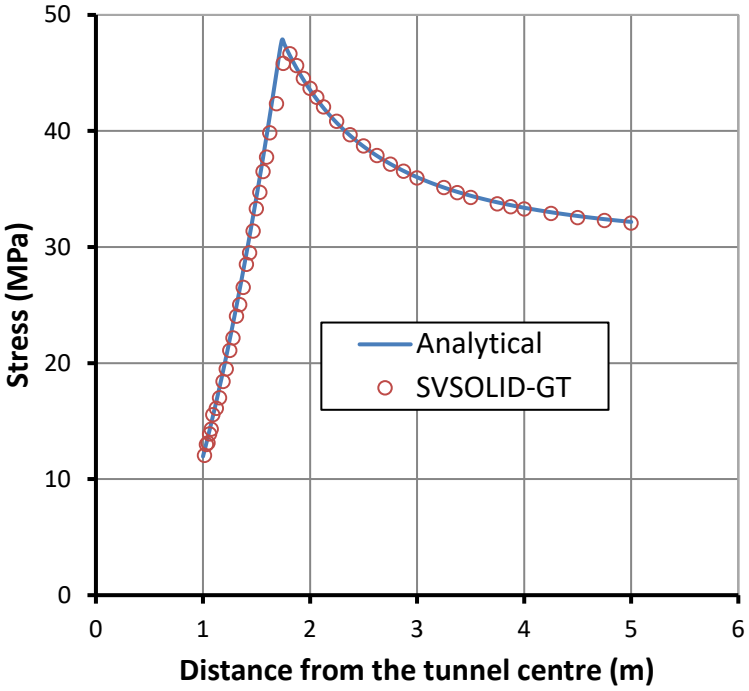

Figure 11. Comparison of the tangential stress, $\psi=0°$ (non-associative flow rule)

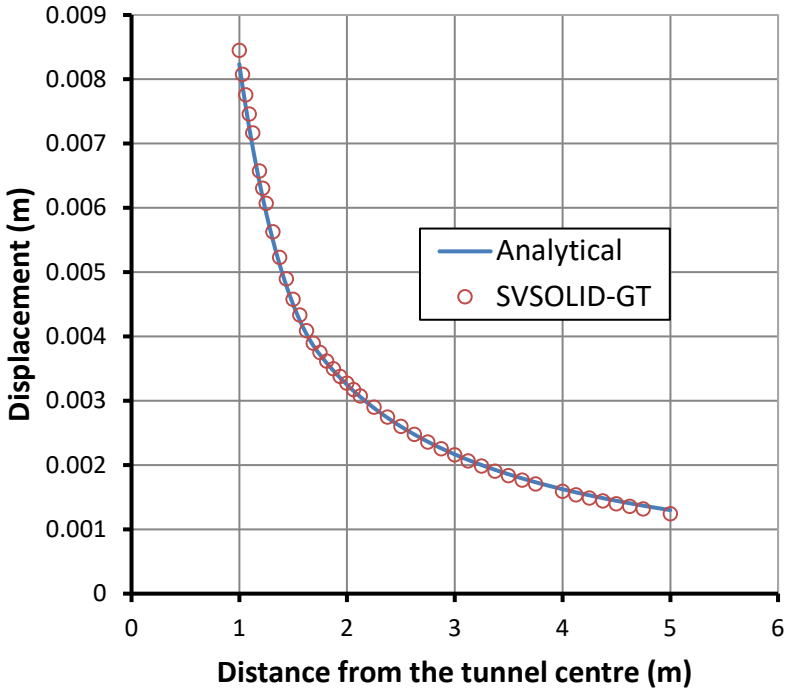

Figure 12. Comparison of the total displacements, $\psi = 0°$ (non-associative flow rule)

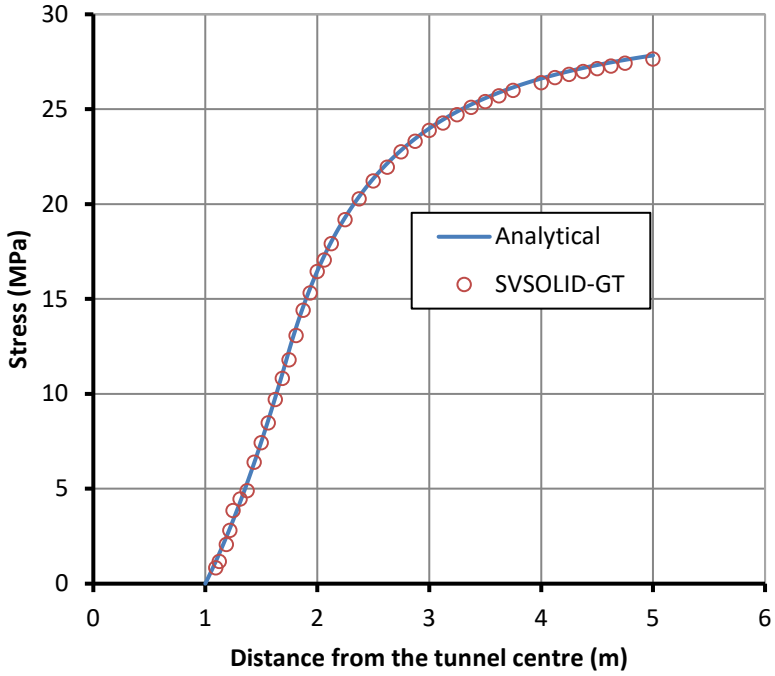

Figure 13. Comparison of the radial stresses, $\psi = 30°$ (associative flow rule)

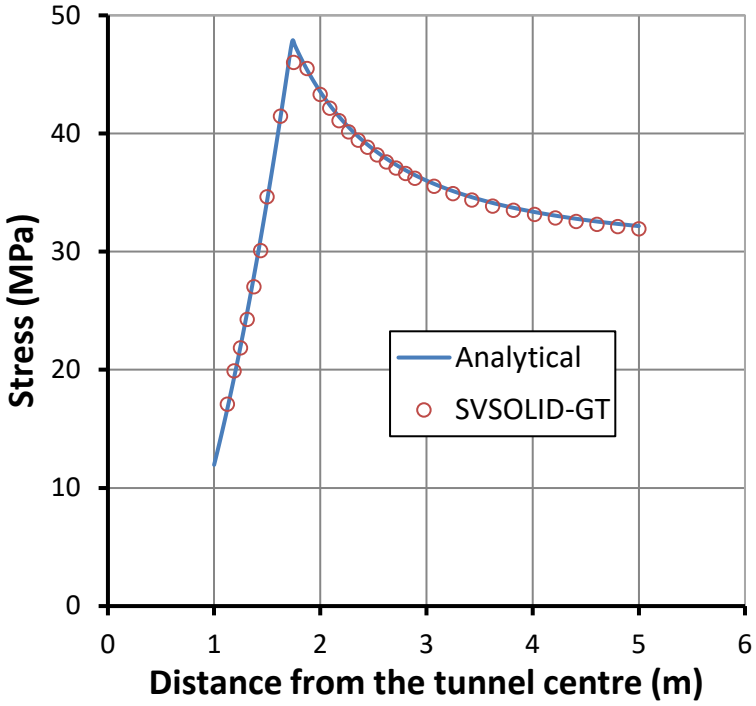

Figure 14. Comparison of the tangential stresses, $\psi = 30°$ (associative flow rule)

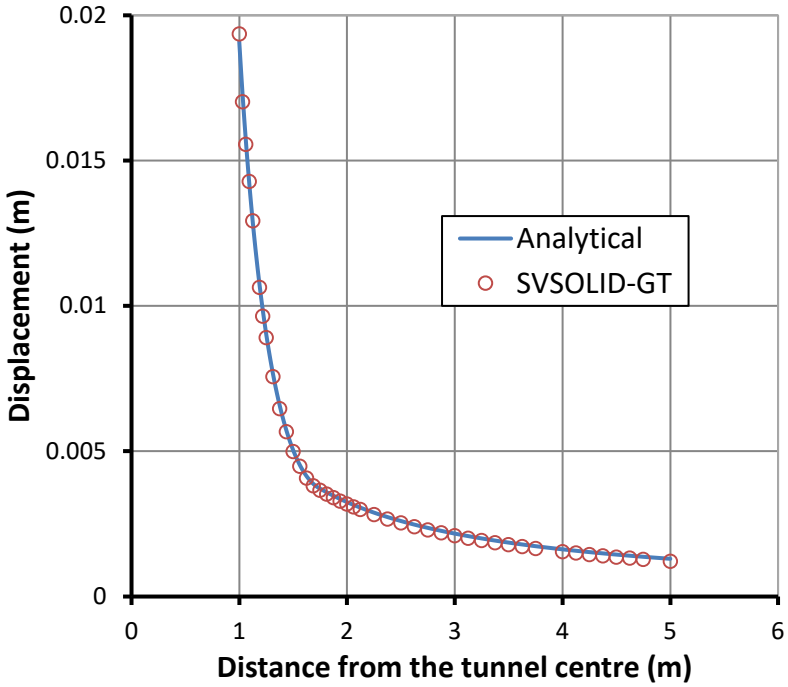

Figure 15. Comparison of the total displacements, $\psi = 30°$ (associative flow rule)

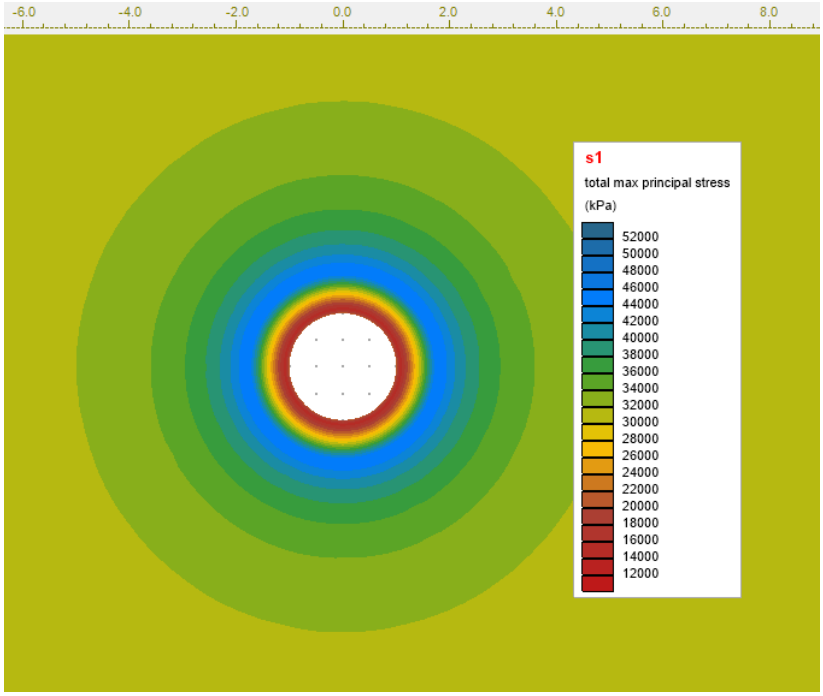

Figure 16. Contour plot of tangential stresses from SVSOLID, $\psi = 0°$ (non-associative flow rule)

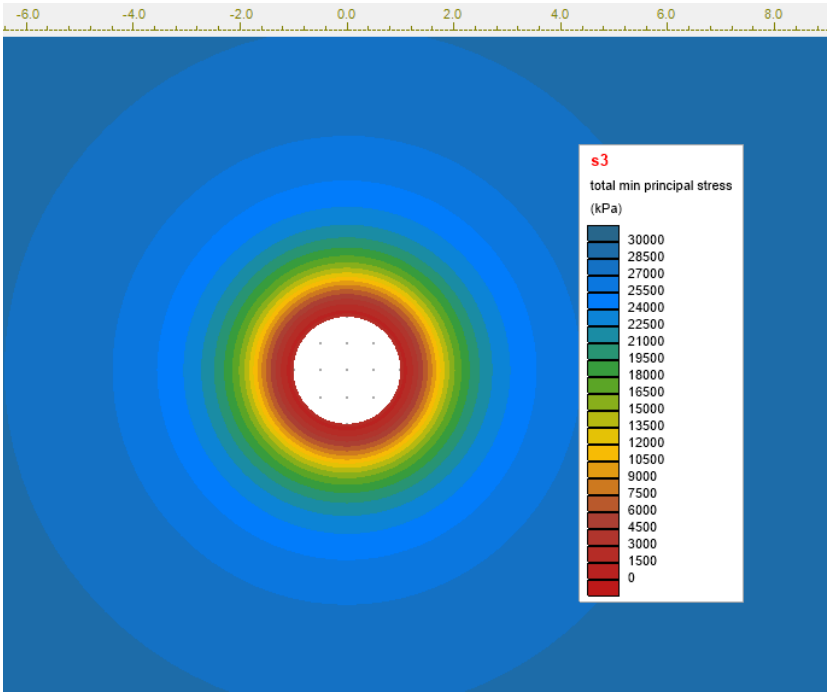

Figure 17. Contour plot of radial stresses from SVSOLID, $\psi = 0°$ (non-associative flow rule)

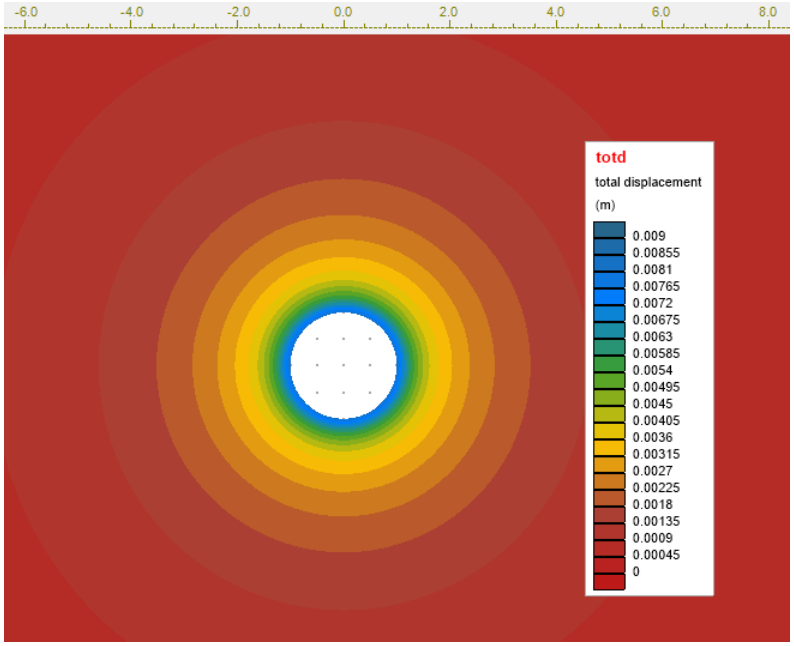

Figure 18. Contour plot of total displacements from SVSOLID, $\psi = 0°$ (non-associative flow rule)

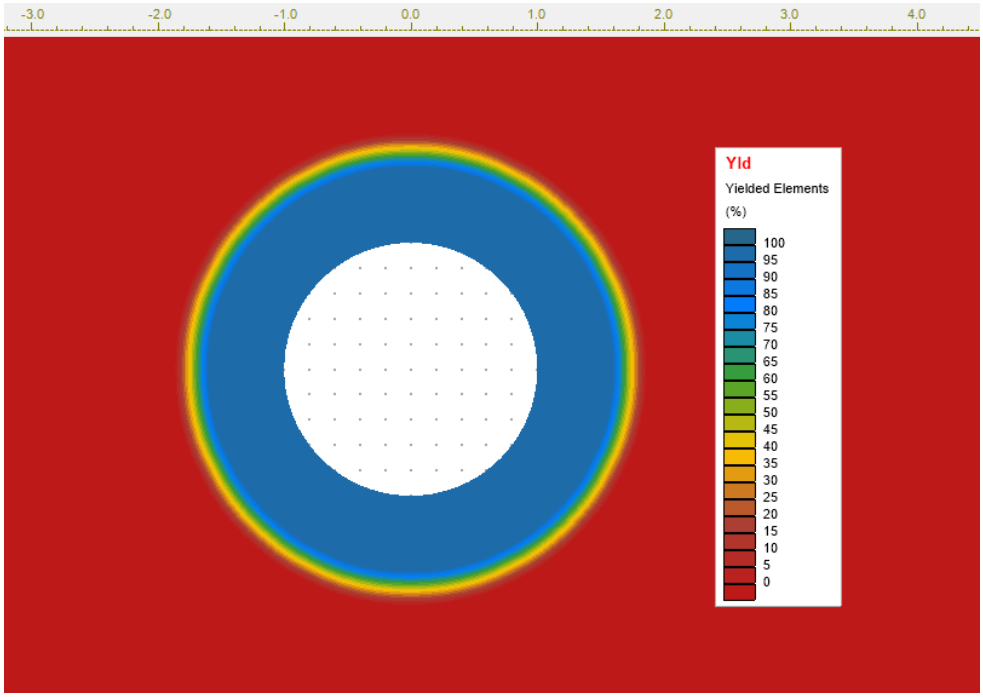

Figure 19. Contour plot of the yield zones from SVSOLID, $\psi = 0°$ (non-associative flow rule)

2.3 Tunnel Heading in Elasto-Plastic Mohr-Coulomb Soil

Reference: Augarde et al., (2013)

Project: Tunnels
Model: TunnelHeading_ElasticPlastic_Case1_GT
to TunnelHeading_ElasticPlastic_Case12_GT

Main Factors Considered:

- Comparison of the SVSOLID solver results to the closed-form solutions for a Mohr-Coulomb soil model under 2D plane strain conditions.

2.3.1 Model Description

In this verification, an internal pressure, σ_t, is estimated to support a tunnel under a surface pressure, σ_s, and the overburden pressure. The values of σ_t to maintain a stable condition depend on several factors including: soil properties, ground surface pressure, σ_s, the tunnel heading diameter, *D*, and the soil overburden thickness, *C*.

2.3.2 Geometry and boundary conditions

Figure 20 shows the geometry and boundary conditions used in this model. A finer mesh was created around the tunnel heading. The Mohr-Coulomb model was used for the cohesive soil. The domain was extended vertically and horizontally to eliminate any boundary effect. There are 12 modeling cases and Young's modulus and Poisson ratio are 20 MPa and 0.3, respectively.

2.3.3 Material Properties

A summary of the material properties is provided in Table 4. There are two dimensionless numbers that define the stability of the problem, namely, load number, *P,* and weight number, *Q*, which are defined as follows (Augarde et al., 2003):

$$P = \frac{\sigma_s - \sigma_t}{c} \qquad [1]$$
$$Q = \frac{\gamma D}{c}$$

The critical load parameter, *P*, was determined for each case by decreasing the internal tunnel pressure, σ_t, until the tunnel became unstable. At this critical internal pressure, the displacement of the tunnel head is large and the solver cannot converge.

Table 4. Input material properties

Case	σ_s (kPa)	γ (kN/m^3)	C/D	**c** (kPa)	Q
1	10	0	2	1	0
2	12	0	5	1	0
3	12	0	8	1	0
4	12	0	10	1	0
5	40	10	2	10	1
6	20	10	5	10	1
7	5	10	8	10	1
8	5	10	10	10	1
9	10	20	2	10	2
10	11	20	5	10	2
11	10	20	8	10	2
12	5	20	10	10	2

2.3.4 Results

A plot is made of the critical load parameter, *P*, versus the ratio, *C/D,* for each simulation case with a particular weight numbers, *Q* (see Figure 21). This plot also shows the upper and lower bound values reported in Augarde et al. (2003).

Figure 22 to Figure 24 show the total displacement contour plots for the cases where *C/D* =2 and *Q* = 0, 1, and 2. These figures clearly show the settlement trough in front of the tunnel heading.

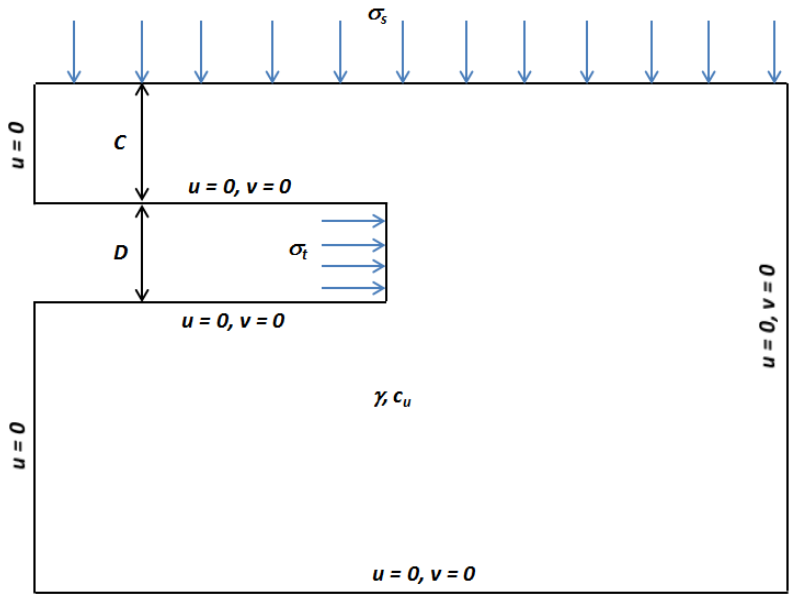

Figure 20. Geometry and boundary conditions with *u = x-displacement and v = y-displacement.*

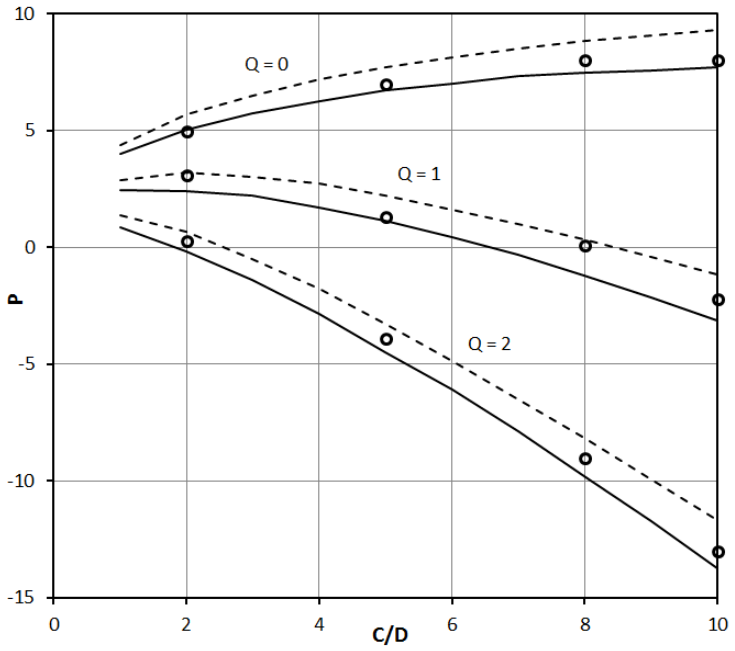

Figure 21. Comparison between the calculated values against upper and lower bound values reported by Augarde et al. (2003).

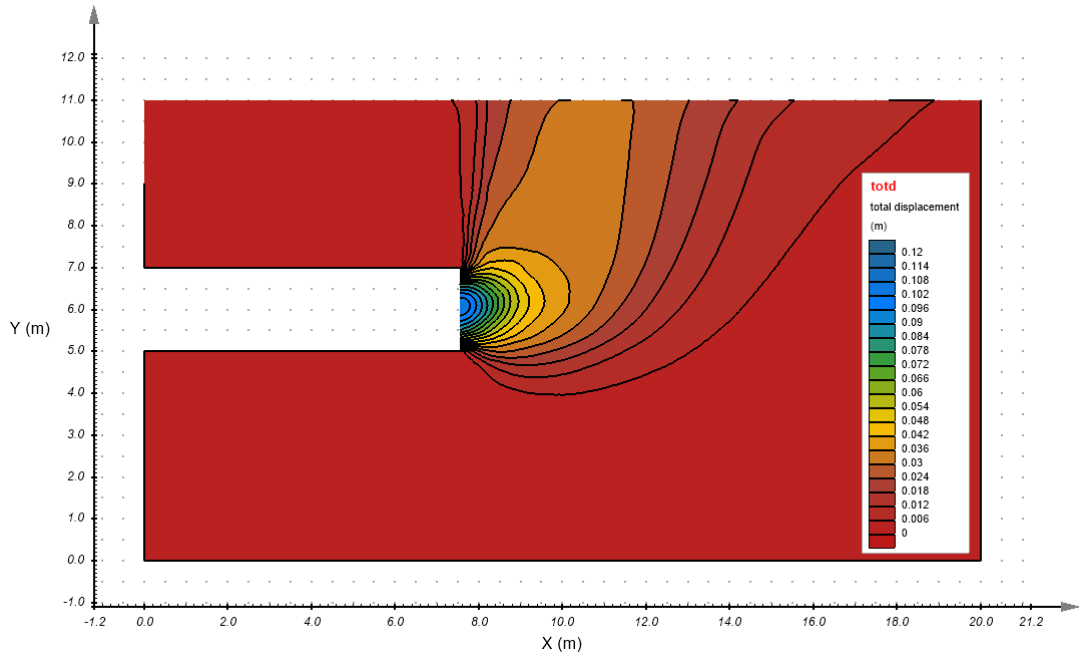

Figure 22. Total displacement contour for *C/D* = 2, and *Q* = 0 at a critical load.

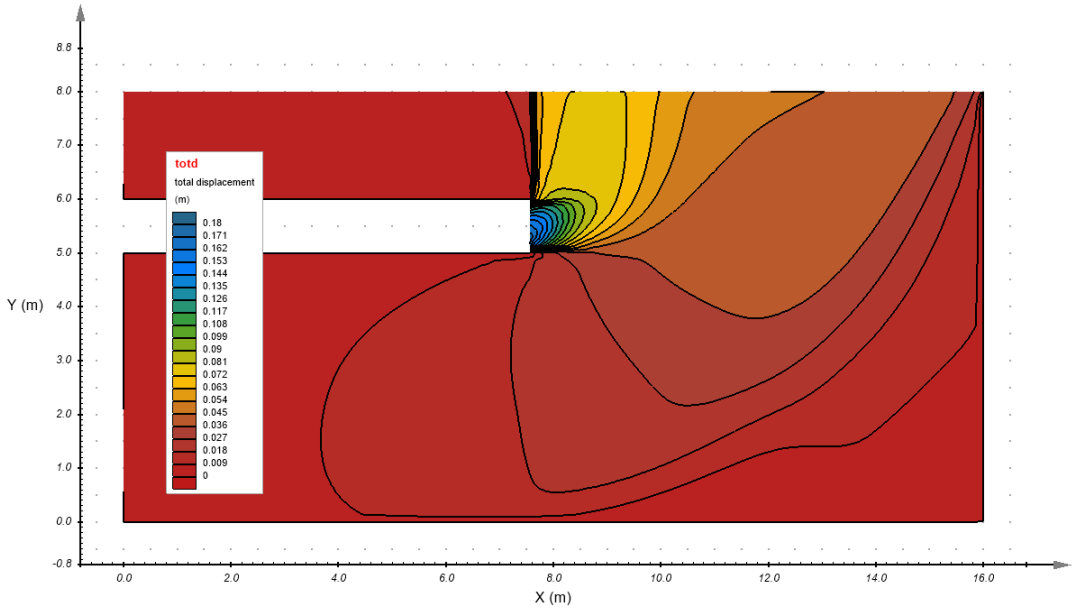

Figure 23. Total displacement contour for *C/D* = 2, and *Q* = 1 at a critical load.

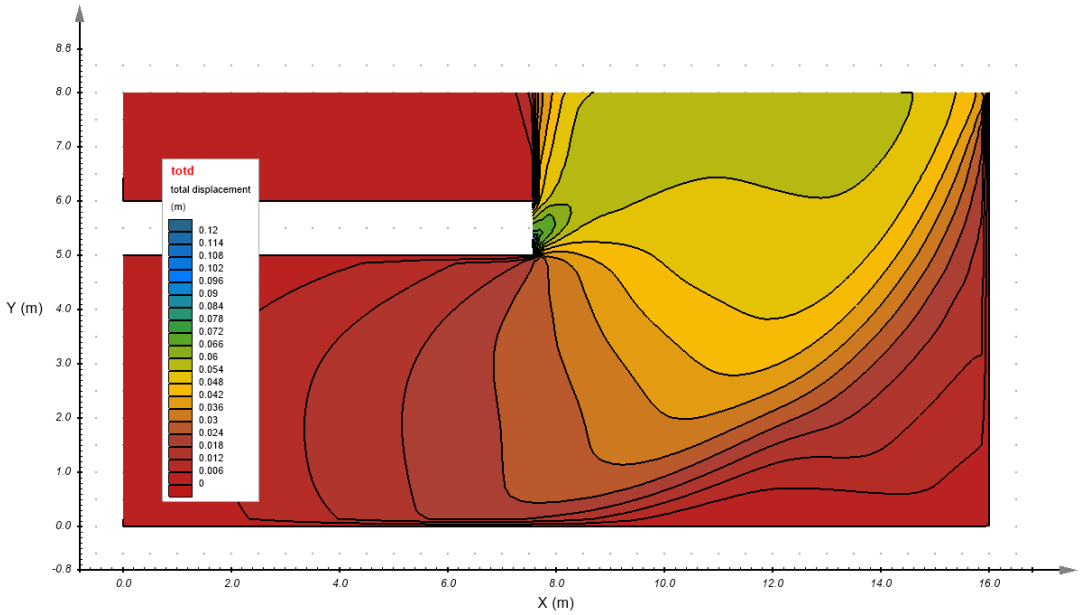

Figure 24. Total displacement contour for *C/D* = 2, and *Q* = 2 at a critical load.

2.4 Strip Footing on Linear Elastic Soil

Reference: Poulos and David (1974)

Project: Foundations
Model: StripFooting_Elastic_GT

Main Factors Considered:

- Comparison between the closed-form solution and the SVSOLID solver for a linear elastic soil model. The geometry is a 2D plane strain representation through the strip footing.

2.4.1 Model Description

A distributed load representing a strip footing is applied to an isotropic elastic soil. The strip footing has a width of *2B*. Due to symmetry, only one half of the footing needs to be modeled. This is a common problem in soil mechanics and a closed-form solution is available.

2.4.2 Geometry and boundary conditions

Figure 25 shows the geometry and boundary conditions used for this example. A distributed load was applied to the surface with a width of B = 0.5 m ($2B$ = 1.0 m). A finer mesh was created around and directly beneath the load. The domain was extended to 20*B* vertically and horizontally to eliminate any boundary effect. Two vertical boundaries are restricted by *x*-displacement and at the base both *x* and *y* displacements are restricted.

2.4.3 Material Properties

A summary of the material properties is provided in Table 5. Calculated stresses are independent of Young's modulus in this example and only affects on computed displacements.

Table 5. Input material properties

Parameter	Value
Young's modulus (E)	20,000 MPa
Poisson's ratio (ν)	0.2
Distributed load (P)	1 kPa
Load width ($2B$)	1 m

2.4.4 Results

Poulos and David (1974) provided an analytical solution for the problem. Stresses at any point in the elastic soil can be determined using the following equations that are independent on Young's modulus and Poisson's ratio:

$$\sigma_y = \frac{P}{\pi}[\alpha + sin\,\alpha\, cos(\alpha + 2\delta)]$$
$$\sigma_x = \frac{P}{\pi}[\alpha - sin\,\alpha\, cos(\alpha + 2\delta)] \qquad [7]$$
$$\sigma_z = \frac{2P}{\pi}\nu\alpha$$

where, the parameters, α and δ, in the above equations are defined in Figure 26. Major and minor principal stresses are given by:

$$\sigma_1 = \frac{P}{\pi}[\alpha + sin\,\alpha] \qquad [8]$$
$$\sigma_3 = \frac{P}{\pi}[\alpha - sin\,\alpha]$$

Comparisons between the analytical and SVSOLID solutions are shown in Figure 27. Along the center vertical line, x = 0, the shear stress τ_{xy} = 0, and therefore, σ_1 = σ_y and σ_3 = σ_x. Figure 27 shows close agreement of the principal stresses from the analytical solution and SVSOLID solutions at the vertical centerline.

Figure 28, Figure 29 and Figure 30 show contour plots of stresses beneath the distributed load. Figure 28 provides an excellent match of contour plots between SVSOLID and the analytical solution for σ_y. According to the analytical solution, the vertical stress of 0.1 kPa (i.e., 10 % of applied load P) at the centerline occurs at a depth of 6.34 m, and the result from the SVSOLID solver shows the corresponding depth to be 6.40 m below the surface.

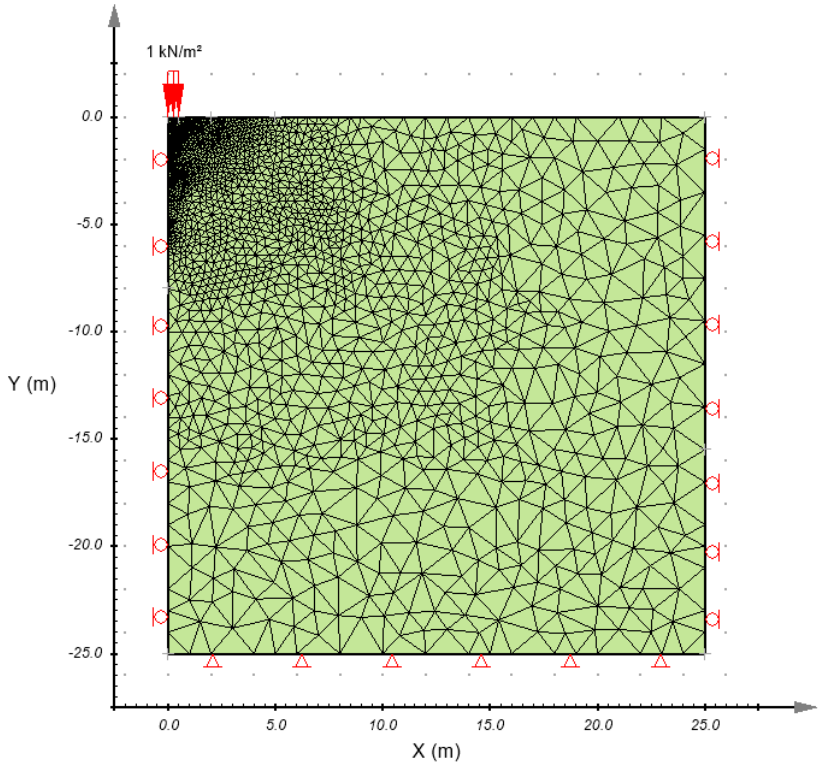

Figure 25. Geometry and boundary conditions

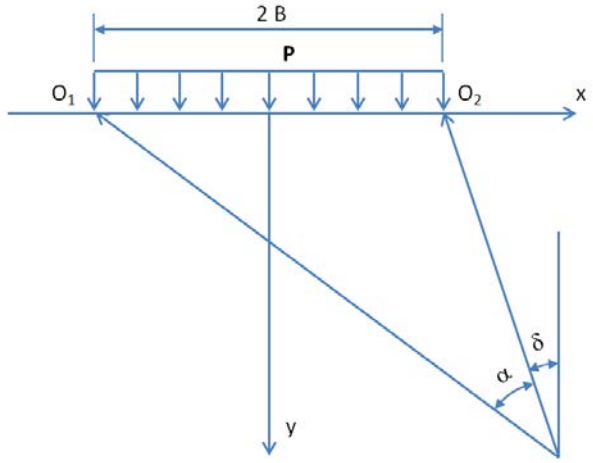

Figure 26. Definition of variables related to the loading scheme

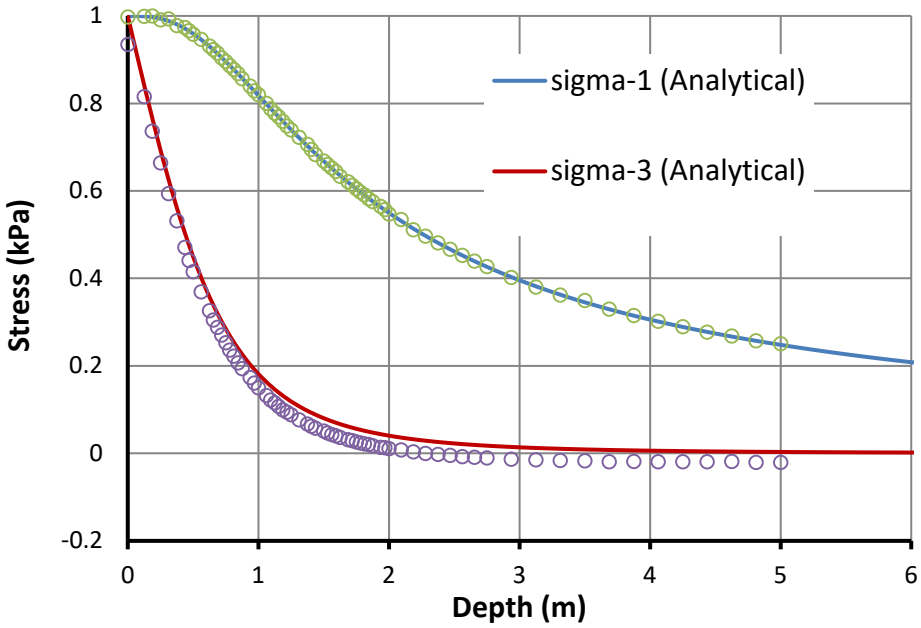

Figure 27. Comparison between the analytical and SVSOLID major and minor principal stresses

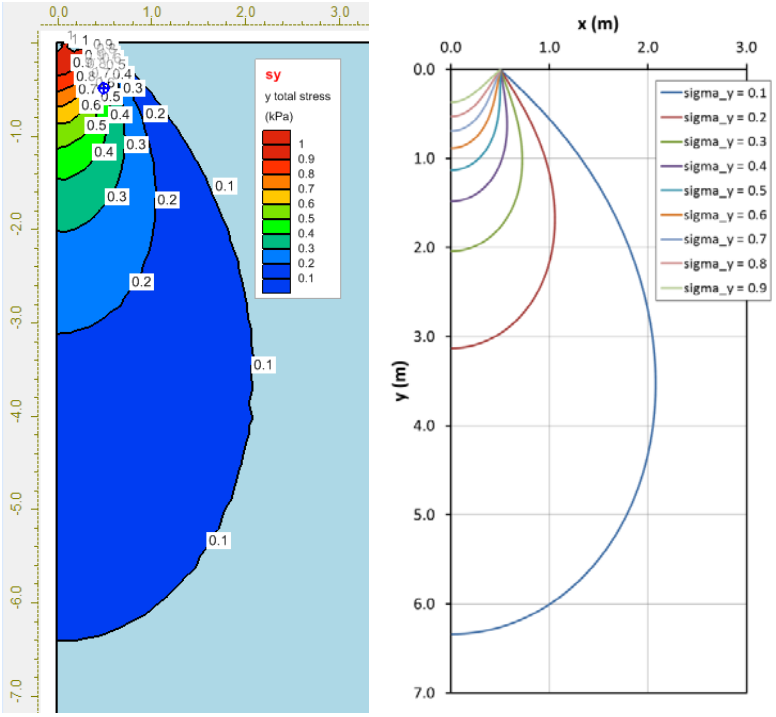

Figure 28. Contour plots of vertical stresses, σ_y, in SVSOLID (left) and analytical solution (right)

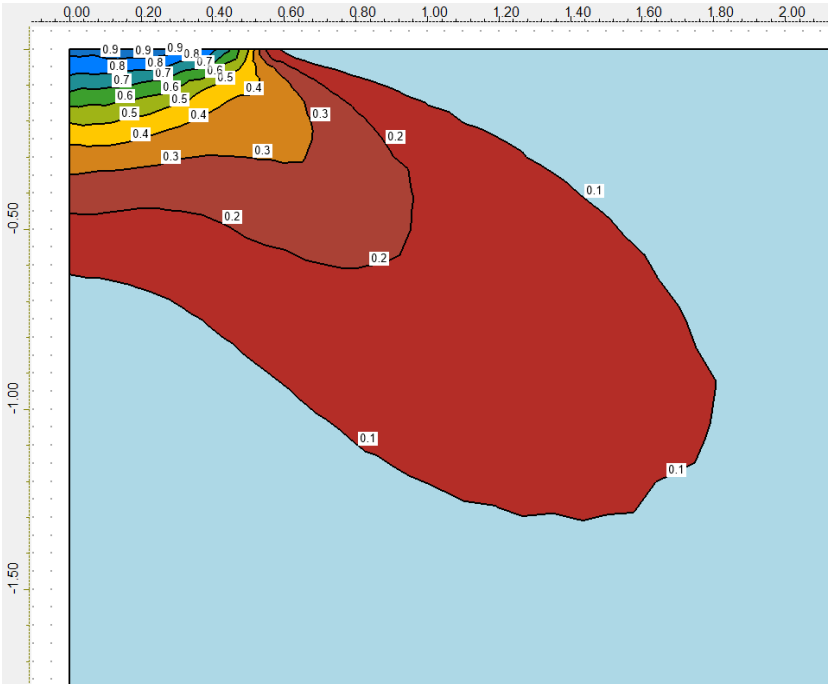

Figure 29. Contour plot of horizontal stresses, σ_x, in SVSOLID

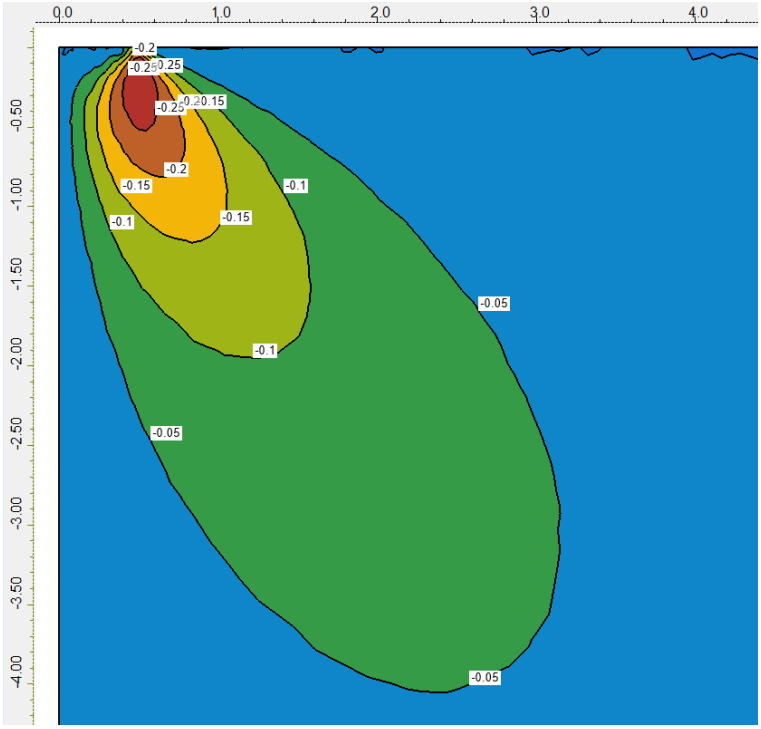

Figure 30. Contour plot of shear stresses, τ_{xy}, in SVSOLID

2.5 Strip Footing on Cohesive Soil

Reference: Chen (2007)

Project: Foundations
Model: StripFooting_CohesiveSoil_GT

Main Factors Considered:

- Comparison of the closed-form solution to the SVSOLID solver solution for a Mohr-Coulomb soil model using a 2D plane strain representation of the strip footing.

2.5.1 Model Description

A distributed load representing a strip footing is applied to a cohesive soil using Mohr-Coulomb failure criterion. The ultimate bearing capacity is of interest. The strip footing has a width of 2*B* and due to the symmetry only one half of the footing was modeled.

2.5.2 Geometry and boundary conditions

Figure 31 shows the geometry and boundary conditions used for this example. A distributed load was applied to the soil surface with a strip footing width of B = 3.0 m ($2B$ = 6.0 m). A finer mesh was created around and directly beneath the applied load.

2.5.3 Material Properties

A summary of the material properties is provided in Table 6.

Table 6. Input material properties

Parameter	Value
Young's modulus (E)	250 MPa
Poisson's ratio (ν)	0.2
Cohesion (c)	0.1 MPa
Friction angle (ϕ)	0°
Haft-width footing (B)	3.0 m

2.5.4 Results

The ultimate bearing capacity is given in Chen (2007).

$$q = (2 + \pi)\ c \qquad [\ 9\ ]$$

where, *c* is the cohesion of soil. The Prandtl's failure mechanism is shown in Figure 32. The ultimate load in this case is 514 kPa when the cohesion is 100 kPa.

Seventeen loading stages were used as the applied load was increased to 530 kPa. Figure 32 shows the failure mechanism at the ultimate load of 514 kPa. Load and displacement curves are shown in Figure 33 and the results indicate that SVSOLID produces an accurate result close to the analytical solution. The displacement beneath the strip footing at the ultimate load is around 5 cm (0.05 m).

SVSOLID failed to converge at a load greater than 520 kPa. Figure 34, Figure 35 and Figure 36 show the contour plots of major and minor principal stresses and total displacement at an applied load of 520 kPa.

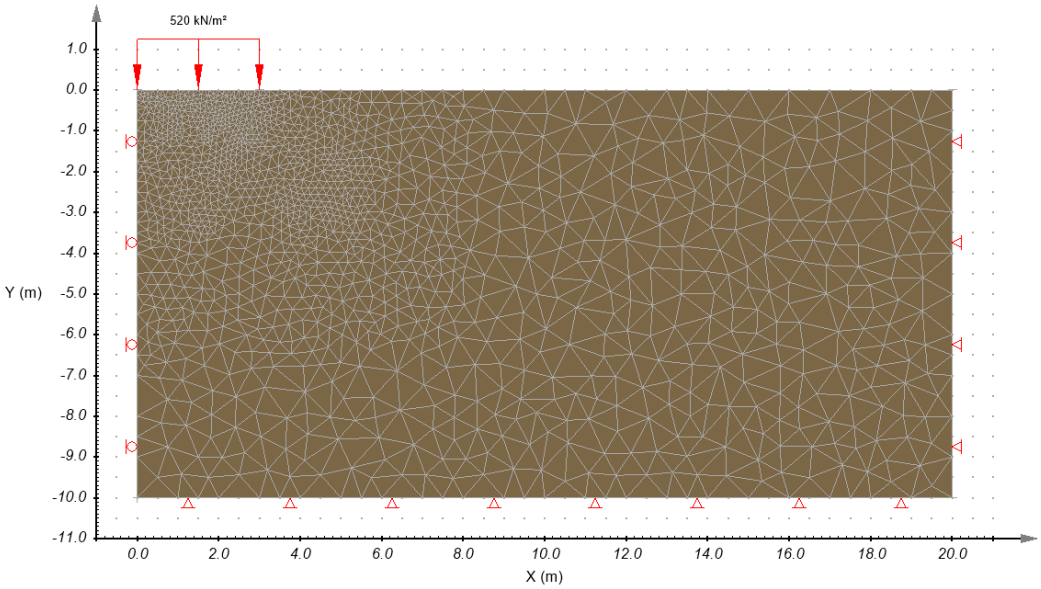

Figure 31. Geometry, mesh and boundary conditions

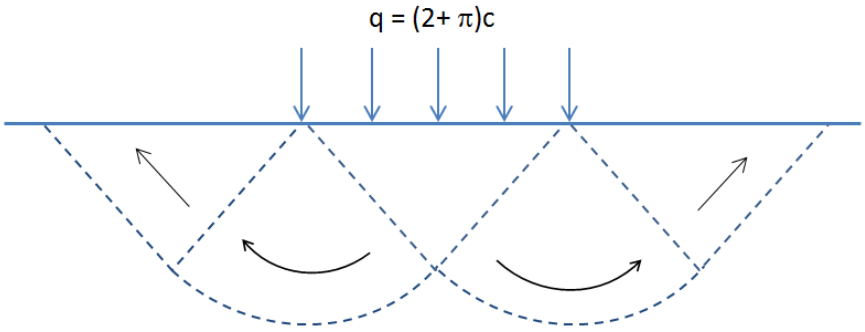

Figure 32. Prandtl's failure mechanism

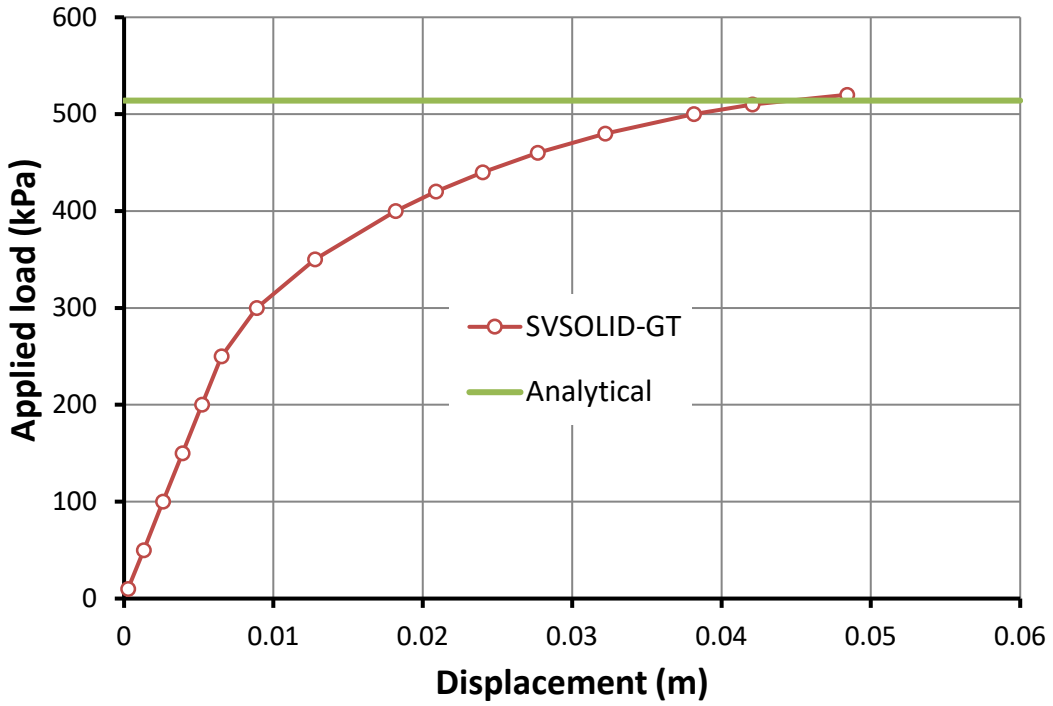

Figure 33. Comparison between the analytical solution and the SVSOLID solution for the ultimate applied load.

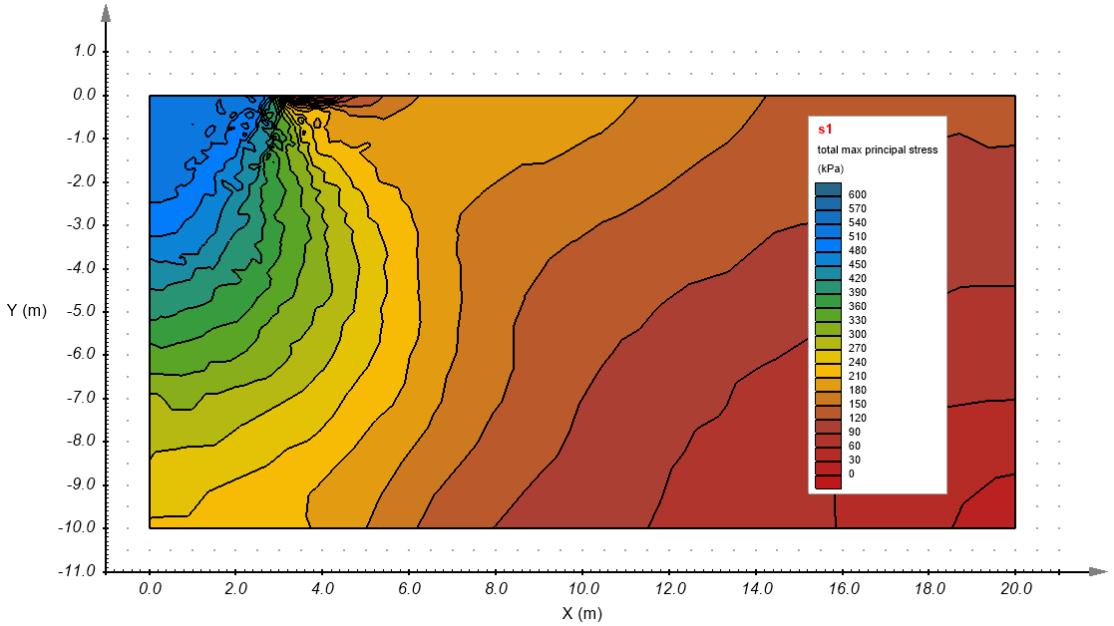

Figure 34. Major principal stress, σ_1, when the applied load is 520 kPa

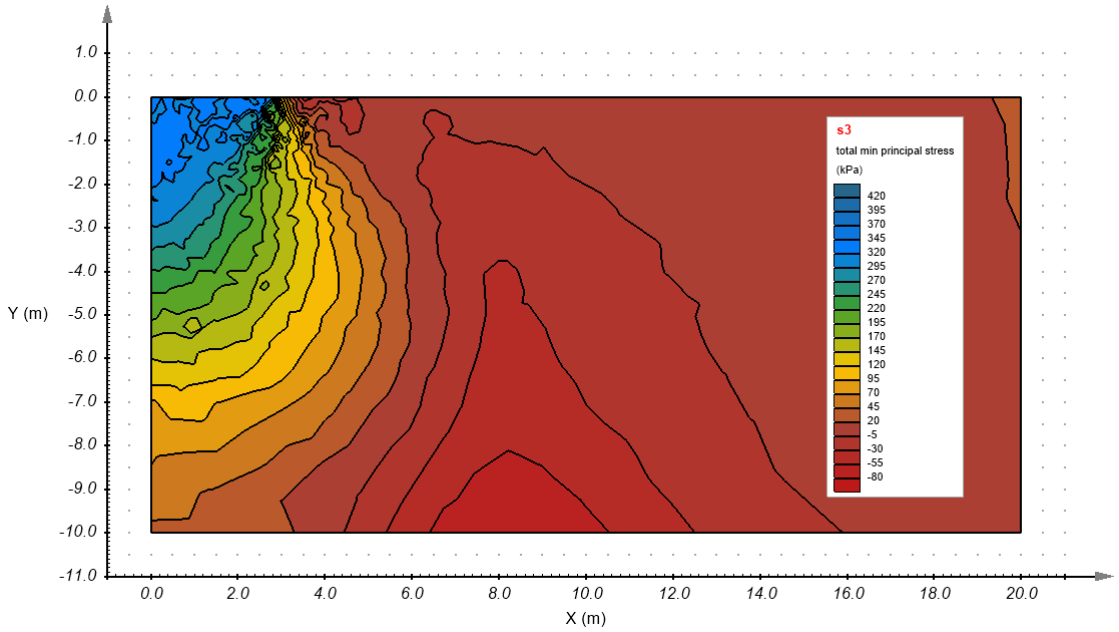

Figure 35. Minor principal stress, σ_3, when the applied load is 520 kPa

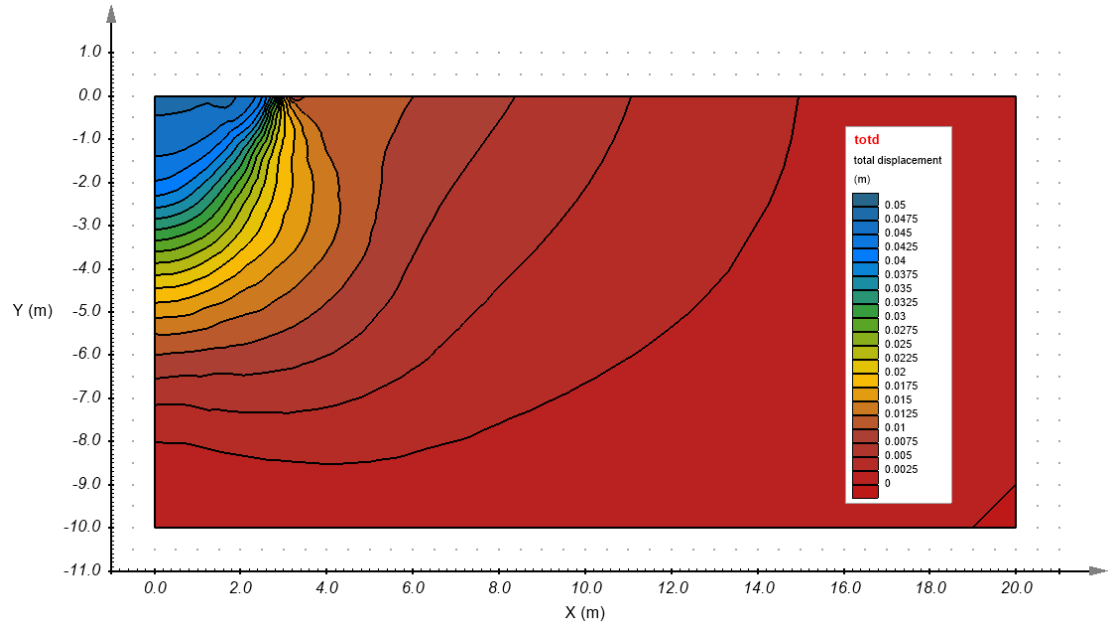

Figure 36. Total displacement when the applied load is 520 kPa

2.6 Ultimate Bearing Capacity of Shallow Foundation on a Cohesive Slope

Reference: Meyerhof (1957)

Project: Foundations
Model: StripFooting_Slope_CohesiveSoil_0degree_Case1_GT to StripFooting_Slope_CohesiveSoil_60degree_Case1_GT
StripFooting_Slope_CohesiveSoil_0degree_Case2_GT to StripFooting_Slope_CohesiveSoil_60degree_Case2_GT

Main Factors Considered:

- Comparing the results of SVSOLID against closed-form solutions of a 2D plane strain representation of a strip footing on a slope.

2.6.1 Model Description

The ultimate bearing capacity of a shallow footing foundation on a cohesive slope is examined. The slope is at an inclination angle of β and the footing has a width B = 1 m. The body load of the soil is not considered and the ultimate load is examined for two cases, Case 1: the depth, D_f, of the footing is 0 m and Case 2: $D_f = B$ = 1 m (Figure 37).

2.6.2 Geometry and boundary conditions

Figure 38 shows the geometry and boundary conditions used in this model. A finer mesh was created around and directly beneath the load. A Mohr-Coulomb model is used for the cohesive soil. The domain is extended vertically and horizontally to eliminate boundary effect. Except at the ground surface, other boundary displacements (i.e., x-displacement and y-displacements) are restricted.

2.6.3 Material Properties

A summary of the material properties is provided in Table 7.

Table 7. Input material properties

Parameter	Value
Young's modulus, E	20,000 kPa
Poisson's ratio, ν	0.3
Cohesion, c	50 kPa
Ultimate load, q_u or N_c	To be determined
Footing width, B	1 m
Footing depth, D_f	0 m (Case 1) and 1 m (Case 2)

2.6.4 Results

Meyerhof (1957) provided an analytical solution for the determination of the ultimate bearing capacity, q_u. The ultimate bearing capacity for purely cohesive soil can be written as:

$$q_u = c_u N_c \qquad [\ 2\ ]$$

where, c_u is the undrained cohesion of the soil and N_c is the bearing capacity factor. The case is solved where the cohesion, c_u, is equal to 50 kPa. The value of N_c is a function of the inclination angle, β and stability number, N_s (Eq. [3]). The stability number, N_s, is defined as:

$$N_s = \gamma \frac{H_s}{c_u} \qquad [\ 3\ ]$$

where, H_s is the height of the slope (Figure 37). In the two cases considered, N_s = 0 as γ = 0 (i.e., neglecting body load).

Figure 40 and Figure 41 show comparisons between the SVSOLID solution and the analytical solution (Meyerhof, 1957). These figures show a close agreement between the SVSOLID and the analytical solution. Table 8 shows the error between the simulated models for both Case 1 and 2 in comparison to the analytical solution.

Table 8. Calculation differences

Simulation case	Difference (%)
Case 1	0.76
Case 2	2.34

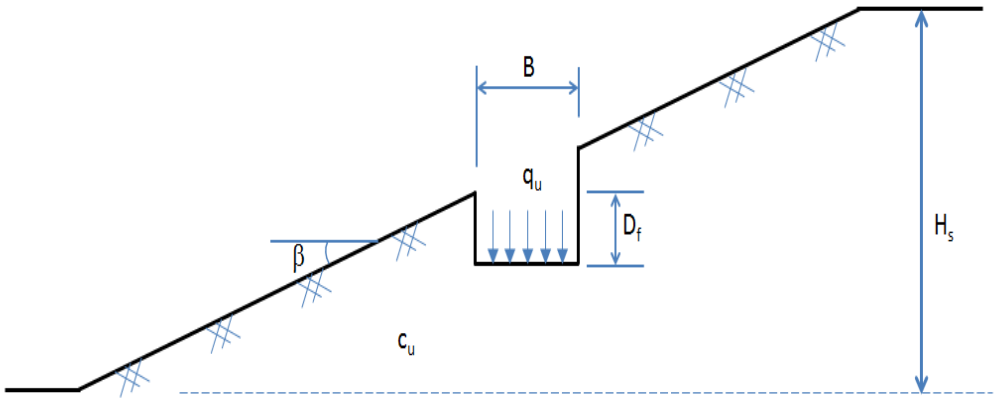

Figure 37. Geometric schematic of the problem

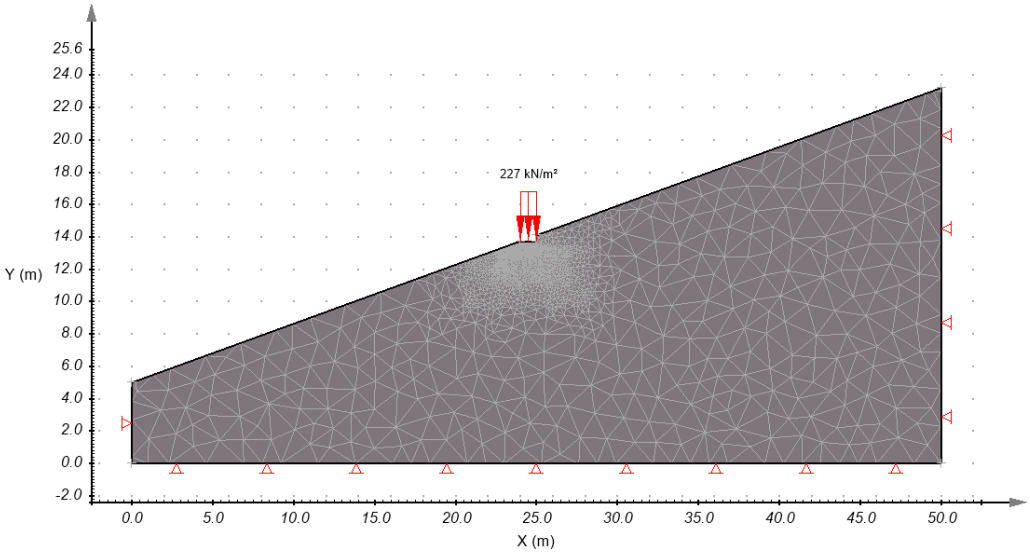

Figure 38. Geometry and boundary conditions

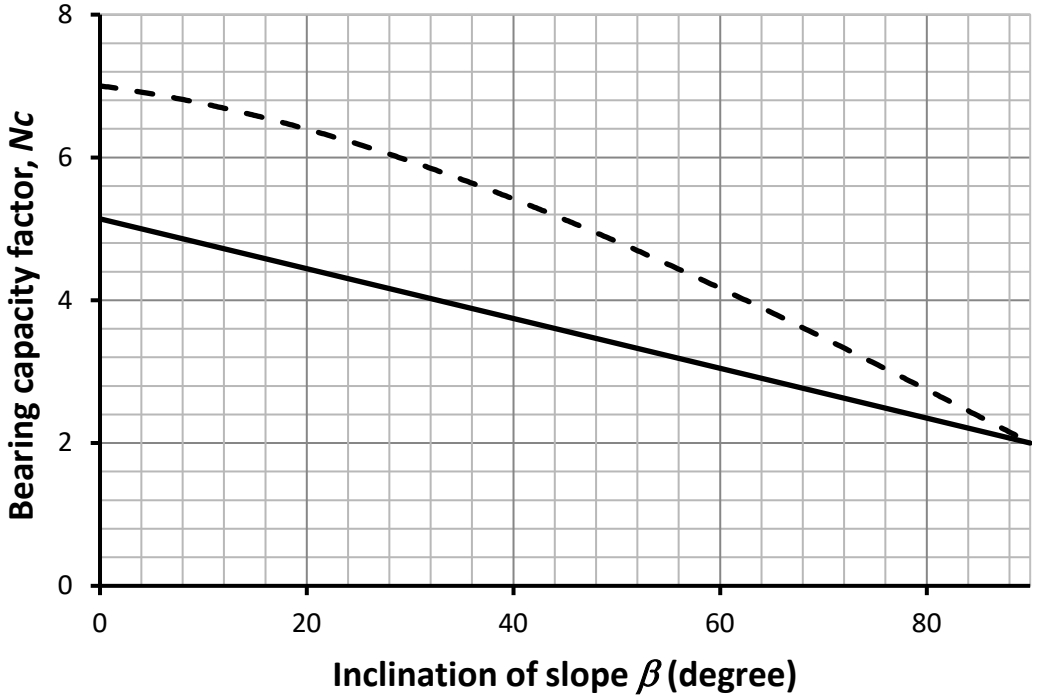

Figure 39. The relation between, N_c and the inclination angle, β. The dashed line for D_f/B = 1 and the solid line for D_f/B = 0 and the stability factor, N_s = 0 (data obtained from Meyerhof, 1957).

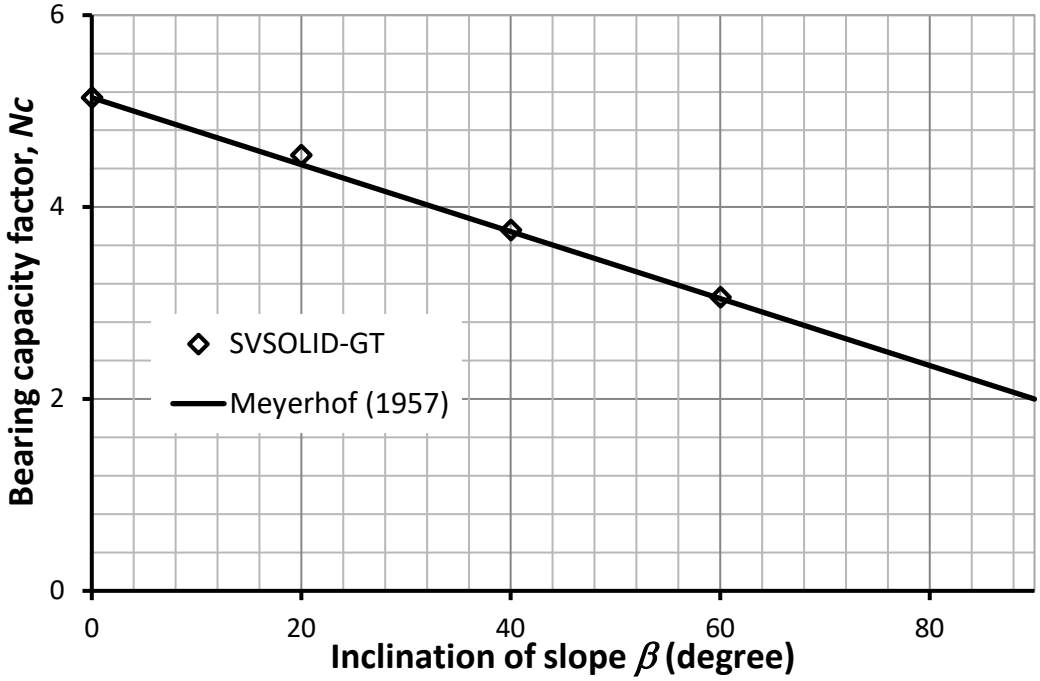

Figure 40. Bearing capacity factors for Case 1

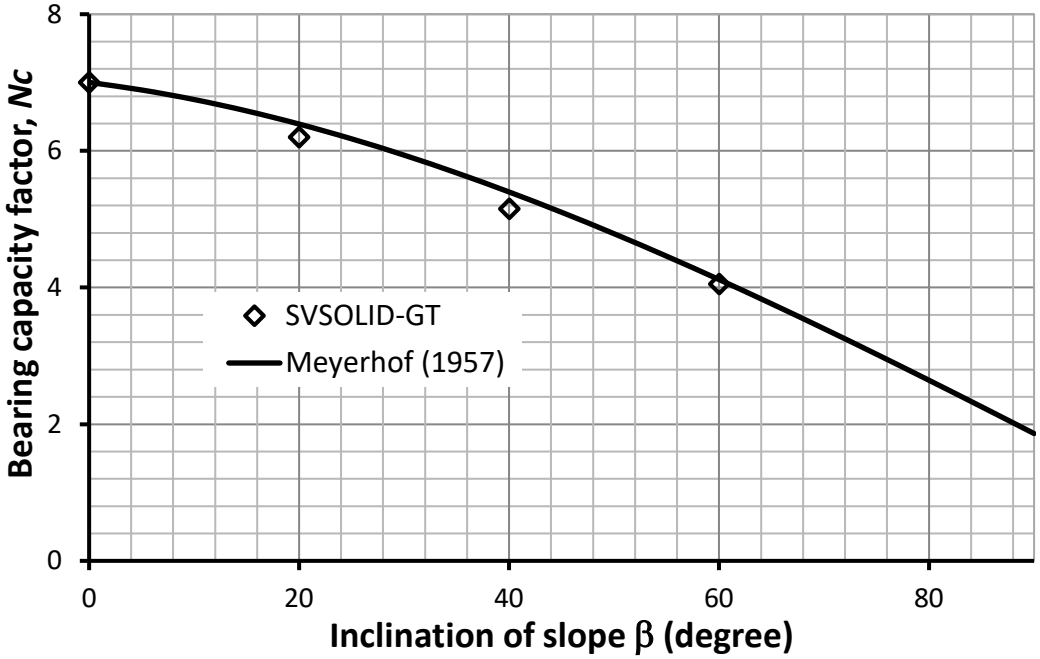

Figure 41. Bearing capacity factors for Case 2

2.7 Bearing Capacity of Footing on Clayey Soil Layers

Reference: Merifield et al. (1999)

Project: Foundations
Model: StripFooting_LayeredCohesiveSoil_Case1_GT and StripFooting_LayeredCohesiveSoil_Case2_GT

Main Factors Considered:

- Comparing SVSOLID results to numerical and closed-form results for a strip footing on two layers of clayey soil under 2D plane strain loading.

2.7.1 Model Description

Bearing capacity of a footing on two cohesive soil layers. Each layer of soil is considered to be isotropic and homogenous. There are two cases that are examined: 1) the upper soil is stronger than the lower soil, (i.e., $c_{u1} > c_{u2}$); and, 2) the lower soil is stronger than the upper soil (i.e., $c_{u2} > c_{u1}$).

2.7.2 Geometry and boundary conditions

Figure 42 shows the geometry and boundary conditions used in this model. A finer mesh was created near the applied load and the Mohr-Coulomb model was used for this purely cohesive soil. The domain is extended vertically and horizontally to eliminate boundary effect.

2.7.3 Material Properties

A summary of the material properties is presented in Table 9.

Table 9. Input material properties

Parameter		Case 1	Case 2
Young's modulus, E (MPa)	Upper clay	500	250
	Lower clay	250	500
Poisson's ratio, ν		0.2	0.2
Cohesion, c_u (kPa)	Upper clay (c_{u1})	200	100
	Lower clay (c_{u2})	100	200
Upper layer thickness, H (m)		1	1
Footing width, B (m)		8	8

2.7.4 Results

The analytical solution for the ultimate bearing capacity of a strip footing on two clay layers with the load applied at the ground surface (without surcharge) is defined as:

$$q_u = N_c c_{u1} \qquad [4]$$

where, N_c is the bearing capacity factor and c_{u1} is the undrained shear strength of the upper layer. In the case, where there are two layers of clay soils beneath the footing, N_c is a function of H/B, which is 0.125 and c_{u1}/c_{u2}.

Merifield et al., (1999) determined upper and lower bound ultimate loads using a finite element analysis. The lower bound solution was obtained using stress nodal variables and the stress discontinuities that can occur at the adjacent element interfaces. The application of stress boundary conditions, equilibrium equations and yield criterion lead to an expression for the lower-bound ultimate load. The upper-bound ultimate load is defined using a kinematically admissible velocity field. The velocity field must satisfy the constraints imposed by compatibility, velocity boundary conditions and the flow rule.

Table 10. Theoretical and computational ultimate loads

c_{u1}/c_{u2}	Lower bound	Upper bound	SVSOLID
2 (Case 1)	2.73	3.09	2.9
0.5 (Case 2)	7.78	10.40	9.20

Table 10 shows the upper and lower bound values of N_c for the two cases. The solution are from Merifield et al., (1999) as well as the results from SVSOLID. This Table shows the values produced by SVSOLID are within the lower and upper bound limits.

Figure 43 and Figure 44 show load-displacement curves for these cases. The curves fall within the lower and upper bound range obtained by Merifield et al., (1999).

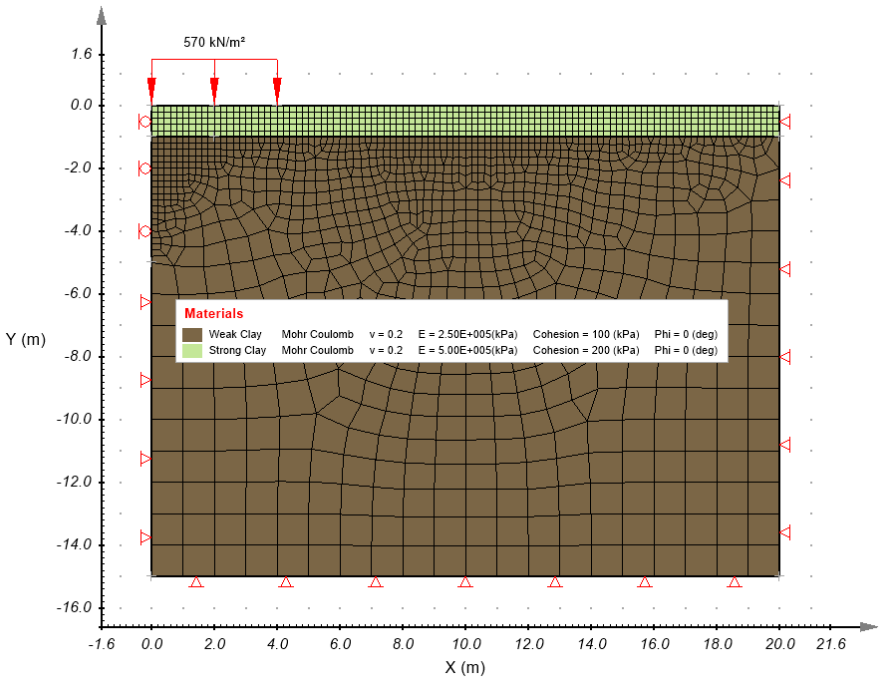

Figure 42. Geometry and boundary conditions

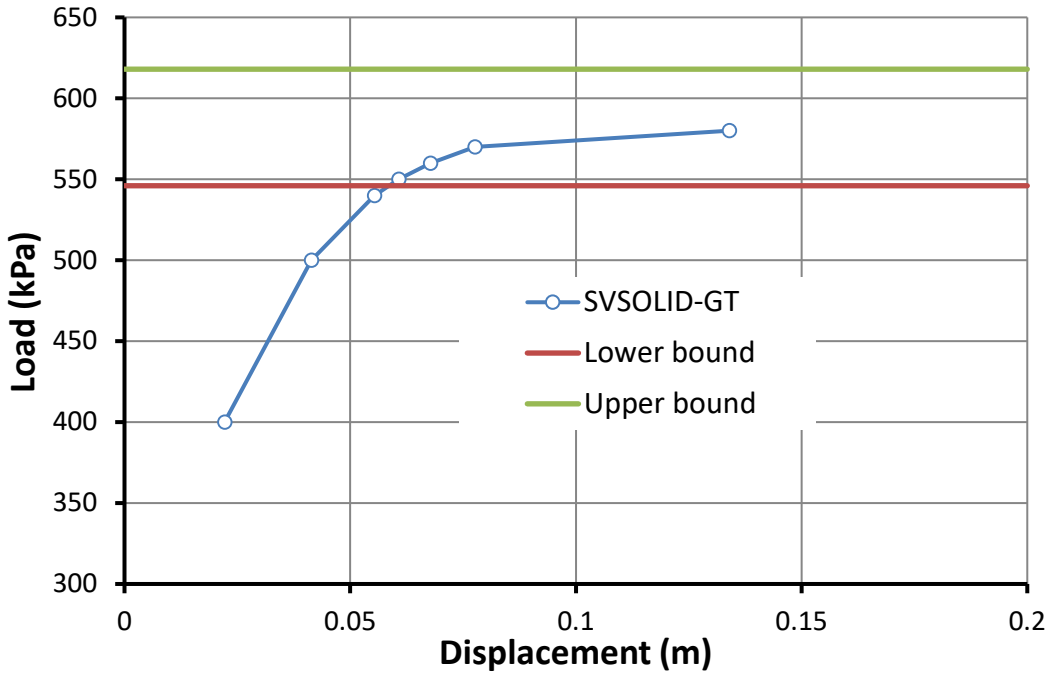

Figure 43. Load-displacement curve for Case 1.

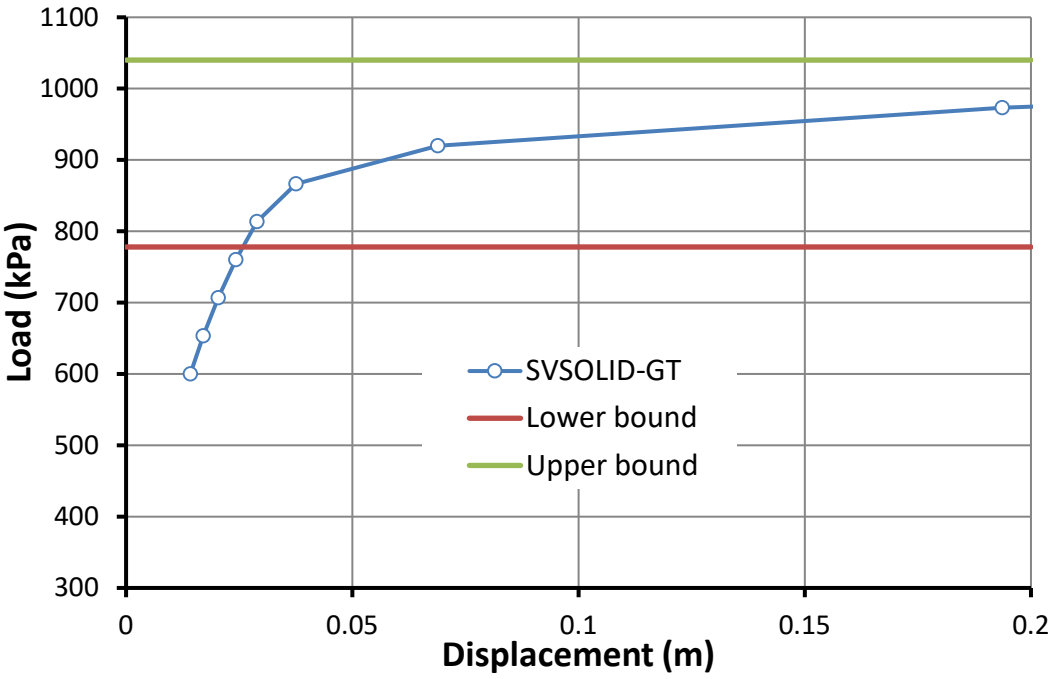

Figure 44. Load-displacement curve for Case 2.

2.8 Passive Load Bearing Capacity of Retaining Wall

Reference: Chen (2007)

Project: RetainingWalls
Model: PassiveLoad_RetainingWall_GT

Main Factors Considered:

- Comparing the results of the SVSOLID solver against the closed-form solutions of a 2D plane strain representation of a retaining wall.

2.8.1 Model Description

The problem involves the determination of the passive bearing capacity of a retaining wall in a purely cohesive soil. A horizontal load is increased until the retaining wall becomes unstable. The self-weight of the soil is neglected.

2.8.2 Geometry and boundary conditions

Figure 45 shows the geometry and boundary conditions used for this model. A finer mesh was created near the applied load and the Mohr-Coulomb model was used for the purely cohesive soil. The domain is extended vertically and horizontally to eliminate boundary effect. Displacements of bottom and right boundaries are restricted in both directions.

2.8.3 Material Properties

A summary of the material properties is provided in Table 11.

Table 11. Input material properties

Parameter	Value
Young's modulus, E	10,000 kPa
Poisson's ratio, ν	0.3
Cohesion, c_u	1 kPa
Wall height	1 m

2.8.4 Results

Chen (2007) published the solution for a critical passive load for this case and it was 2 kPa = $2c_u$. A load–displacement curve is provided in Figure 46 and it shows SVSOLID produces similar results that compared to the analytical solution. Figure 47 shows the displacement contour plot at the critical load of 2 kPa. The results show a large displacement near the ground surface.

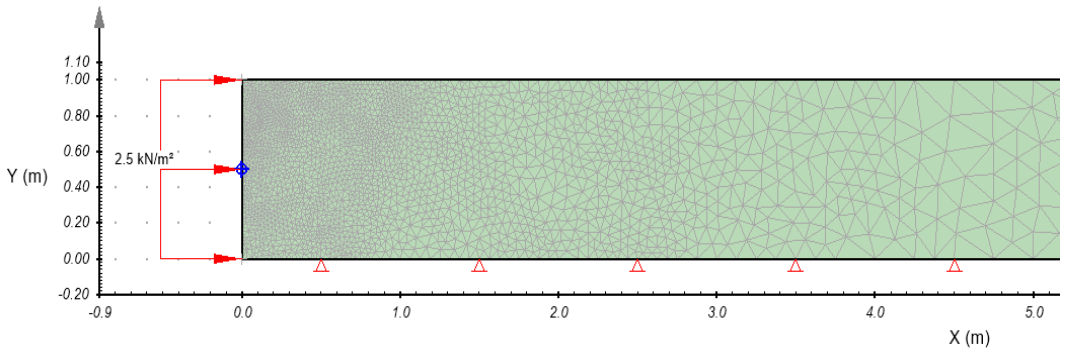

Figure 45. Geometry and boundary conditions

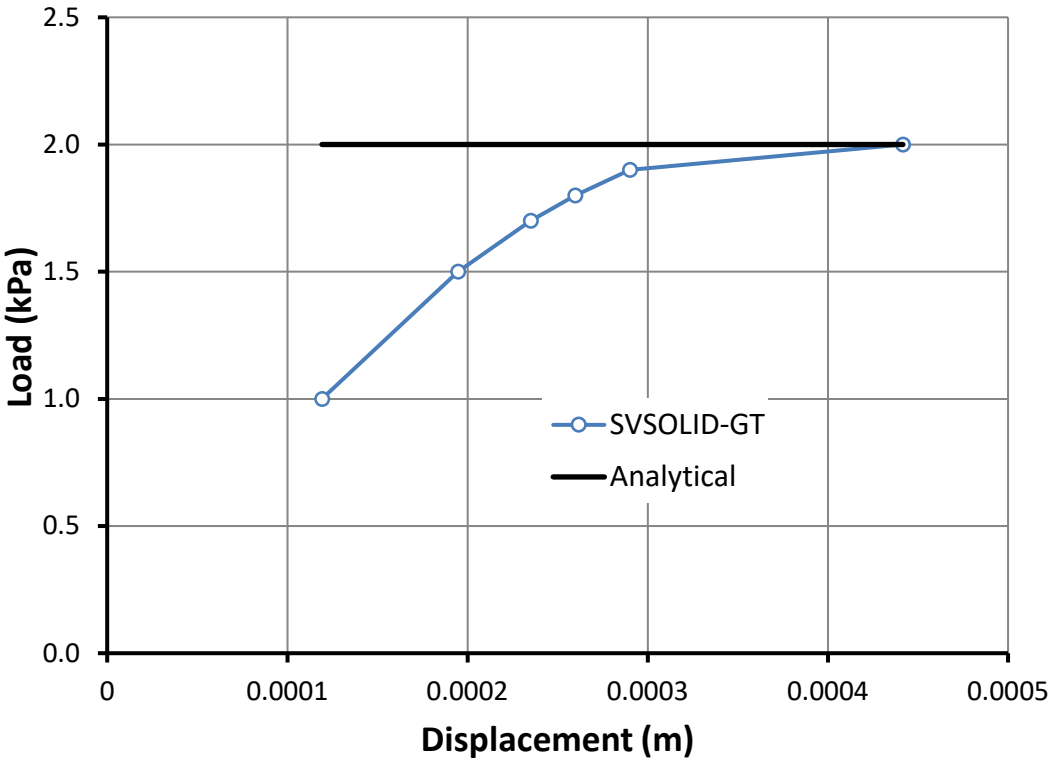

Figure 46. Load-displacement curve for the passive loading capacity problem

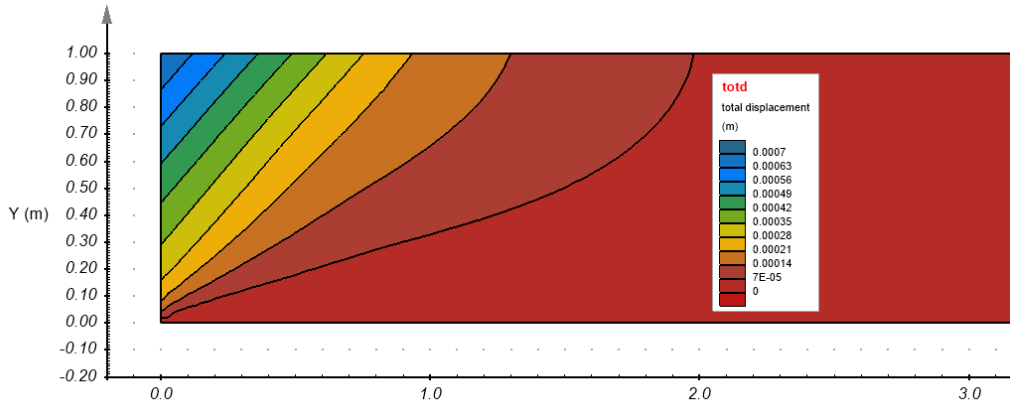

Figure 47. Displacement contours for an applied load of 2 kPa.

2.9 Anchor in 2D Elastic Rock Mass

Reference: Farmer (1975)

Project: Foundations
Model: 2D_Anchor_GT

Main Factors Considered:

- Comparing the results of the SVSOLID solver against the closed-form solutions of an anchor installed in 2D plane strain elastic rock mass.

2.9.1 Model Description

This problem concerns the elastic behavior of an anchor grouted in 2D elastic rock mass. The shear stress distribution along the anchor/rock interface is examined if a pull-out force of 100 kN is applied to the anchor head.

2.9.2 Geometry and boundary conditions

Figure 48 shows the geometry and boundary conditions used in this model. The model geometry has a cross-sectional area of 0.4 m x 0.4 m, and 0.6 m in height. An anchor/rock bolt is installed at the model center and 0.5 m in length from the ground surface. The displacements of the model are restricted at the bottom surface, while at the top surface y-displacement is restricted.

2.9.3 Material Properties

The anchor and rock properties are summarized in Table 12.

Table 12. Input material properties

Parameter	Value
Rock mass properties	
Young's modulus (E_R)	5.0×10^7 kPa
Poisson's ratio (ν)	0.25
Drill hole radius (R)	11 mm
Anchor properties	
Tributary area (A)	243.3 mm^2
Anchor radius (a)	8.8 mm
Young's modulus (E_a)	1.0×10^8 kPa
Bond shear stiffness (K_b)	1.4×10^7 kPa

2.9.4 Results

The shear stress developed along the anchor/grout interface is given in the following (Farmer, 1975)

$$\frac{\tau}{\sigma_o} = 0.1 \times e^{\frac{-0.2x}{a}} \qquad [\ 10\ ]$$

where, τ is the shear stress along the rock bolt/grout interface, σ_o is the applied pull-out stress, x is the distance from the head of the anchor, and a is the radius of anchor. The following assumptions were made by Farmer (1975)

- The shear modulus of grout is $G_b = 0.005\ E_a$
- The drill hole radius is $R = 1.25\ a$

The shear stiffness were determined using the following equation (St. John and Van Dillen, 1983; Dey, 2001)

$$K_b = \frac{2\pi G_b}{ln\left(1 + {}^{t}/_{a}\right)} \qquad [\ 11\ ]$$

where, t = 2.2 mm is the annulus thickness and it is defined in Figure 49. The second assumption indicates he drill hole radius, R is 1.25 × 8.8 mm = 11 mm.

The shear stress along the bolt/grout interface is:

$$\tau = \frac{F_s}{2\pi a} \qquad [\ 12\ ]$$

where, F_s is the shear force per unit length. Similarly, the shear stress along the rock/grout interface can be calculated using Equation [12] with R instead of a.

Figure 54 shows a comparison between the results of shear stress using Equation [10] and SVSOLID. The SVSOLID results match closely to the analytical results. A figure of total displacement contours is shown in Figure 55.

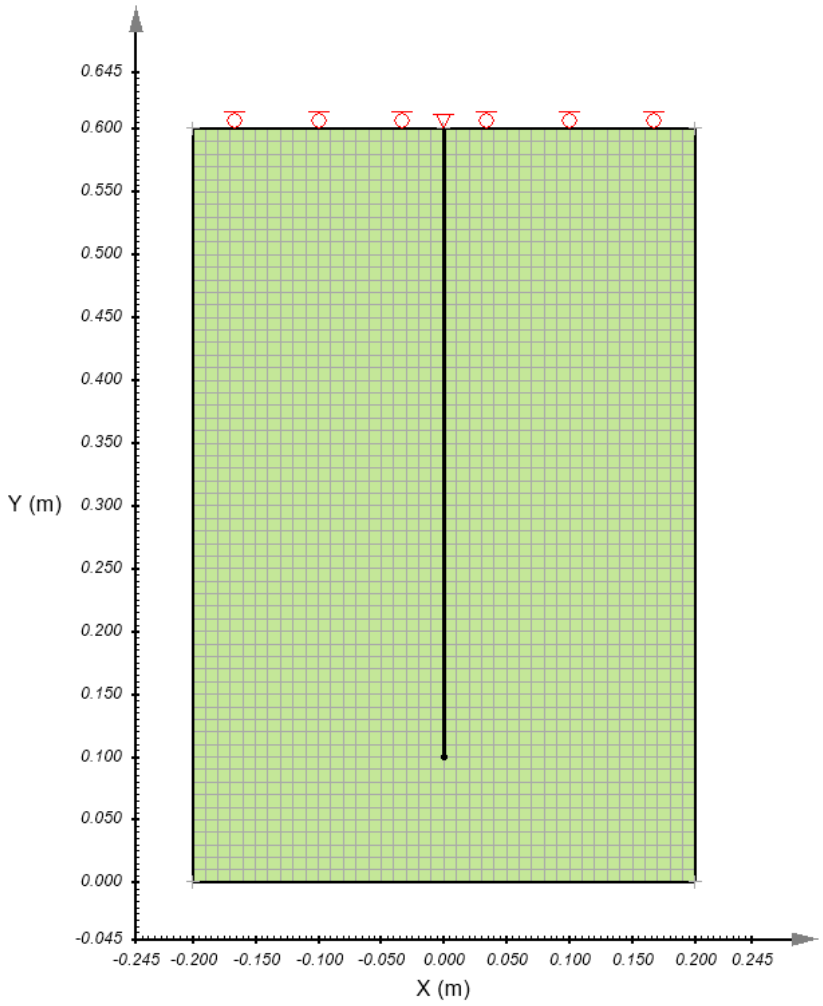

Figure 48. Geometry and boundary conditions

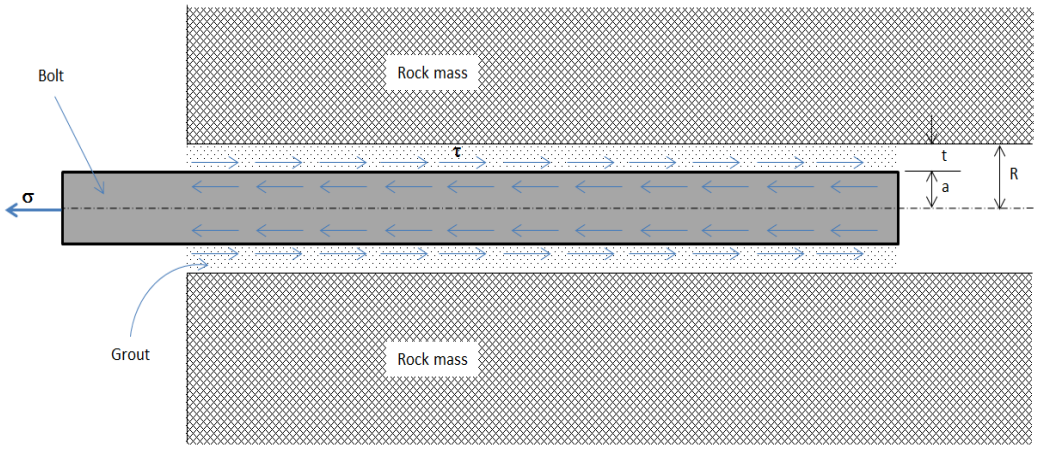

Figure 49. Schematic of rock bolt

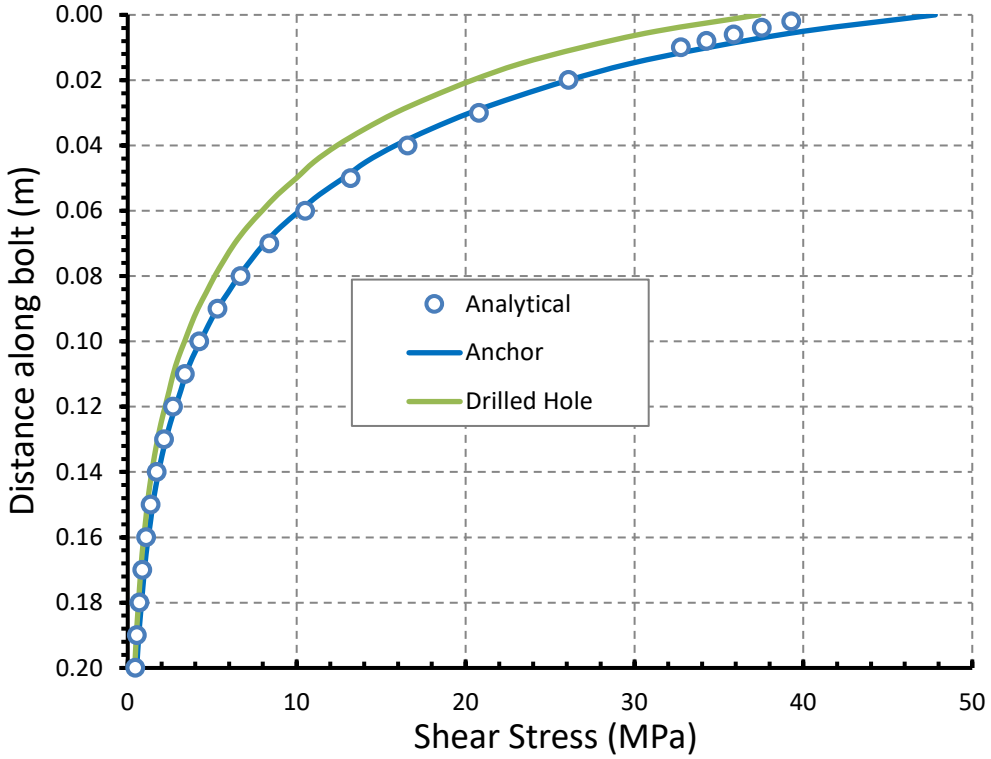

Figure 50. Shear stress along the bolt / grout (anchor) and grout / rock (drilled hole) interfaces

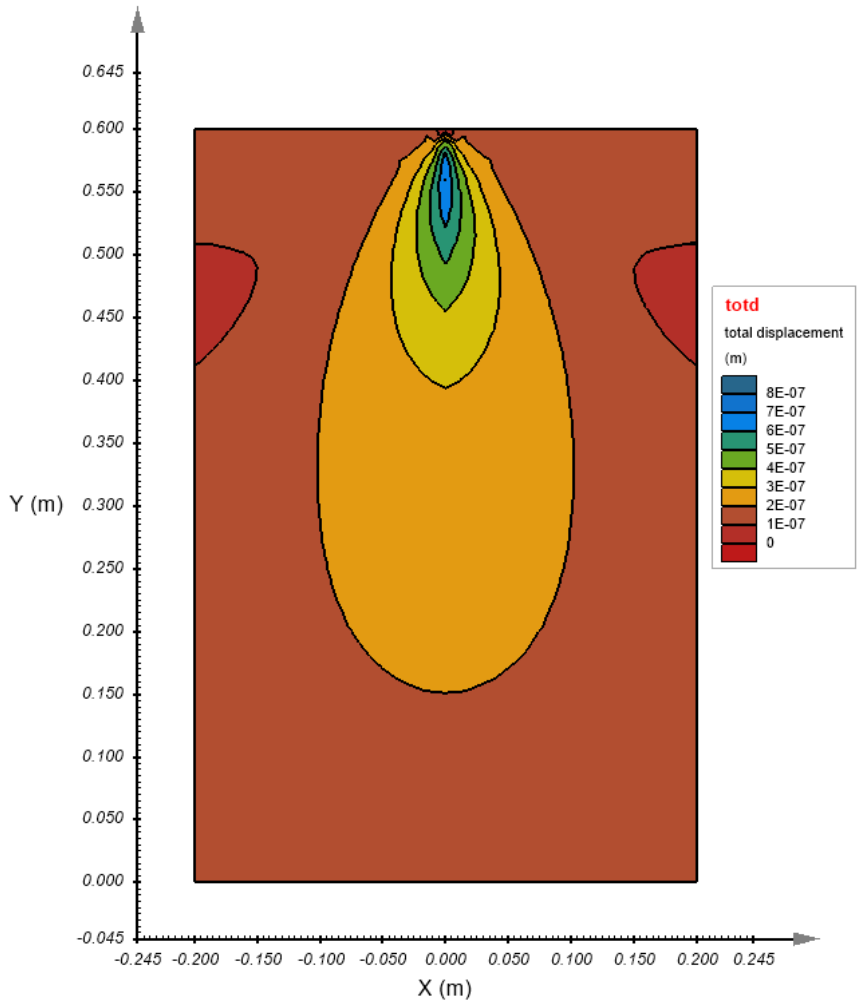

Figure 51. Total displacement contours

3 TWO-DIMENSIONAL SHEAR STRENGTH REDUCTION

This section presents 2D shear strength reduction (SSR) problems that can be solved using SVSOLID.

3.1 Heterogeneous One Layer Slope - SSR

Project: Slopes_SSR
Model: HetrogenousOneLayerSlope_SSR_GT

Main Factors Considered:

- Shear strength reduction factor of safety calculations.
- Limit Equilibrium method (LEM) factor of safety calculations.
- A single soil layer

3.1.1 Model Description

This model consists of a hetrogenous slope comprised a single material. The factor of safety (FoS) from the SSR analysis is compared to the limit equilibrium method (LEM) using the General Limit Equilibrium (GLE) formulation in SVSLOPE.

3.1.2 Geometry and boundary conditions

Figure 52 shows the geometry and boundary conditions in SVSOLID. Displacements are fixed in both *x* and *y* directions at the base. Two vertical boundaries are only fixed in the *x*-direction.

3.1.3 Material Properties

A summary of the material properties is provided in Table 13.

Table 13. Input material properties

Parameter	Value
Young's modulus, E	50,000 kPa
Poisson's ratio, ν	0.4
Cohesion, c	3 kPa
Friction angle, ϕ	19.6
Unit weight, γ	20 kN/m^3

3.1.4 Results

Figure 53 and Figure 54 show the total displacement contours in SVSOLID and the critical slip surface from the SVSLOPE solution, respectively. These figures show that the slip surfaces from both SVSOLID and SVSLOPE are similar. Table 14 shows the FoS results of SVSLOPE and SVSOLID.

Table 14. FoS comparison

SVSLOPE	SVSOLID	Difference (%)
0.99 (GLE*)	1.02	2.9

*GLE = General Limit Equilibrium formulation

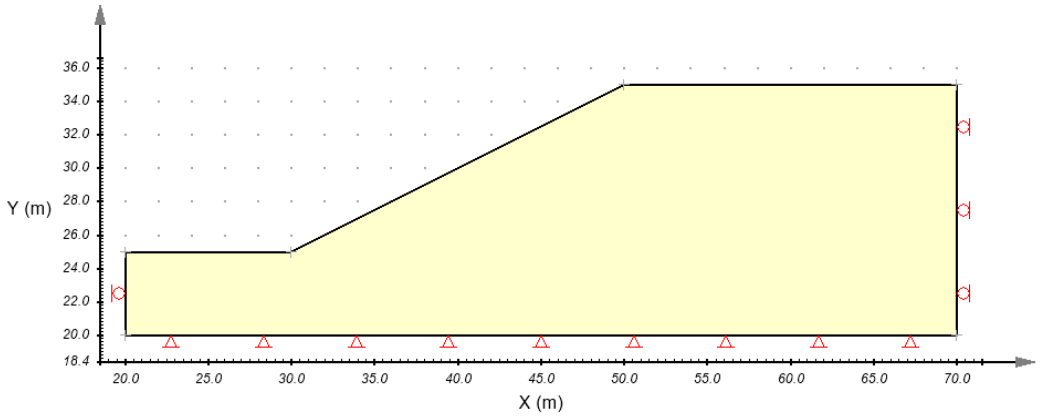

Figure 52. Geometry and boundary conditions

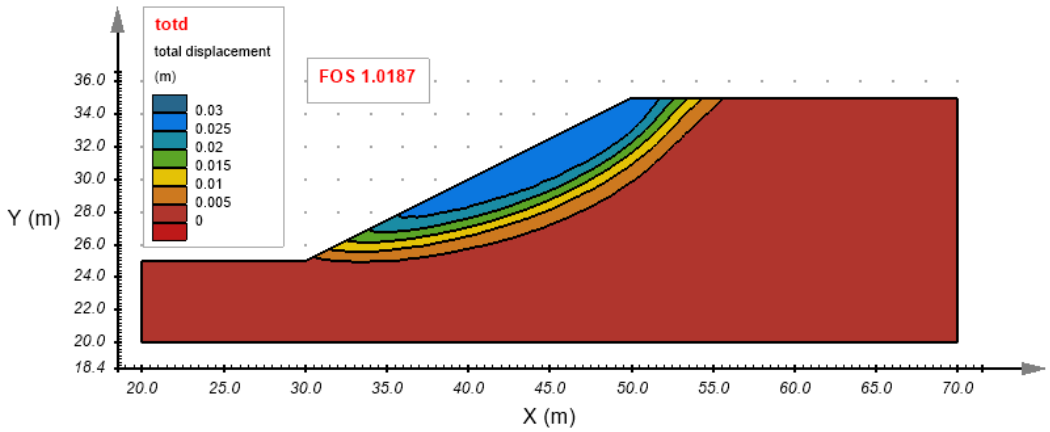

Figure 53. Total displacement contours from SVSOLID with a FoS = 1.02

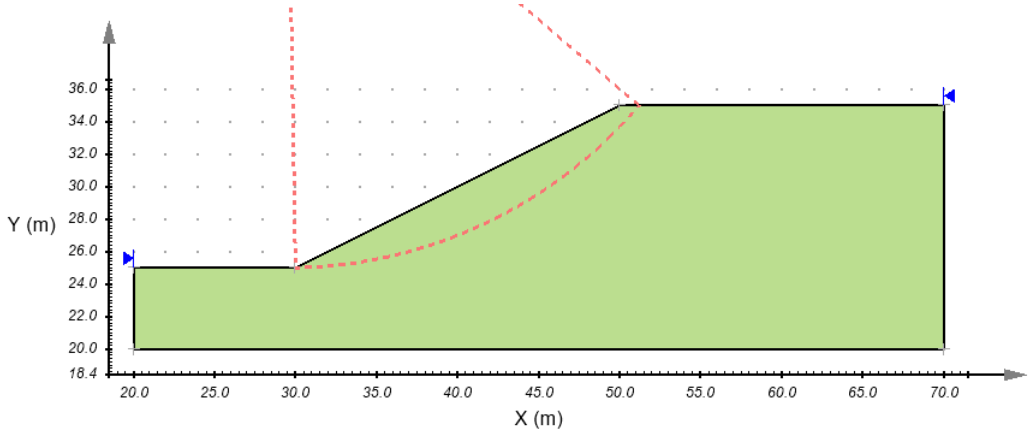

Figure 54. Critical slip surface from SVSLOPE with a FoS = 0.99

3.2 Multi-Layer Slope - SSR

Project: Slopes_SSR
Model: MultiLayerSlope_SSR_GT

Main Factors Considered:

- Shear strength reduction factor of safety calculations.
- Limit Equilibrium method (LEM) factor of safety calculations.
- Multiple layers of soil in the slope

3.2.1 Model Description

This model has multiple layers of soil with differing material properties. The factor of safety (FoS) result from SVSOLID using the SSR solver is compared to the FoS obtained when using the limit equilibrium method (LEM) in SVSLOPE.

3.2.2 Geometry and boundary conditions

Figure 55 shows the geometry and boundary conditions in SVSOLID. Displacements are fixed in both *x* and *y*-directions at the base. Two vertical boundaries are only fixed in the *x*-direction.

3.2.3 Material Properties

A summary of the material properties is provided in Table 15.

Table 15. Input material properties

Parameter	Soil 1	Soil 2	Soil 3
Young's modulus, E (kPa)	50,000	50,000	50,000
Poisson's ratio, ν	0.4	0.4	0.4
Cohesion, c (kPa)	0	5.3	7.2
Friction angle, ϕ	38	23	20
Unit weight, γ (kN/m^3)	19.5	19.5	19.5

3.2.4 Results

Figure 56 and Figure 57 show the total displacement contours in SVSOLID and critical slip surface in SVSLOPE, respectively. These figures show the critical slip surfaces from both the SVSOLID solver and the SVSLOPE solver are similar. Table 16 shows the calculation of FoS results from the SVSOLID and SVSLOPE are also similar.

Table 16. FoS comparison

SVSLOPE	SVSOLID	Difference (%)
1.39 (GLE*)	1.38	0.7

*GLE = General Limit Equilibrium formulation

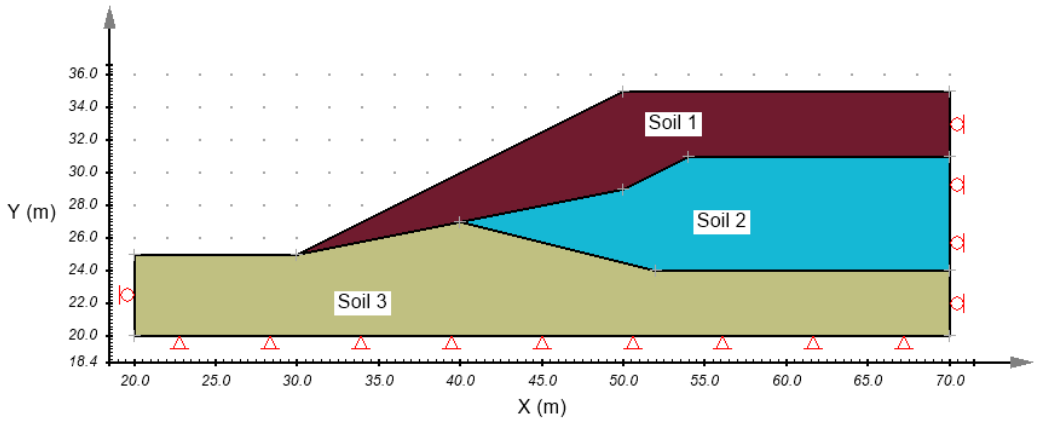

Figure 55. Geometry and boundary conditions

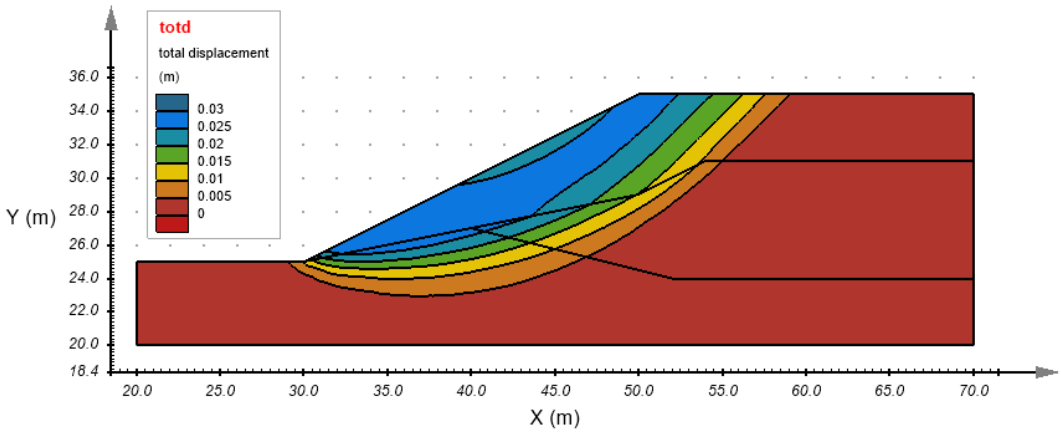

Figure 56. Total displacement contours from the SVSOLID solver giving a FoS = 1.38

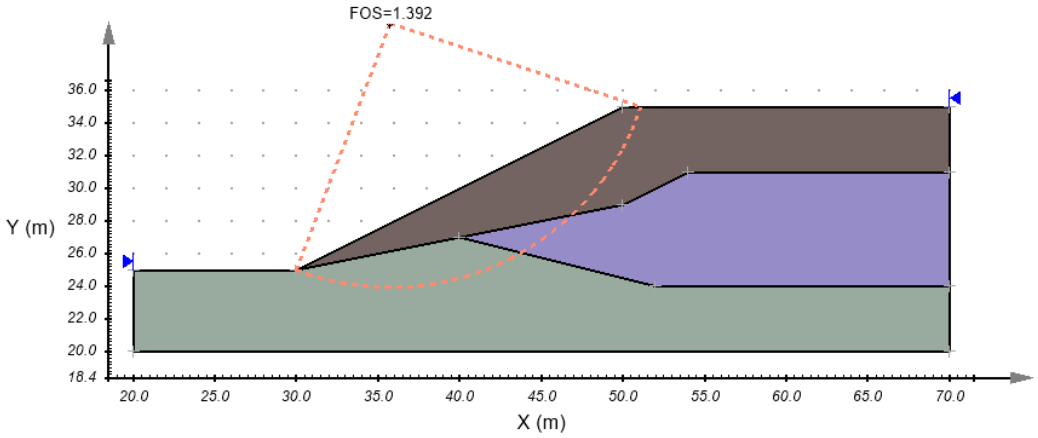

Figure 57. Critical slip surface form the SVSLOPE solver giving a FoS = 1.39

3.3 Multi-Layer Slope with Seismic Load - SSR

Project: Slopes_SSR
Model: MultiLayerSlope_Seismic_SSR_GT

Main Factors Considered:

- Shear strength reduction factor of safety calculations.
- Limit Equilibrium method (LEM) factor of safety calculations.
- Multiple layers of soil in the slope
- Seismic load

3.3.1 Model Description

This model has multiple layers of soil with differing material properties. The factor of safety (FoS) result from SVSOLID using the SSR solver is compared to the FoS obtained when using the limit equilibrium method (LEM) in SVSLOPE with seismic load of 0.15*g*.

3.3.2 Geometry and boundary conditions

Figure 58 shows the geometry and boundary conditions in SVSOLID. Displacements are fixed in both *x* and *y*-directions at the base. Two vertical boundaries are only fixed in the *x*-direction.

3.3.3 Material Properties

A summary of the material properties is provided in Table 17.

Table 17. Input material properties

Parameter	Soil 1	Soil 2	Soil 3
Young's modulus, E (kPa)	50,000	50,000	50,000
Poisson's ratio, ν	0.4	0.4	0.4
Cohesion, c (kPa)	0	5.3	7.2
Friction angle, ϕ	38	23	20
Unit weight, γ (kN/m^3)	19.5	19.5	19.5
Seismic load (g)	Horizontal = 0.15; Vertical = 0.00		

3.3.4 Results

Figure 59 and Figure 61 show the total displacement contours in SVSOLID and critical slip surface in SVSLOPE, respectively. These figures show the critical slip surfaces from both the SVSOLID solver and the SVSLOPE solver are similar. A potential slip surface is clearly shown in Figure 60, which is plotted in term of principal strain difference. Table 18 shows the calculation of FoS results from the SVSOLID and SVSLOPE are also similar.

Table 18. FoS comparison

SVSLOPE	SVSOLID	Difference (%)
1.01 (GLE*)	0.98	3.0

*GLE = General Limit Equilibrium formulation

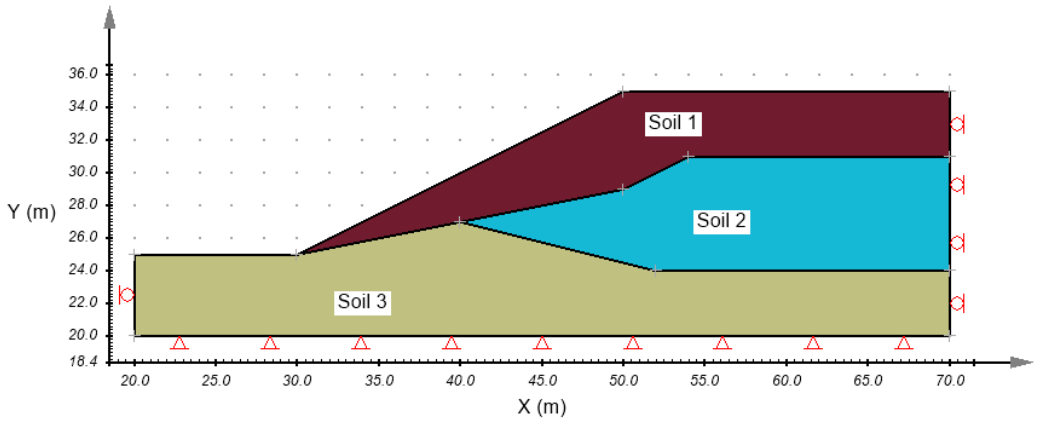

Figure 58. Geometry and boundary conditions

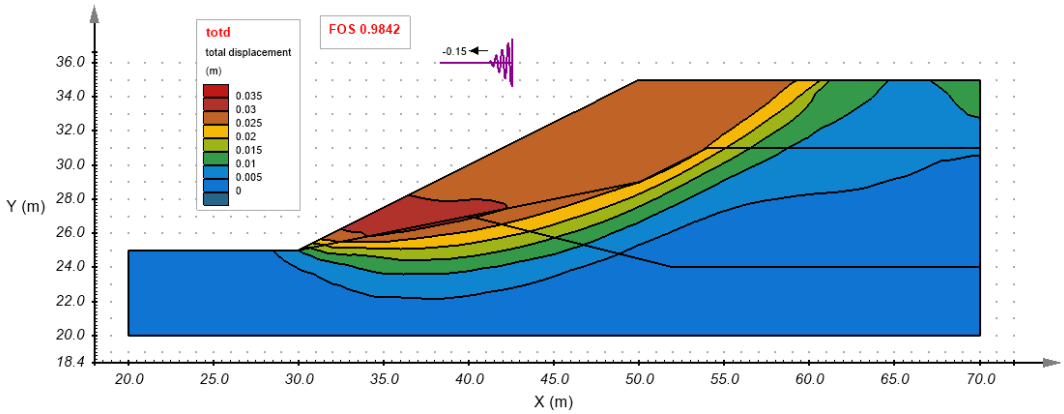

Figure 59. Total displacement contours from SVSOLID

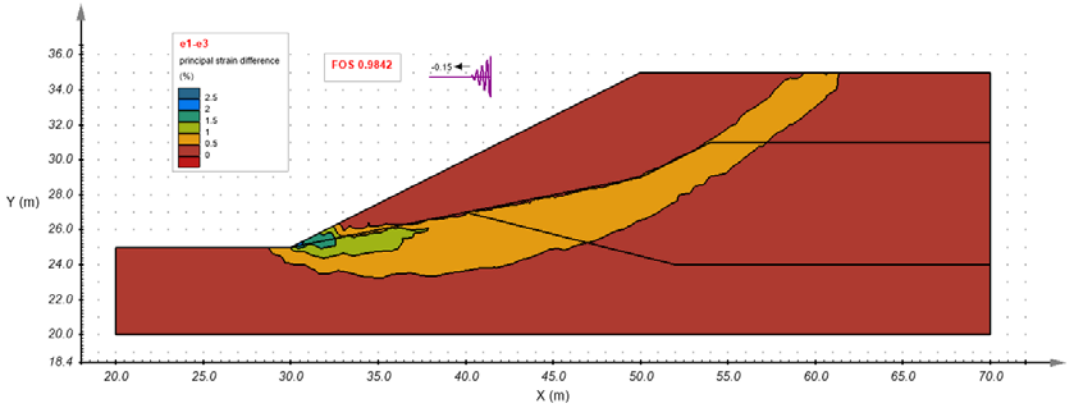

Figure 60. Principle strain difference contours from SVSOLID

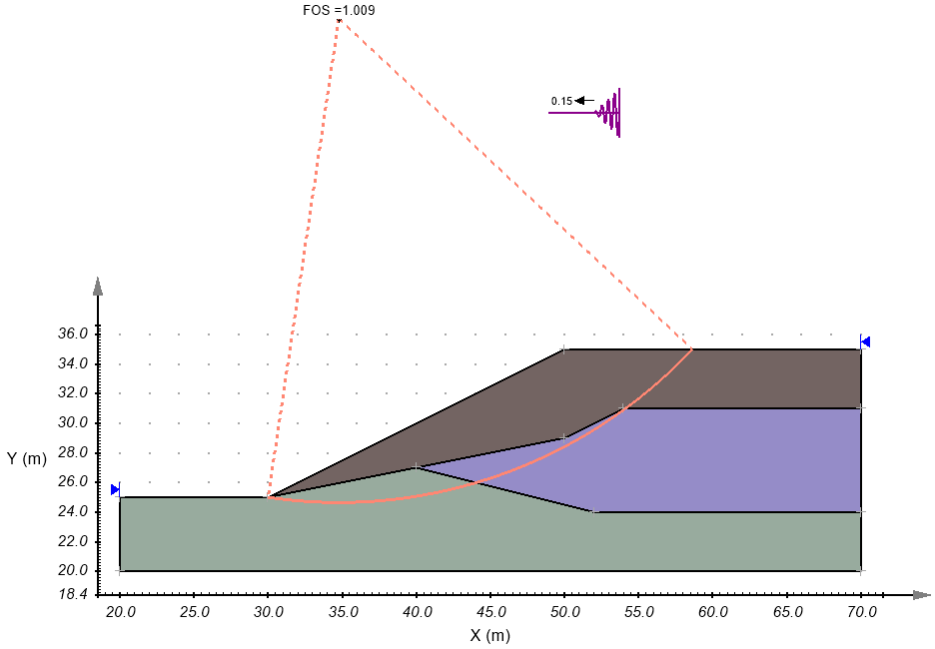

Figure 61. Critical slip surface from SVSLOPE

3.4 Homogenous Slope - SSR

Project: Slopes_SSR
Model: HomogenousSlope_SSR_GT

Main Factors Considered:

- Shear strength reduction factor of safety calculations.
- Limit Equilibrium method (LEM) factor of safety calculations.
- A single soil layer

3.4.1 Model Description

This model is comprised of a homogenous one-layer slope. The factor of safety (FoS) result using the SSR technique is compared against the FoS calculated using the limit equilibrium method (LEM) in SVSLOPE.

3.4.2 Geometry and boundary conditions

Figure 62 shows the geometry and boundary conditions in SVSOLID. Displacements are fixed in both *x* and *y* directions at the base. Two vertical boundaries are only fixed in the *x* direction.

3.4.3 Material Properties

A summary of the material properties for the model is provided in Table 19.

Table 19. Input material properties

Parameter	Soil 1
Young's modulus, E (kPa)	50,000
Poisson's ratio, ν	0.4
Cohesion, c (kPa)	41.65
Friction angle, ϕ	15
Unit weight, γ (kN/m^3)	18.82

3.4.4 Results

Figure 63 and Figure 64 show the total displacement contours from the SVSOLID solver and the critical slip surface location from SVSLOPE, respectively. These figures show that the slip surfaces from SVSOLID and SVSLOPE solvers are similar. Table 20 shows the FoS results from SVSOLID and SVSLOPE.

Table 20. FoS comparison

SVSLOPE	SVSOLID	Difference (%)
1.47 (GLE*)	1.46	0.7

*GLE = General Limit Equilibrium formulation

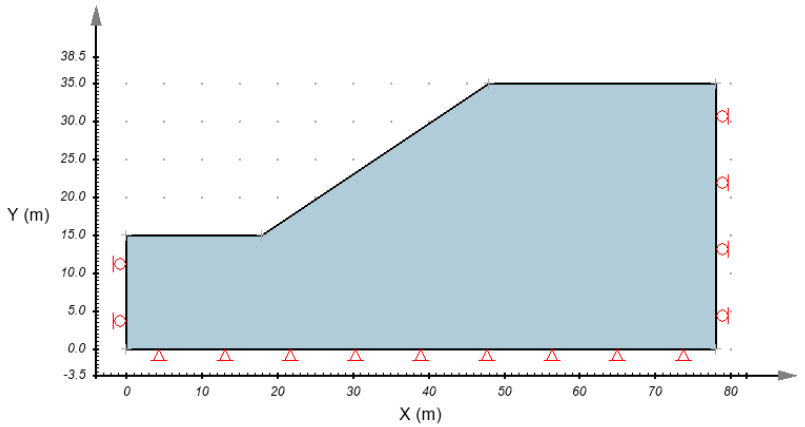

Figure 62. Geometry and boundary conditions

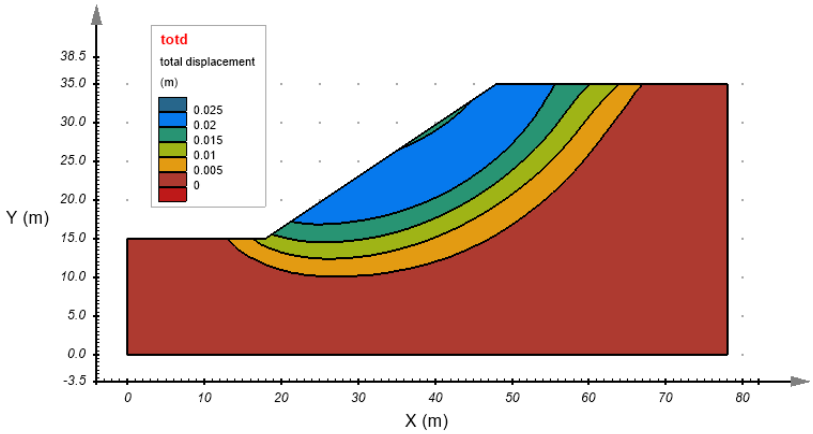

Figure 63. Total displacement contours from the SVSOLID solver giving a FoS = 1.46

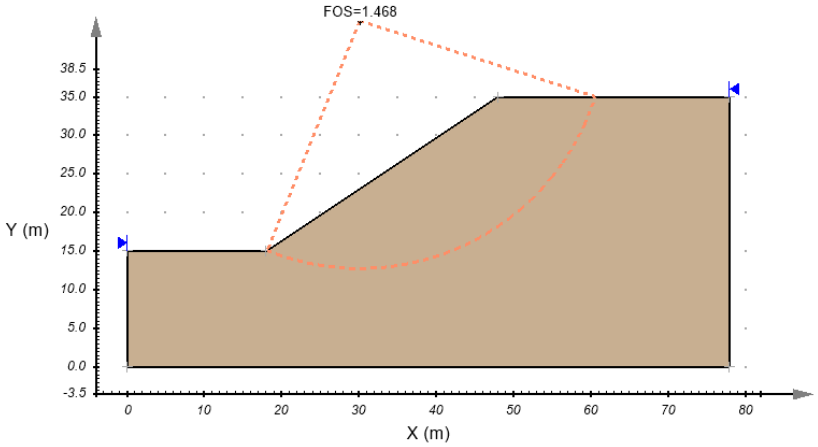

Figure 64. Critical slip surface from the SVSLOPE giving a FoS = 1.47

3.5 Layered Slope - SSR

Project: Slopes_SSR
Model: LayeredSlope_SSR_GT

Main Factors Considered:

- Shear strength reduction factor of safety calculation
- Limit Equilibrium method (LEM) factor of safety calculations.Multiple layers of soil in the slope

3.5.1 Model Description

This model has multiple layers of soil comprising the slope. There is one layer with a low shear strength sandwiched between two layers of higher strength. The factor of safety (FoS) result from the SSR solver is compared to the FoS from the limit equilibrium method (LEM) using SVSLOPE.

3.5.2 Geometry and boundary conditions

Figure 65 shows the geometry and boundary conditions in SVSOLID. Displacements are fixed in both *x* and *y*-directions at the base. Two vertical boundaries are only fixed in the *x*-direction.

3.5.3 Material Properties

A summary of the material properties for the model is provided in Table 21.

Table 21. Input material properties

Parameter	Upper layer	Middle layer	Lower layer
Young's modulus, E (kPa)	50,000	50,000	50,000
Poisson's ratio, ν	0.4	0.4	0.4
Cohesion, c (kPa)	29.4	9.8	5.0
Friction angle, ϕ	12	5	40
Unit weight, γ (kN/m^3)	18.82	18.82	18.82

3.5.4 Results

Figure 66 and Figure 67 show the total displacement contours from the SVSOLID solver and the critical slip surface from the SVSLOPE solver, respectively. These figures show the slip surfaces from both SVSOLID solver and SVSLOPE solver are similar. Table 22 shows the FoS results from the SVSOLID and SVSLOPE solvers.

Table 22. FoS comparison

SVSLOPE	SVSOLID	Difference (%)
0.43 (GLE*)	0.42	2.3

*GLE = General Limit Equilibrium formulation

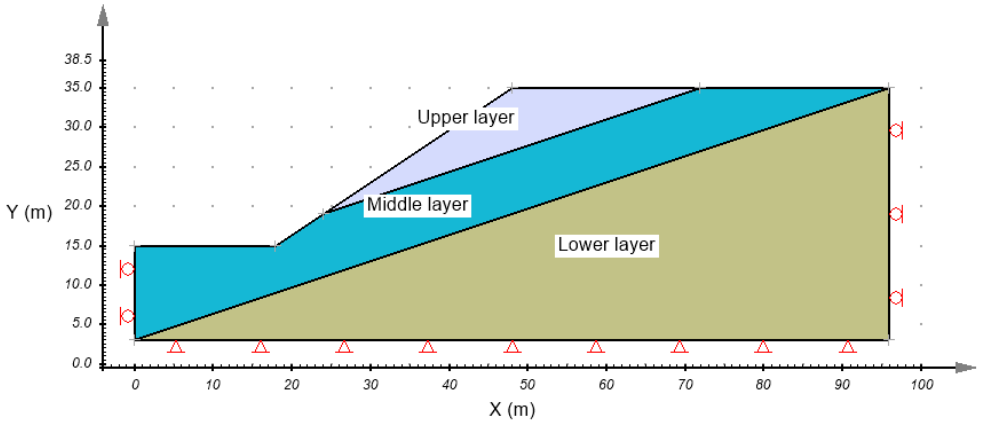

Figure 65. Geometry and boundary conditions

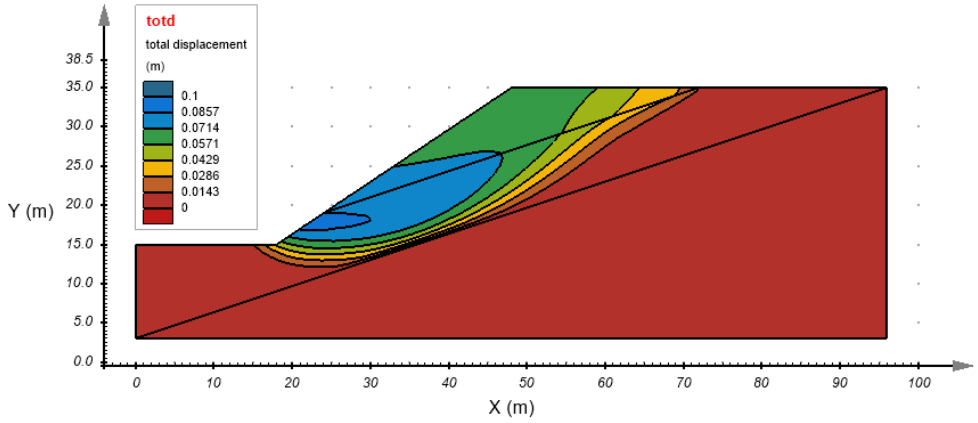

Figure 66. Total displacement contours from the SVSOLID solver giving a FoS = 0.42

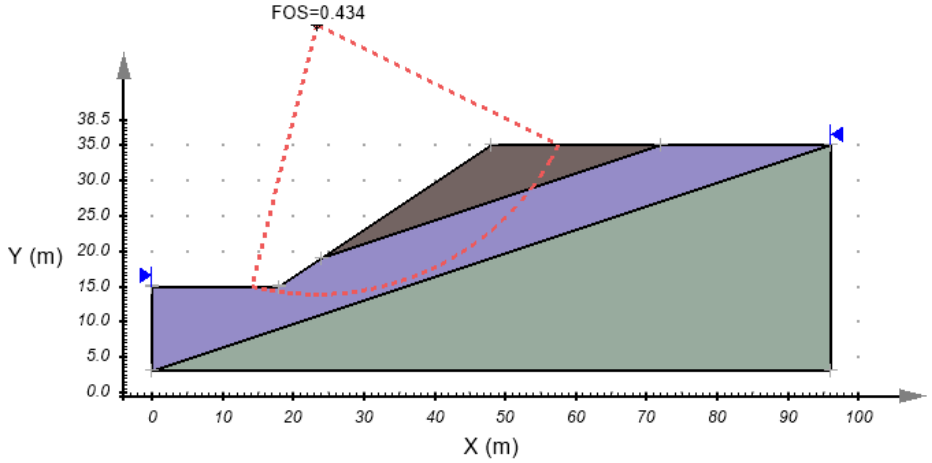

Figure 67. Critical slip surface from the SVSLOPE giving a FoS = 0.43

3.6 Homogenous Slope with Water Table - SSR

Project: Slopes_SSR
Model: HomSlopewWaterTable_SSR_GT

Main Factors Considered:

- Shear strength reduction factor of safety calculations
- Limit Equilibrium method (LEM) factor of safety calculations.
- Input of pore-water pressures

3.6.1 Model Description

This model consists of a homogenous slope comprised of one soil layer. There is a water table within the soil layer. The factor of safety (FoS) result from the SSR solution is compared to the FoS calculated using the limit equilibrium method (LEM) within the SVSLOPE solver.

3.6.2 Geometry and boundary conditions

Figure 68 shows the geometry and boundary conditions used in SVSOLID. Displacements are fixed in both *x* and *y*-directions at the base. Two vertical boundaries are only fixed in the *x*-direction.

3.6.3 Material Properties

A summary of the material properties for the model is provided in Table 23.

Table 23. Input material properties

Parameter	Soil 1
Young's modulus, E (kPa)	50,000
Poisson's ratio, ν	0.4
Cohesion, c (kPa)	41.65
Friction angle, ϕ	15
Unit weight, γ (kN/m^3)	18.82

3.6.4 Results

Figure 69 and Figure 70 show the total displacement contours from the SVSOLID solver and the critical slip surface from the SVSLOPE solver, respectively. These figures show the slip surfaces from the SVSOLID solver are similar to those obtained from the SVSLOPE solution. Table 24 shows the FoS results of SVSOLID and SVSLOPE.

Table 24. FoS comparison

SVSLOPE	SVSOLID	Difference (%)
1.14 (GLE*)	1.12	1.8

*GLE = General Limit Equilibrium formulation

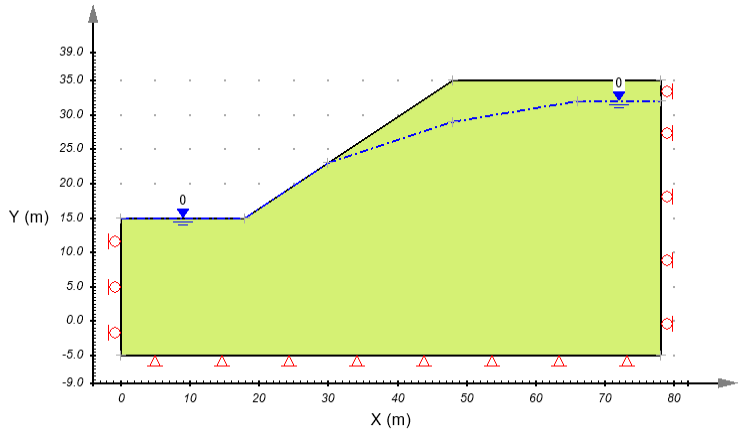

Figure 68. Geometry and boundary conditions

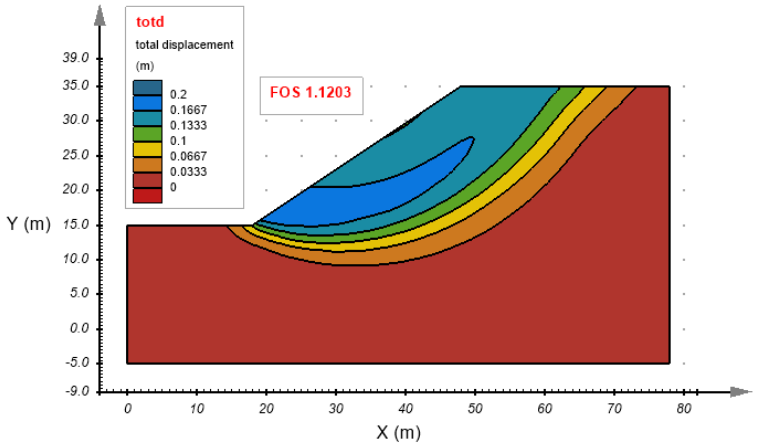

Figure 69. Total displacement contours from the SVSOLID giving a FoS = 1.12

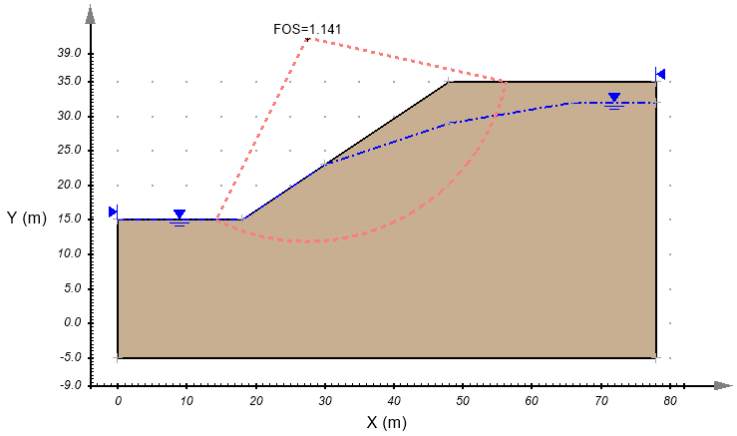

Figure 70. Critical slip surface from the SVSLOPE giving a FoS = 1.14

3.7 Simple Homogenous Slope - SSR

Project: Slopes_SSR
Model: SimpleHomSlope_SSR_GT

Main Factors Considered:

- Shear strength reduction factor of safety calculations
- Limit Equilibrium method (LEM) factor of safety calculations.
- One homogeneous soil layer

3.7.1 Model Description

This model consists of a single homogenous layer of soil in the slope. The factor of safety (FoS) result from the SSR method is compared to the FoS obtained when using the limit equilibrium method (LEM) with the SVSLOPE solver.

3.7.2 Geometry and boundary conditions

Figure 71 shows the geometry and boundary conditions used in SVSOLID. Displacements are fixed in both *x* and *y*-directions at the base. Two vertical boundaries are only fixed in the *x*-direction.

3.7.3 Material Properties

A summary of the material properties for the model is provided in Table 25.

Table 25. Input material properties

Parameter	Soil 1
Young's modulus, E (kPa)	50,000
Poisson's ratio, ν	0.4
Cohesion, c (kPa)	41.65
Friction angle, ϕ	15
Unit weight, γ (kN/m^3)	18.82

3.7.4 Results

Figure 72 and Figure 73 show the total displacement contours from the SVSOLID solver and the critical slip surface location from the SVSLOPE solver, respectively. These figures show the slip surfaces from both SVSOLID solver and SVSLOPE solver are similar. Table 26 shows the FoS results from the SVSOLID and SVSLOPE solutions.

Table 26. FoS comparison

SVSLOPE	SVSOLID	Difference (%)
1.35 (GLE*)	1.36	0.7

*GLE = General Limit Equilibrium

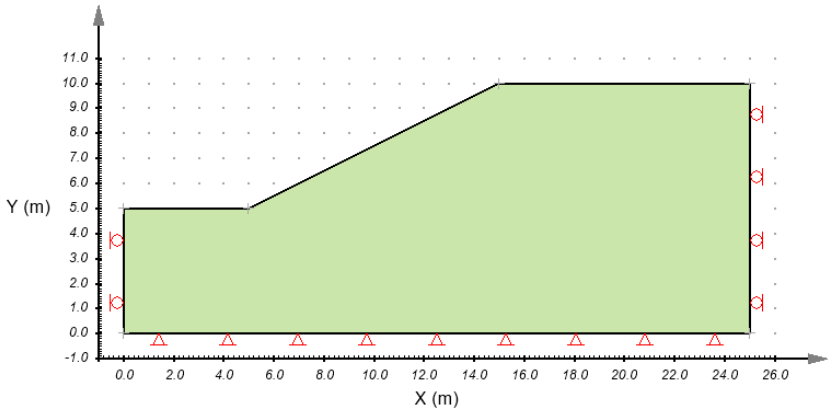

Figure 71. Geometry and boundary conditions

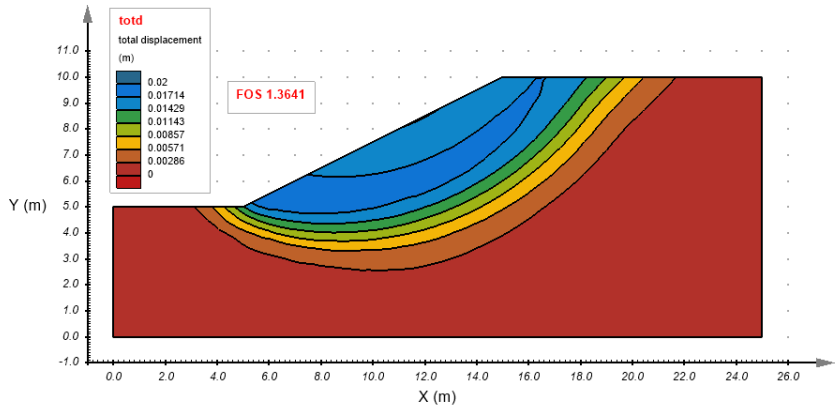

Figure 72. Total displacement contours in SVSOLID with FoS = 1.36

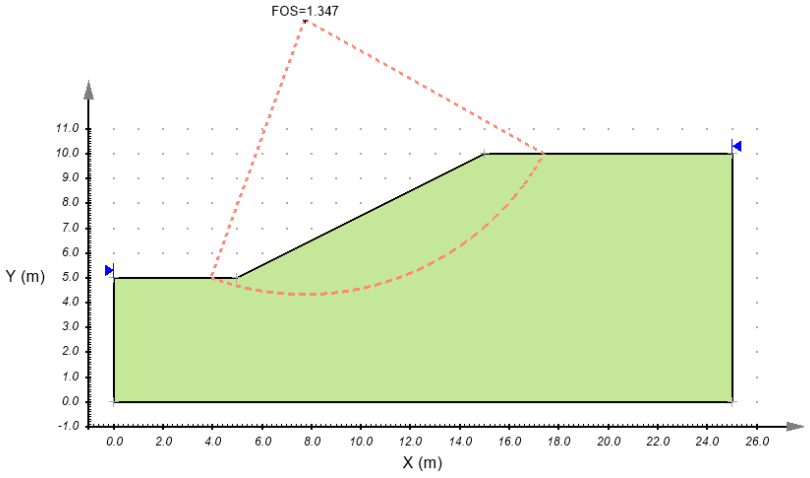

Figure 73. Critical slip surface in SVSLOPE with FoS = 1.35

3.8 Layered Embankment Slope - SSR

Project: Slopes_SSR
Model: LayeredEmbankmentSlope_SSR_GT

Main Factors Considered:

- Shear strength reduction factor of safety calculations
- Limit Equilibrium method (LEM) factor of safety calculations.
- Multiple soil layers comprising a slope embankment

3.8.1 Model Description

This model has multiple layers of soil comprising the slope. There is one layer with a low shear strength sandwiched between two layers of higher strength. The factor of safety (FoS) result from the SSR solver is compared to the FoS from the limit equilibrium method (LEM) using SVSLOPE.

3.8.2 Geometry and boundary conditions

Figure 74 shows the geometry and boundary conditions in SVSOLID. Displacements are fixed in both *x* and *y* directions at the base. Two vertical boundaries are only fixed in the *x* direction.

3.8.3 Material Properties

A summary of the material properties for the model is provided in Table 27.

Table 27. Input material properties

Parameter	Upper layer	Layer 2	Layer 3	Bottom layer
Young's modulus, E (kPa)	50,000	50,000	50,000	50,000
Poisson's ratio, ν	0.4	0.4	0.4	0.4
Cohesion, c (kPa)	49	0	7.84	0
Friction angle, ϕ	29	30	20	30
Unit weight, γ (kN/m^3)	20.38	17.64	20.38	17.64

3.8.4 Results

Figure 75 and Figure 76 show the total displacement contours from the SVSOLID solver and the critical slip surface from the SVSLOPE solver, respectively. These figures show the slip surfaces from both SVSOLID solver and SVSLOPE solver are similar. Table 28 shows the FoS results of SVSOLID and SVSLOPE solvers.

Table 28. FoS comparison

SVSLOPE	SVSOLID	Difference (%)
1.48 (GLE*)	1.38	6.7

*GLE = General Limit Equilibrium

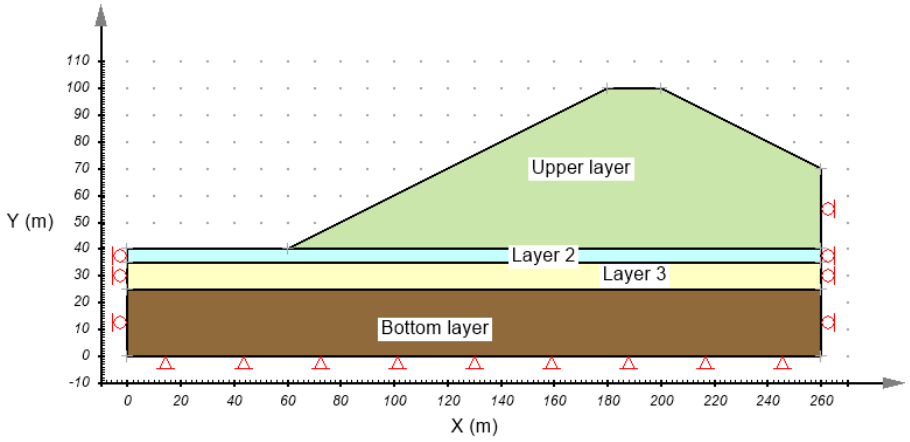

Figure 74. Geometry and boundary conditions

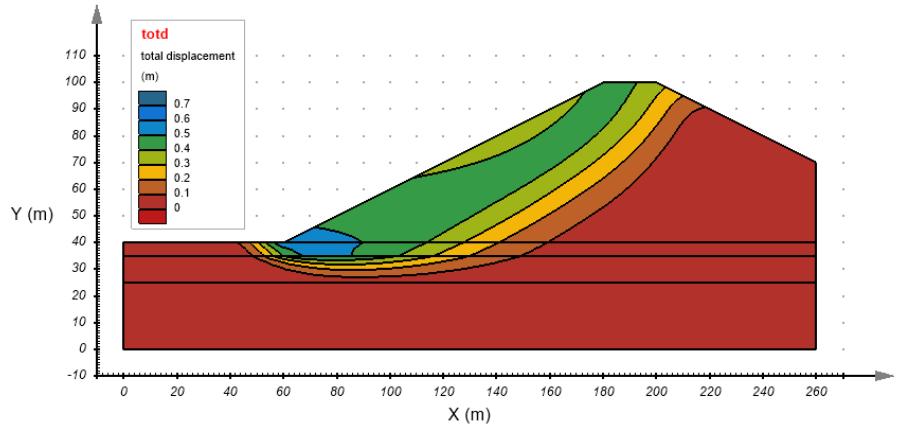

Figure 75. Total displacement contours from the SVSOLID giving a FoS = 1.38

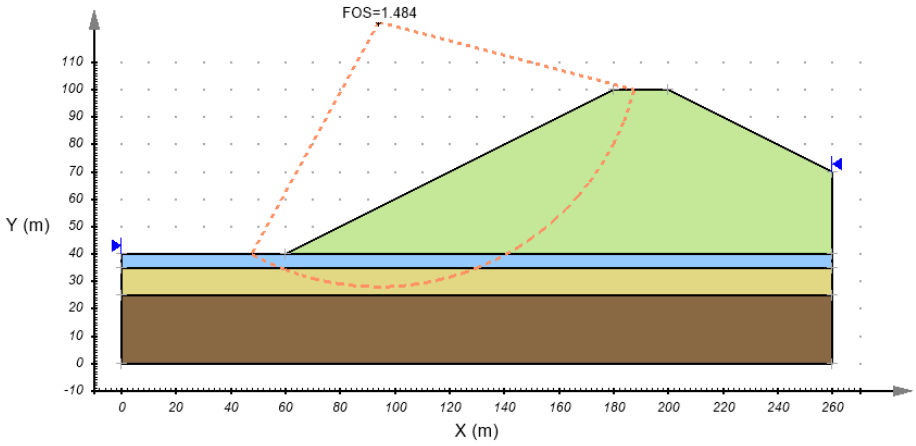

Figure 76. Critical slip surface from the SVSLOPE giving a FoS = 1.48

3.9 Simple Slope with Water Table - SSR

Project: Slopes_SSR
Model: SimpleSlopewWaterTable_SSR_GT

Main Factors Considered:

- Shear strength reduction factor of safety calculations
- Limit Equilibrium method (LEM) factor of safety calculations.Pore-water pressures defined using a water table

3.9.1 Model Description

This model consists of a homogenous slope with one soil layer. There is a water table within the soil layer. The factor of safety (FoS) result from the SSR solution is compared to the FoS calculated using the limit equilibrium method (LEM) within the SVSLOPE solver.

3.9.2 Geometry and boundary conditions

Figure 77 shows the geometry and boundary conditions used in SVSOLID. Displacements are fixed in both *x* and *y*-directions at the base. Two vertical boundaries are only fixed in the *x*-direction.

3.9.3 Material Properties

A summary of the material properties for the model is provided in Table 29.

Table 29. Input material properties

Parameter	Soil 1
Young's modulus, E (psf)	1,000,000
Poisson's ratio, ν	0.4
Cohesion, c (psf)	600
Friction angle, ϕ	20
Unit weight, γ (lbf/ft^3)	120

3.9.4 Results

Figure 78 and Figure 79 show the total displacement contours from the SVSOLID solver and the critical slip surface from the SVSLOPE solver, respectively. These figures show the slip surfaces from the SVSOLID solver is similar to that obtained from the SVSLOPE solution. Table 30 shows the FoS results of SVSOLID and SVSLOPE solvers.

Table 30. FoS comparison

SVSLOPE	SVSOLID	Difference (%)
1.78 (GLE*)	1.78	0.0

*GLE = General Limit Equilibrium formulation

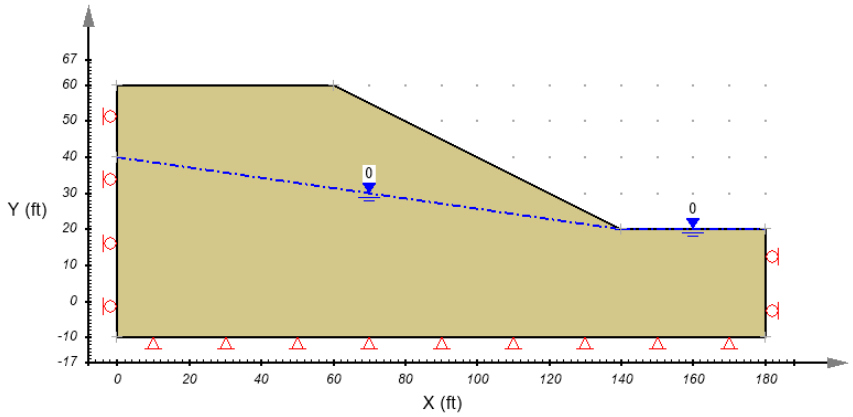

Figure 77. Geometry and boundary conditions

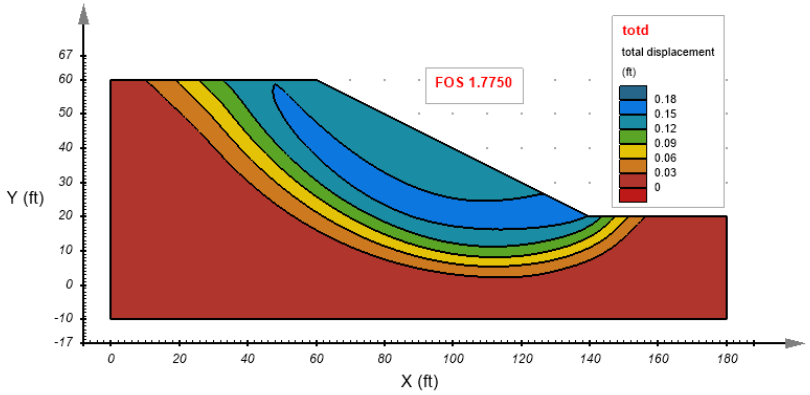

Figure 78. Total displacement contours from the SVSOLID giving a FoS = 1.78

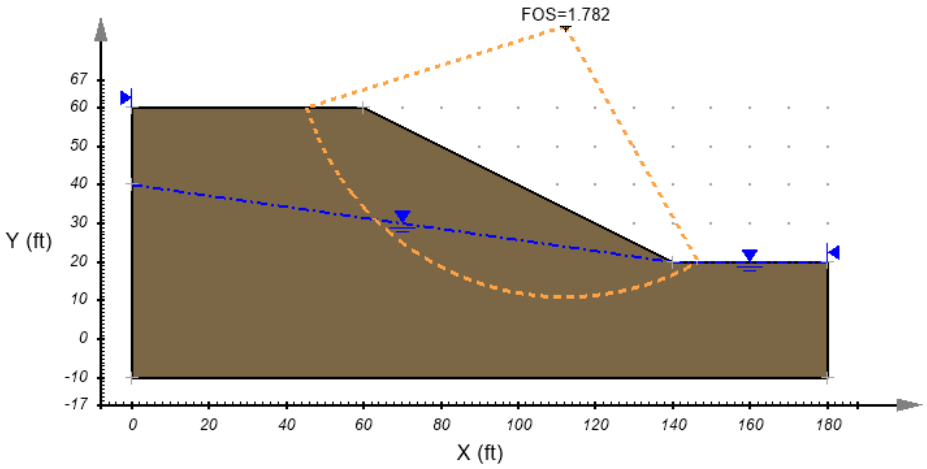

Figure 79. Critical slip surface from the SVSLOPE giving a FoS = 1.78

3.10 Layered Embankment Slope with Weak Layer - SSR

Project: Slopes_SSR
Model: LayeredEmbankmentSlopewWeakLayer_SSR_GT

Main Factors Considered:

- Shear strength reduction factor of safety calculations
- Limit Equilibrium method (LEM) factor of safety calculations.
- Multiple soil layers comprising a slope embankment

3.10.1 Model Description

This model has multiple layers of soil comprising the slope. There is one layer with a low shear strength sandwiched between two layers of higher strength. The factor of safety (FoS) result from the SSR solver is compared to the FoS from the limit equilibrium method (LEM) using SVSLOPE.

3.10.2 Geometry and boundary conditions

Figure 80 shows the geometry and boundary conditions in SVSOLID. Displacements are fixed in both *x* and *y*-directions at the base. Two vertical boundaries are only fixed in the *x*-direction.

3.10.3 Material Properties

A summary of the material properties for the model is provided in Table 31. Bedrock is simulated using linear elastic material.

Table 31. Input material properties

Parameter	Upper soil	Weak layer	Bedrock
Young's modulus, E (psf)	50,000	50,000	70,000,000,000
Poisson's ratio, ν	0.4	0.4	0.4
Cohesion, c (psf)	600	0	---
Friction angle, ϕ	20	10	---
Unit weight, γ (lbf/ft^3)	120	120	127

3.10.4 Results

Figure 81 and Figure 82 show the total displacement contours from the SVSOLID solver and the critical slip surface from the SVSLOPE solver, respectively. These figures show the slip surfaces from both SVSOLID solver and SVSLOPE solver are similar. Table 32 shows the FoS results between SVSOLID and SVSLOPE solvers.

Table 32. FoS comparison

SVSLOPE	SVSOLID	Difference (%)
1.34 (GLE*)	1.32	1.5

*GLE = General Limit Equilibrium

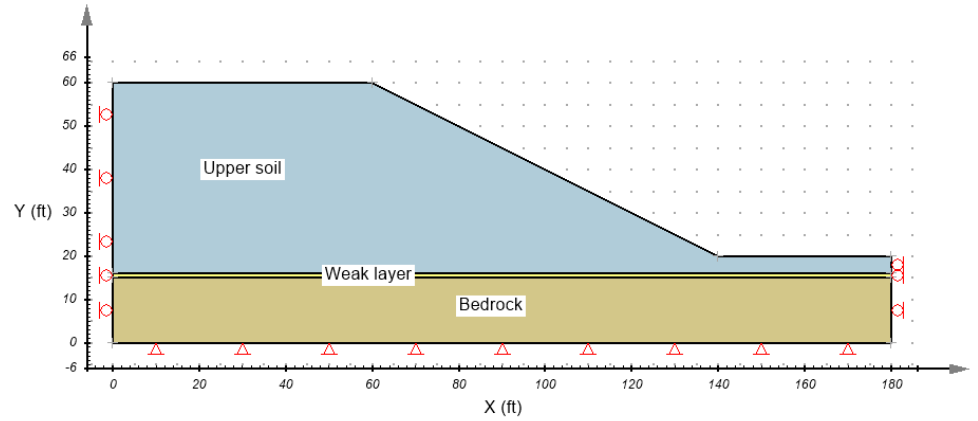

Figure 80. Geometry and boundary conditions

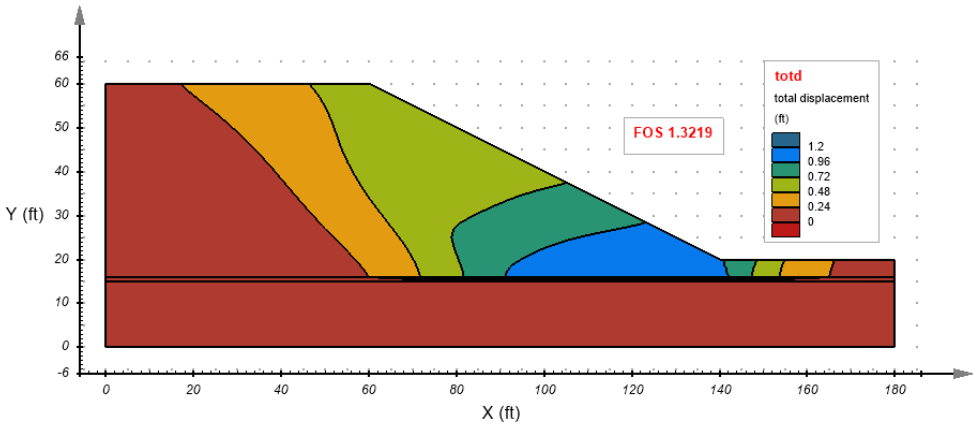

Figure 81. Total displacement contours from the SVSOLID giving a FoS = 1.32

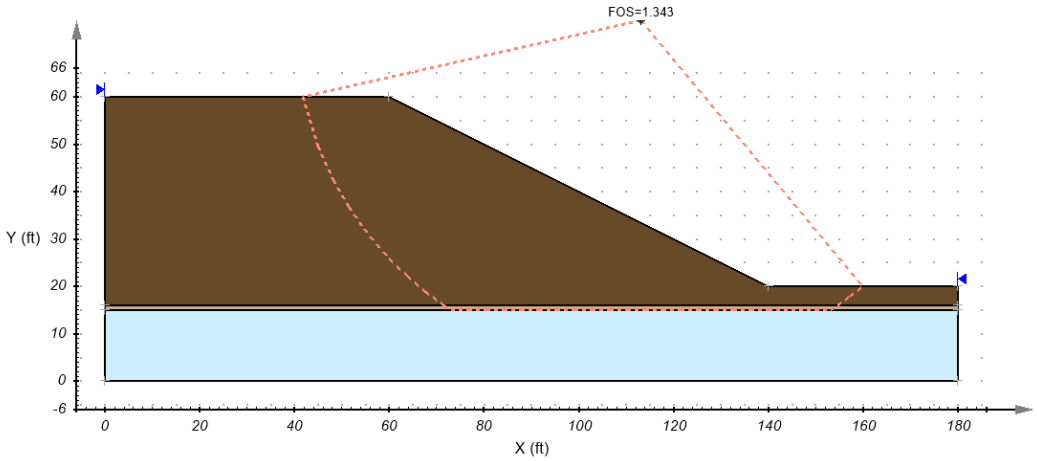

Figure 82. Critical slip surface from the SVSLOPE giving a FoS = 1.34

3.11 Multi-Layer Undrained Clay Slope - SSR

Project: Slopes_SSR
Model: MultiLayerUndrainedClaySlope_SSR_GT

Main Factors Considered:

- Shear strength reduction factor of safety calculations
- Limit Equilibrium method (LEM) factor of safety calculations.
- Undrained shear strength for clays
- Multiple soil layers comprising a slope embankment

3.11.1 Model Description

This model is a multi-layer slope of clays that fail in an undrained mode. The factor of safety (FoS) result from the SSR solver is compared to the FoS from the limit equilibrium method (LEM) using SVSLOPE.

3.11.2 Geometry and boundary conditions

Figure 83 shows the geometry and boundary conditions in SVSOLID. Displacements are fixed in both *x* and *y*-directions at the base. The two vertical boundaries are only fixed in the *x*-direction.

3.11.3 Material Properties

A summary of the material properties for the model is provided in Table 33.

Table 33. Input material properties

Parameter	Upper layer	Middle layer	Bottom layer
Young's modulus, E (kPa)	50,000	50,000	50,000
Poisson's ratio, ν	0.4	0.4	0.4
Cohesion, c_u (kPa)	30	20	150
Unit weight, γ (kN/m^3)	18	18	18

3.11.4 Results

Figure 84 and Figure 85 show the total displacement contours from the SVSOLID solver and the critical slip surface from the SVSLOPE solver, respectively. These figures show the slip surfaces from both SVSOLID solver and SVSLOPE solver are similar. Table 34 shows the FoS results of SVSOLID and SVSLOPE solvers.

Table 34. FoS comparison

SVSLOPE	SVSOLID	Difference (%)
1.48 (GLE*)	1.44	2.7

*GLE = General Limit Equilibrium formulation

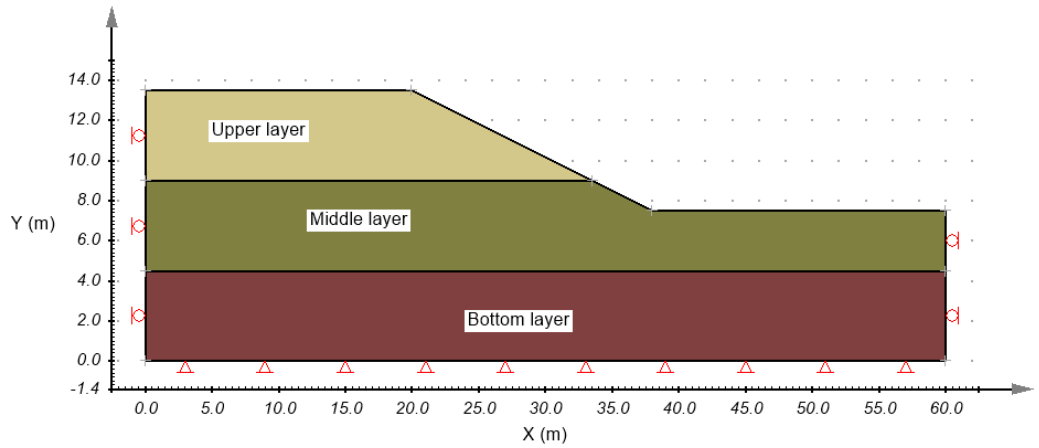

Figure 83. Geometry and boundary conditions

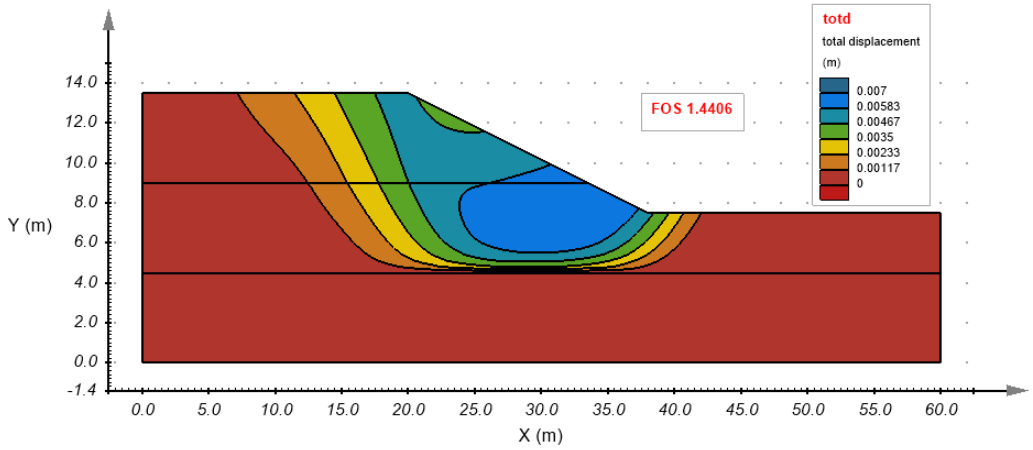

Figure 84. Total displacement contours from the SVSOLID giving a FoS = 1.44

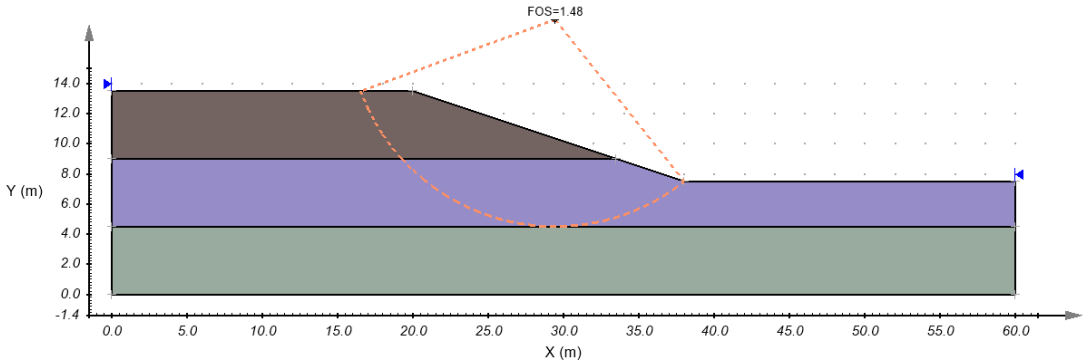

Figure 85. Critical slip surface from the SVSLOPE giving a FoS = 1.48

3.12 Bearing Capacity of Strip Footing - SSR

Project: Slopes_SSR
Model: BearingCapacityStripFooting_SSR_GT

Main Factors Considered:

- Shear strength reduction factor of safety calculations
- Limit Equilibrium method (LEM) factor of safety calculations.
- Undrained shear strength for clay
- Prandtl's failure mechanism

3.12.1 Model Description

This model calculates the bearing capacity according to the Prandt solution for undrained loading of a clay. The factor of safety (FoS) result from the SSR solution is compared to the FoS calculated using the limit equilibrium method (LEM) within the SVSLOPE solver.

3.12.2 Geometry and boundary conditions

Figure 86 shows the geometry and boundary conditions used in SVSOLID. Displacements are fixed in both *x* and *y*-directions at the base. The two vertical boundaries are only fixed in the *x*-direction. The applied distributed load is the ultimate bearing capacity of strip footing = 5.14 c_u = 102.83 kPa.

3.12.3 Material Properties

A summary of the material properties for the model is provided in Table 35.

Table 35. Input material properties

Parameter	Undrained clay
Young's modulus, E (kPa)	50,000
Poisson's ratio, ν	0.4
Cohesion, c (kPa)	20
Friction angle, ϕ	0
Unit weight, γ (kN/m^3)	---

3.12.4 Results

Figure 87 and Figure 88 show the total displacement contours from the SVSOLID solver and the critical slip surface from the SVSLOPE solver, respectively. These figures show the slip surfaces from the SVSOLID solver is similar to that obtained from the SVSLOPE solution. Table 36 shows the FoS results between SVSOLID and SVSLOPE solvers.

Table 36. FoS comparison

SVSLOPE	SVSOLID	Difference (%)
1.08 (GLE*)	1.03	4.6

*GLE = General Limit Equilibrium

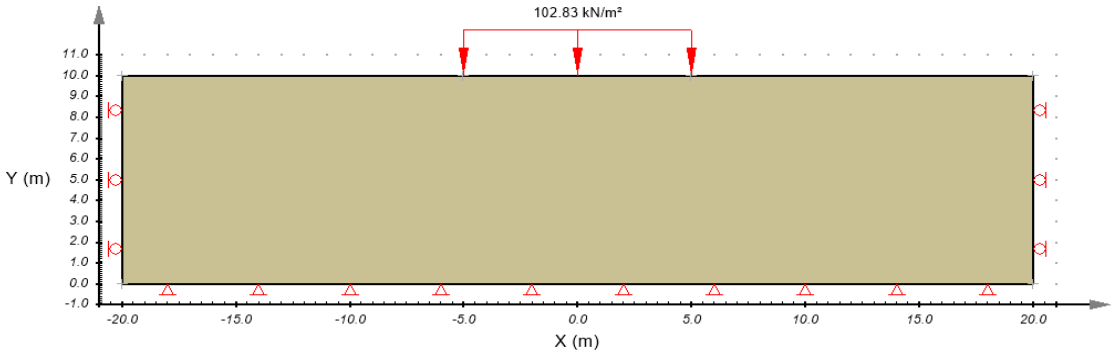

Figure 86. Geometry and boundary conditions

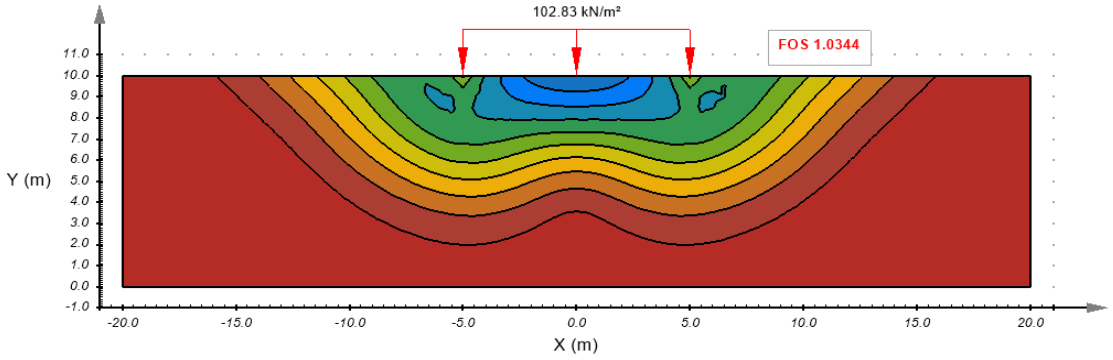

Figure 87. Total displacement contours from the SVSOLID giving a FoS = 1.03

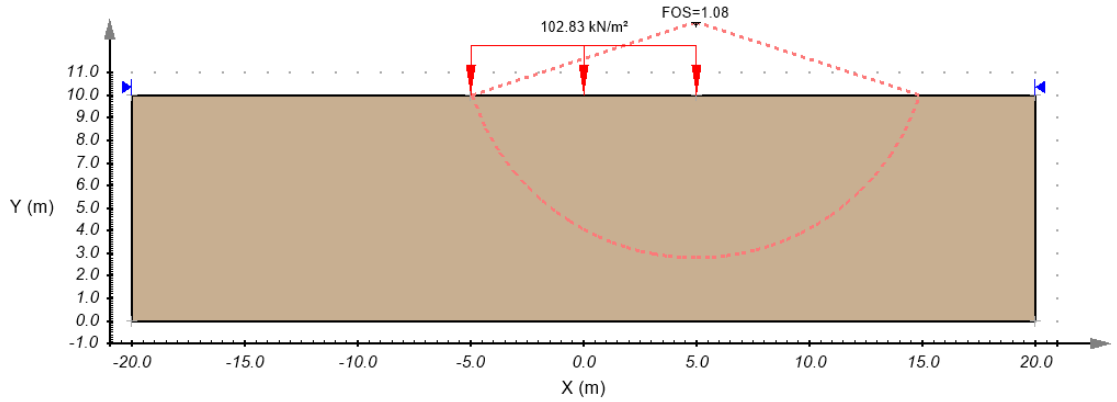

Figure 88. Critical slip surface from the SVSLOPE giving a FoS = 1.08

3.13 Complex Geometry Slope with Applied Load and Water Table - SSR

Project: Slopes_SSR
Model: ComplexSlopewAppliedLoadwWaterTable_SSR_GT

Main Factors Considered:

- Shear strength reduction factor of safety calculations
- Limit Equilibrium method (LEM) factor of safety calculations.
- Applied load and water table

3.13.1 Model Description

This model consists of a homogenous slope with one soil layer along with a complex geometry. There is a water table within the soil layer. The factor of safety (FoS) result from the SSR solution is compared to the FoS calculated using the limit equilibrium method (LEM) within the SVSLOPE solver.

3.13.2 Geometry and boundary conditions

Figure 89 shows the geometry and boundary conditions used in SVSOLID. Displacements are fixed in both *x* and *y*-directions at the base. The two vertical boundaries are only fixed in the *x*-direction.

3.13.3 Material Properties

A summary of the material properties for the model is provided in Table 37.

Table 37. Input material properties

Parameter	Soil
Young's modulus, E (psf)	1,000,000
Poisson's ratio, ν	0.4
Cohesion, c (psf)	500
Friction angle, ϕ	14
Unit weight, γ (lb/ft^3)	124.2

3.13.4 Results

Figure 90 and Figure 91 show the total displacement contours from the SVSOLID solver and the critical slip surface from the SVSLOPE solver, respectively. These figures show the slip surfaces from the SVSOLID solver is similar to that obtained from the SVSLOPE solution. Table 38 shows the FoS results of SVSOLID and SVSLOPE solvers.

Table 38. FoS comparison

SVSLOPE	SVSOLID	Difference (%)
1.50 (GLE*)	1.56	3.8

*GLE = General Limit Equilibrium

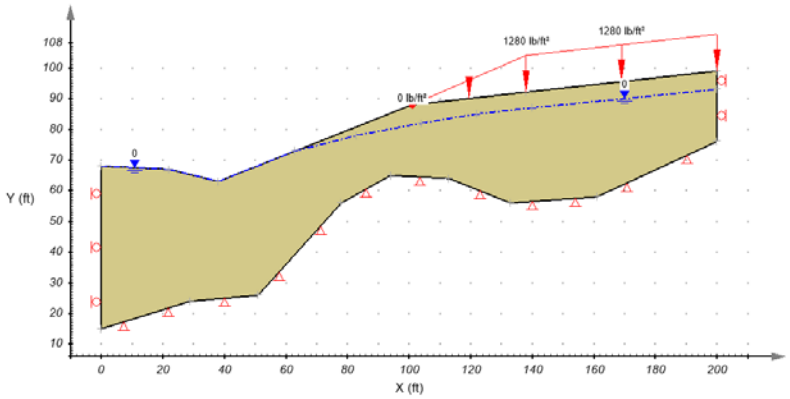

Figure 89. Geometry and boundary conditions

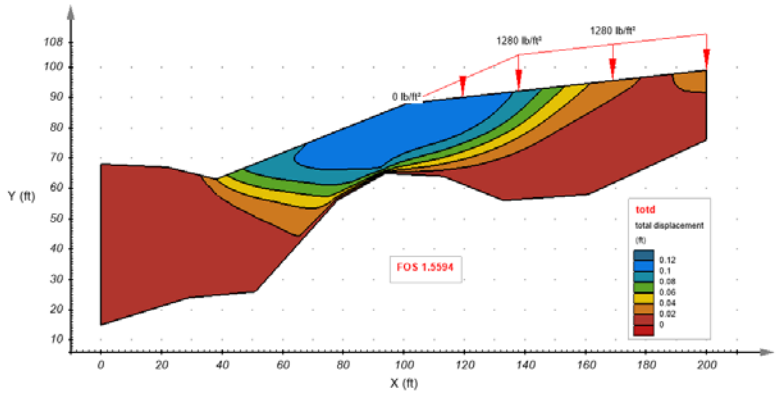

Figure 90. Total displacement contours from the SVSOLID giving a FoS = 1.56

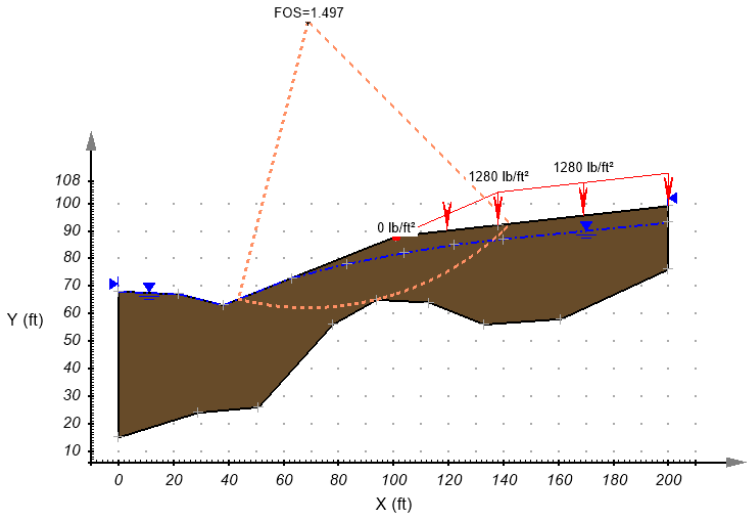

Figure 91. Critical slip surface from the SVSLOPE giving a FoS = 1.50

3.14 Tailings Dyke Slope - SSR

Project: Slopes_SSR
Model: TailingsDykeSlope_SSR_GT

Main Factors Considered:

- Shear strength reduction factor of safety calculation
- Limit Equilibrium method (LEM) factor of safety calculations.
- Complex geometry and multiple layers of soil

3.14.1 Model Description

The geometry of this model is complex with multiple layers of soil and a bedrock layer at the base. The factor of safety (FoS) result from the SSR solution is compared to the FoS calculated using the limit equilibrium method (LEM) within the SVSLOPE solver.

3.14.2 Geometry and boundary conditions

Figure 92 shows the geometry and boundary conditions used in SVSOLID. Displacements are fixed in both *x* and *y* directions at the base. The two vertical boundaries are only fixed in the *x* direction.

3.14.3 Material Properties

A summary of the material properties for the model is provided in Table 39.

Table 39. Input material properties

Parameter	Tailings sand	Glacio-fluvial sand	Sandy till	Distributed clay shale	Clayey till	Bedrock
Young's modulus, E (kPa)	50,000	50,000	50,000	50,000	50,000	50,000
Poisson's ratio, ν	0.4	0.4	0.4	0.4	0.4	0.4
Cohesion, c (kPa)	0	0	0	0	0	---
Friction angle, ϕ	34	34	34	7.5	7.5	---
Unit weight, γ (kN/m^3)	20.0	17.0	17.0	17.0	17.0	20.0

3.14.4 Results

Figure 93 and Figure 94 show the total displacement contours from the SVSOLID solver and the critical slip surface from the SVSLOPE solver, respectively. These figures show the slip surfaces from the SVSOLID solver is similar to that obtained from the SVSLOPE solution. Table 40 shows the FoS results of SVSOLID and SVSLOPE solvers.

Table 40. FoS comparison

SVSLOPE	SVSOLID	Difference (%)
1.85 (GLE*)	1.84	0.5

*GLE = General Limit Equilibrium

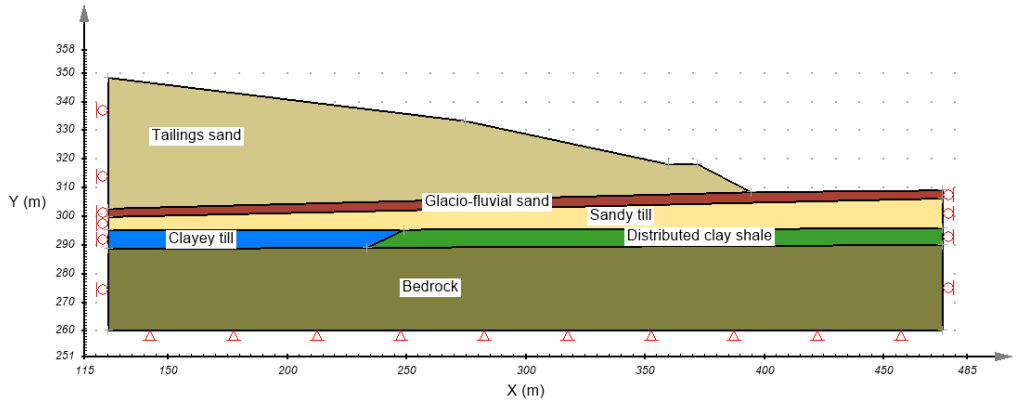

Figure 92. Geometry and boundary conditions

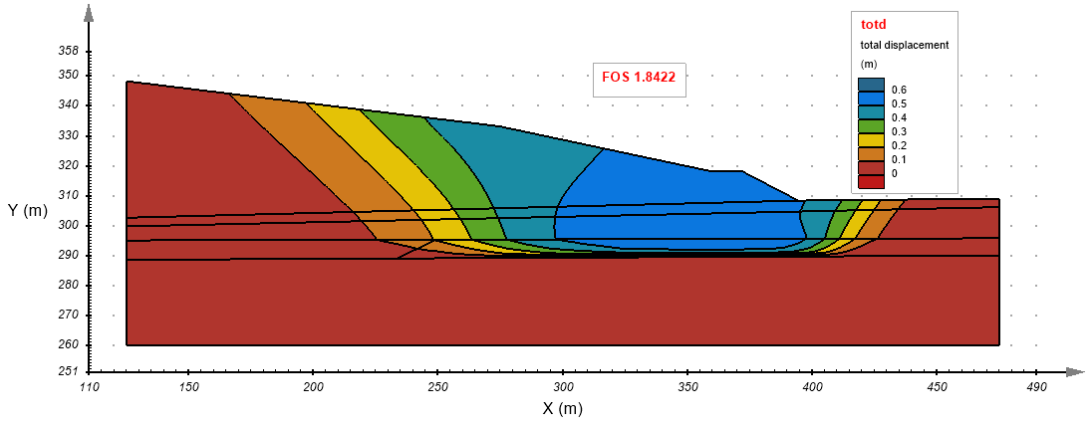

Figure 93. Total displacement contours from the SVSOLID giving a FoS = 1.84

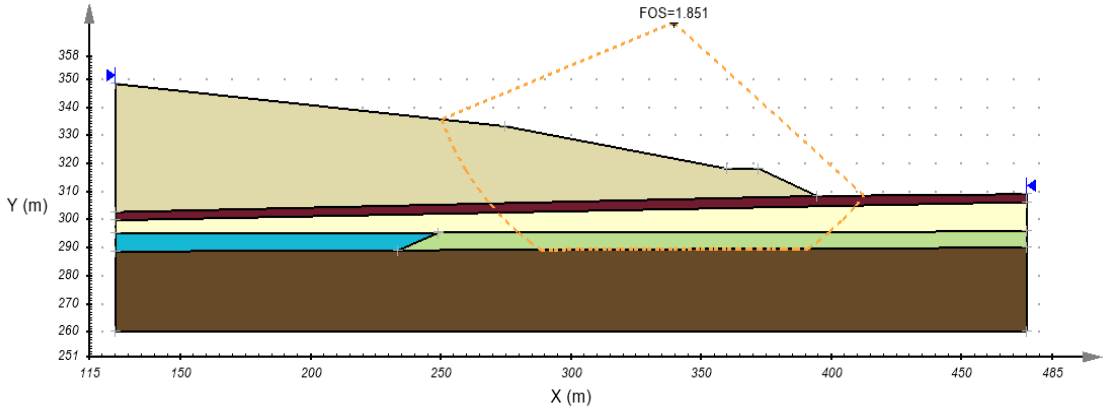

Figure 94. Critical slip surface from the SVSLOPE giving a FoS = 1.85

3.15 Embankment Slope of Undrained Clay - SSR

Project: Slopes_SSR
Model: EmbankmentSlopeUndrainedClay_SSR_GT

Main Factors Considered:

- Shear strength reduction factor of safety calculations.
- Limit Equilibrium method (LEM) factor of safety calculations.
- Undrained shear strength clays
- Application of distributed load

3.15.1 Model Description

This model includes two layers of undrained clays with a distributed load applied at the ground surface. The factor of safety (FoS) result from the SSR solution is compared to the FoS calculated using the limit equilibrium method (LEM) within the SVSLOPE solver.

3.15.2 Geometry and boundary conditions

Figure 95 shows the geometry and boundary conditions used in SVSOLID. Displacements are fixed in both *x* and *y* directions at the base. The two vertical boundaries are only fixed in the *x* direction.

3.15.3 Material Properties

A summary of the material properties for the model is provided in Table 41.

Table 41. Input material properties

Parameter	Clay fill embankment	Soft clay foundation
Young's modulus, E (kPa)	50,000	50,000
Poisson's ratio, ν	0.4	0.4
Cohesion, c (kPa)	20	20
Friction angle, ϕ	0	0
Unit weight, γ (kN/m^3)	19.4	19.4

3.15.4 Results

Figure 96 and Figure 97 show the total displacement contours from the SVSOLID solver and the critical slip surface from the SVSLOPE solver, respectively. These figures show the slip surfaces from the SVSOLID solver is similar to that obtained from the SVSLOPE solution. Table 42 shows the FoS results of SVSOLID and SVSLOPE solvers.

Table 42. FoS comparison

SVSLOPE	SVSOLID	Difference (%)
1.04 (GLE*)	0.94	9.6

*GLE = General Limit Equilibrium

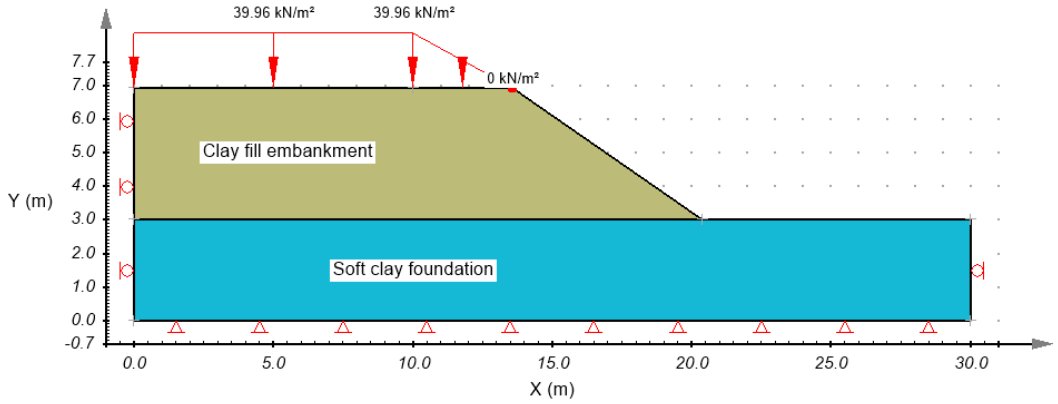

Figure 95. Geometry and boundary conditions

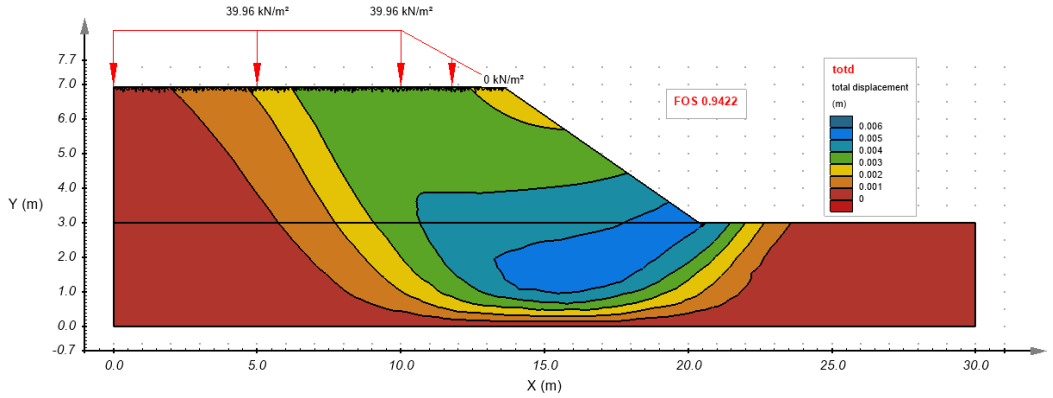

Figure 96. Total displacement contours from the SVSOLID giving a FoS = 0.94

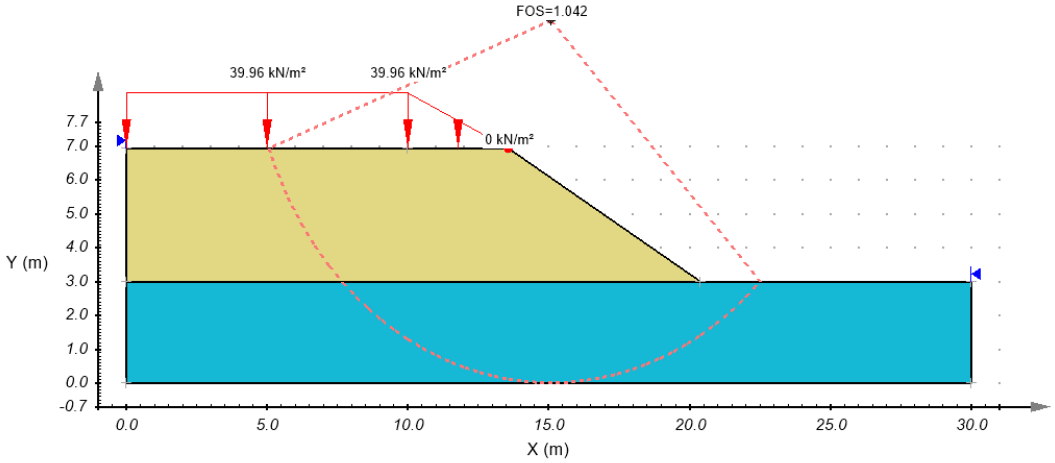

Figure 97. Critical slip surface from the SVSLOPE giving a FoS = 1.04

4 THREE DIMENSIONAL SOIL MECHANICS

This section presents 3D soil mechanics problems solved by SVSOLID.

4.1 Triaxial Tests of Hyperbolic Duncan-Chang Model

Reference: Duncan and Chang (1970)

Project: Foundations
Model: TriaxialTest_Hyperbolic_Case1_GT to TriaxialTest_Hyperbolic_Case6_GT

Main Factors Considered:

- Comparison of SVSOLID solver results to the closed-form solutions
- Use of the Duncan-Chang constitutive model
- Application of triaxial test results to a 3D cube sample
- Various loading scenarios are considered

4.1.1 Model Description

Various triaxial test results were fit with the Duncan-Chang hyperbolic type model. The Duncan-Chang model was then used in SVSOLID to simulate loading scenarios including:

- Consolidation of the sample under an initial stress state
- Drained strain-controlled test
- Load-unload-reload stress path
- Triaxial extension test

4.1.2 Geometry and Duncan-Chang model

A 3D cube was used to present the triaxial sample with edges that was 1 m. The 3D geometry was meshed using eight 4-noded tetrahedron elements. A coarse mesh was used in the simulations since the model cases are independent of the mesh density. Figure 98 shows the geometry and boundary conditions.

The Duncan-Chang model is a nonlinear hyperbolic model, in which the model stiffness depends on the major and minor principal stresses, σ_1 and σ_3. The Mohr-Coulomb's failure criterion is also applied in the model. The Duncan-Chang soil model is mathematically described as follows:

$$E_t = E_i \left[1 - \frac{R_f(1 - sin\,\varphi)(\sigma_1 - \sigma_3)}{2c\,cos\,\varphi + 2\sigma_3\,sin\,\varphi}\right]^2 \qquad [\ 13\ ]$$

where: E_t is the tangent modulus; $E_i = Kp_a\left(\frac{\sigma_3}{p_a}\right)^n$, which is the initial modulus; n is the modulus exponent; K is the modulus number; P_a is the atmospheric pressure; R_f is the failure ratio; c is the cohesion of the soil; and ϕ is the friction angle of the soil.

4.1.3 Material Properties

A summary of the material properties is provided in Table 43 and Table 44.

Table 43. Input material properties

Parameter	Value
Modulus number (K)	50
Modulus exponent	0
Failure ratio (R_f)	0.1 MPa
Atmospheric pressure (P_a)	0°
Poisson's ratio (assumed)	0.3

Table 44. Soil strength parameters

Case	Cohesion, c (kPa)	Friction angle, ϕ (°)
Case 1	100	0
Case 2	100	0
Case 3	100	0
Case 4	0	30
Case 5	0	30
Case 6	0	30

4.1.4 Results

4.1.4.1 Case 1: Unconfined compression test

An unconfined compression test is simulated. Ten stages were used to apply equal vertical displacements at the specimen surface are linearly increased. The final vertical strain in the soil specimen was 30 %. The unconfined compression strength is $q_u = \sigma_1 = 2\ c = 200\ kPa$. The shear strength in the soil specimen is $\tau_f = c$.

Figure 99 shows the stress-strain curve related to the simulation. It shows that at 30 % strain the vertical stress reached the ultimate unconfined compression strength of 200 *kPa* with a tangent modulus of 70.3 kPa (Figure 100). The minimum tangent modulus is based on the following equation:

$$E_t^{min} = E_i\left[1 - R_f\right]^2 = 5000[1 - 0.9]^2 = 50 \text{ kPa} \quad [\ 14\ ]$$

where,

$$E_i = Kp_a\left(\frac{\sigma_3}{p_a}\right)^n = 5000 \text{ kPa} \quad [\ 15\ ]$$

4.1.4.2 Case 2: Loading-unloading-reloading test

The soil properties remain the same as in the previous simulation. However the soil specimen is loaded, then unloaded and then reloaded. Figure 101 shows the applied strain experienced by the soil specimen.

Figure 102 shows the stress-strain response of the soil specimen during the simulation. During the unloading, the vertical stress decreases to a value of 57.4 kPa before being increased to the value attained before unloading for the reloading step. The final vertical stress at 30 % strain was 196.2 kPa.

The values of tangent modulus versus the load steps are shown in Figure 103. Its limiting initial value modulus is set to $E_t = E_i = 5000$ kPa during the unloading steps. E_t is maintained at this value until the vertical stress reaches its previous maximum value.

4.1.4.3 Case 3: Confined compression test on a cohesive soil

This analysis repeats the test in section 4.1.4.1 while using an all-round confining pressure of 100 kPa prior the applied strain (i.e., vertical displacement) at the surface of the soil specimen. In this case, the maximum vertical stress is increased to 300 kPa and the shear strength of the soil specimen remains at 100 kPa (i.e., $(\sigma_1 - \sigma_3)/2$).

Figure 104 and Figure 105 shows the stress-strain curve and the tangent modulus during the confined compression test. Figure 104 indicates that the vertical stress approaches the confined compression strength of 300 kPa and at this stress the tangent modulus reaches its minimum value of 50 kPa.

4.1.4.4 Case 4: Confined compression test on a frictional soil

For this simulation, the shear strength parameters of the soil are comprised of a frictional angle, $\phi = 30°$ and cohesion, $c = 0$ kPa. The confining pressure on the soil specimen is 100 kPa. At failure, the following equation is defined:

$$\frac{\sigma_1}{\sigma_3} = \frac{1 + sin\,\varphi}{1 - sin\,\varphi} = 3 \quad [\ 16\ ]$$

The confining pressure, $\sigma_3 = 100$ kPa; and the maximum vertical stress, $\sigma_1 = 100$ kPa. These values are confirmed by Figure 106.

4.1.4.5 Case 5: Loading-unloading-reloading on a frictional soil

This simulation is similar the one presented in section 4.1.4.2 for a frictional soil and an applied strain (i.e., vertical displacement) as shown in Figure 107. The stress-strain curve is shown in Figure 108, and the soil specimen response is similar to that shown in section 4.1.4.2. The maximum shear strength in this case was 300 kPa.

4.1.4.6 Case 6: Extension test on a frictional soil

This is an extension test simulation. The applied extension strain (i.e., vertical displacement) increases from zero to 8 %. The confining pressure is also 100 kPa. In this case, the maximum principal stress is in the horizontal direction and the maximum vertical stress is 100/3 = 33.3 kPa (Eq. [16]). Figure 109 provides a confirmation of the simulation results.

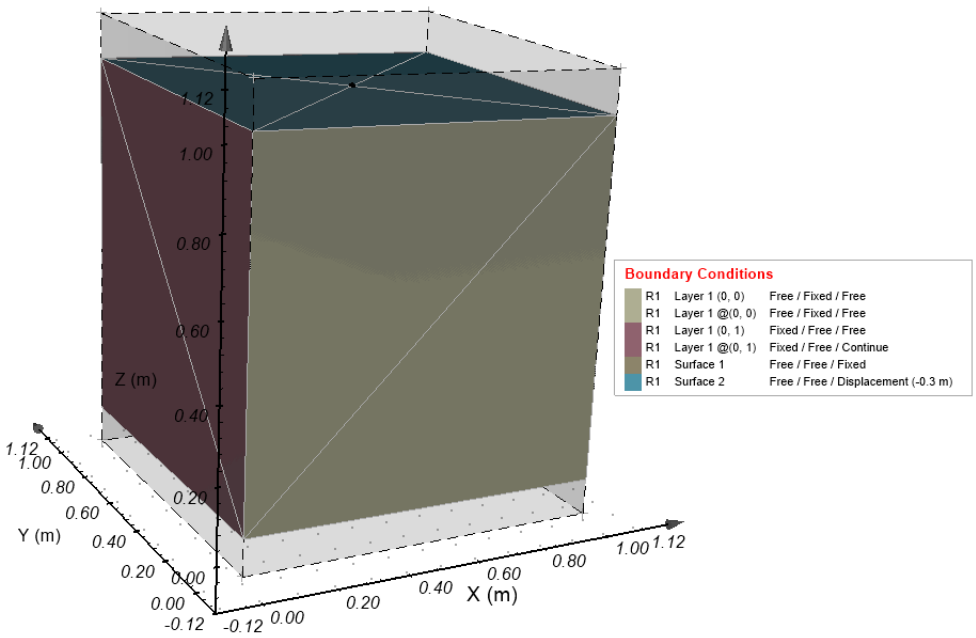

Figure 98. Geometry and boundary conditions (color coded).

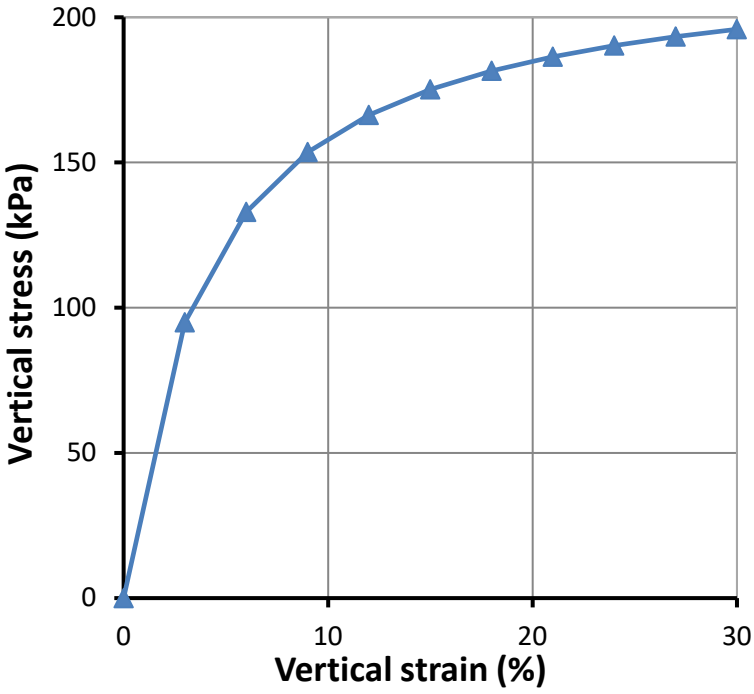

Figure 99. Stress - strain curve for the unconfined compression test with c_u = 100 kPa (Case 1).

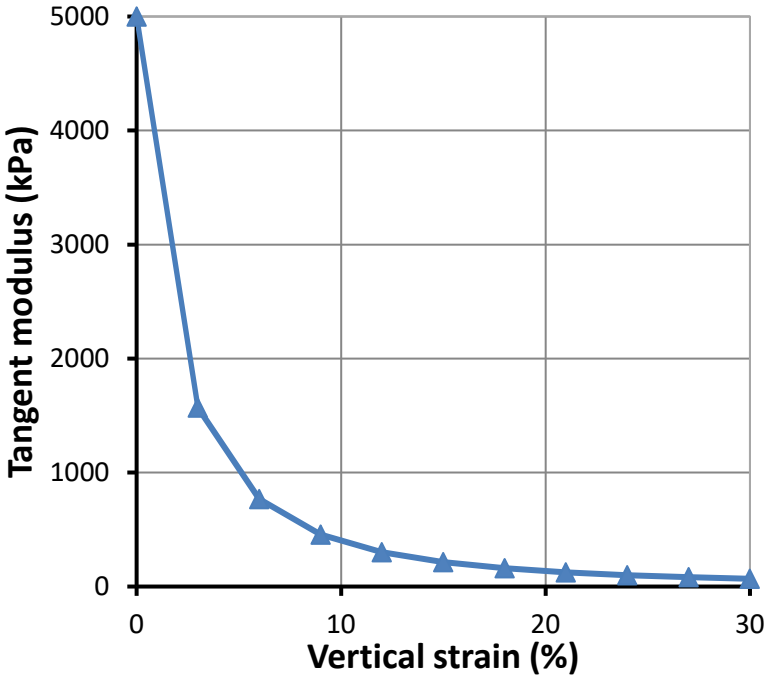

Figure 100. Tangent modulus at various strain values (Case 1).

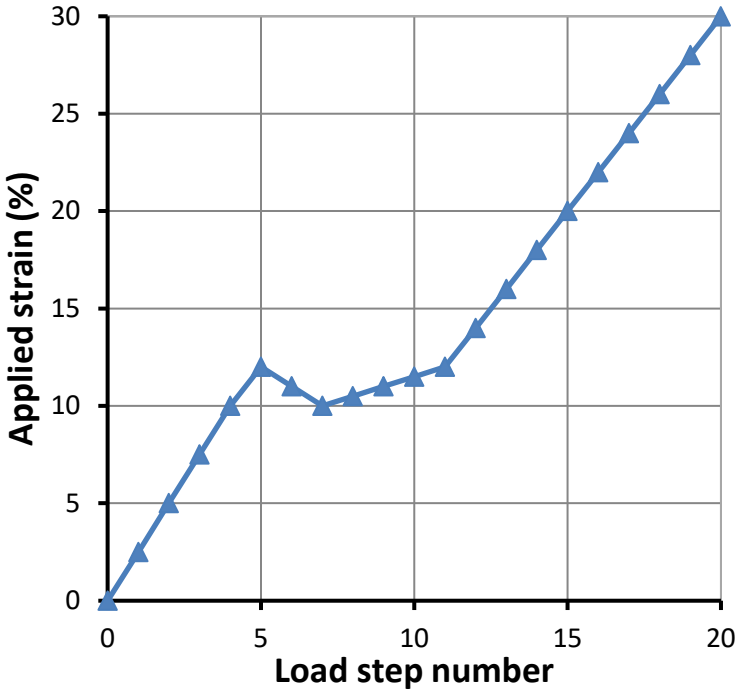

Figure 101. Applied strain on the soil specimen for loading-unloading-reloading tests (Case 2).

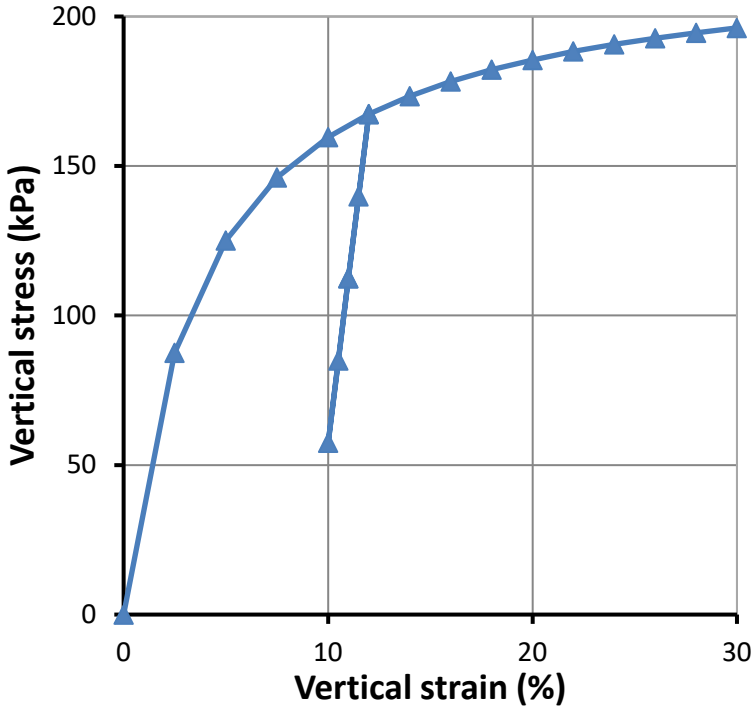

Figure 102. Stress – strain curve during loading-unloading-reloading tests (Case 2).

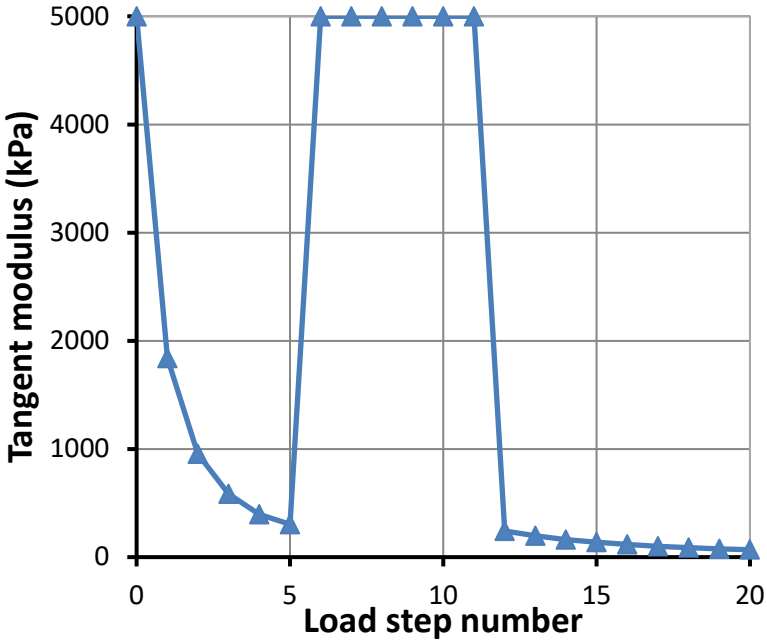

Figure 103. Load step – tangent moduli during loading-unloading-reloading tests (Case 2).

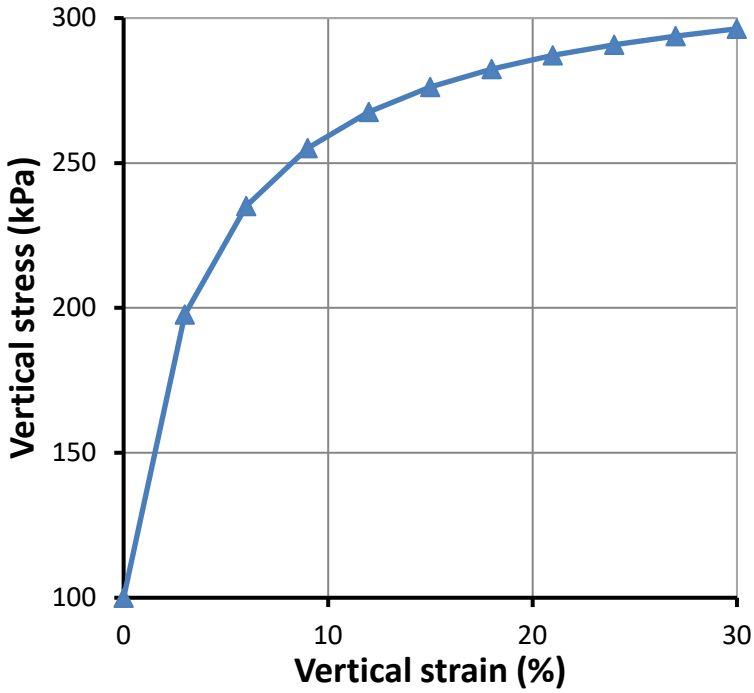

Figure 104. Stress – strain curve during confined compression test (Case 3).

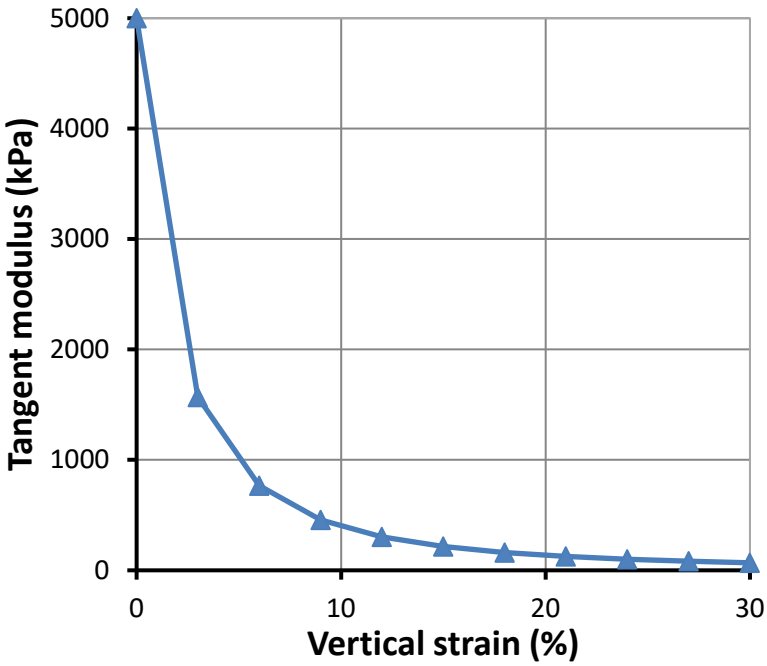

Figure 105. Tangent moduli versus vertical strain during confined compression test (Case 3).

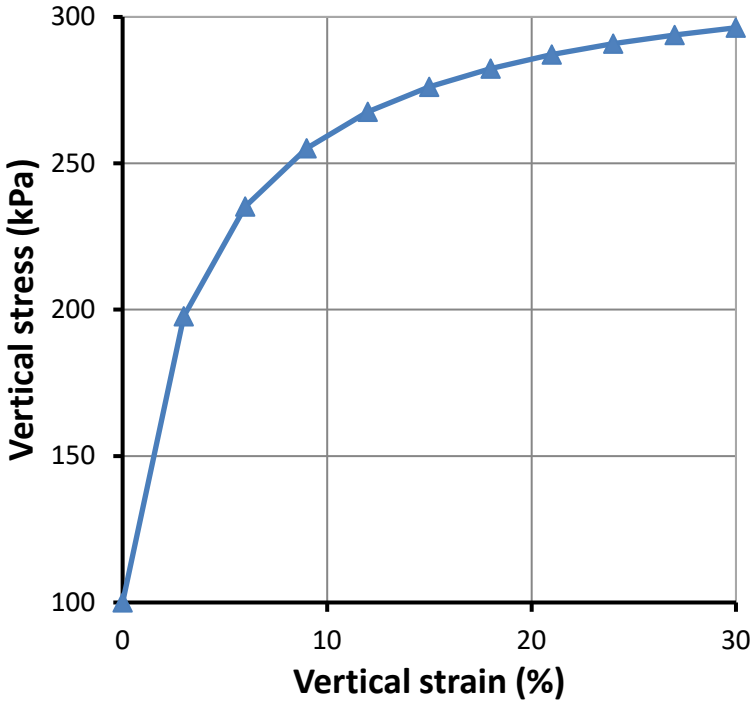

Figure 106. Stress – strain curve during confined compression test on a fictional soil (Case 4).

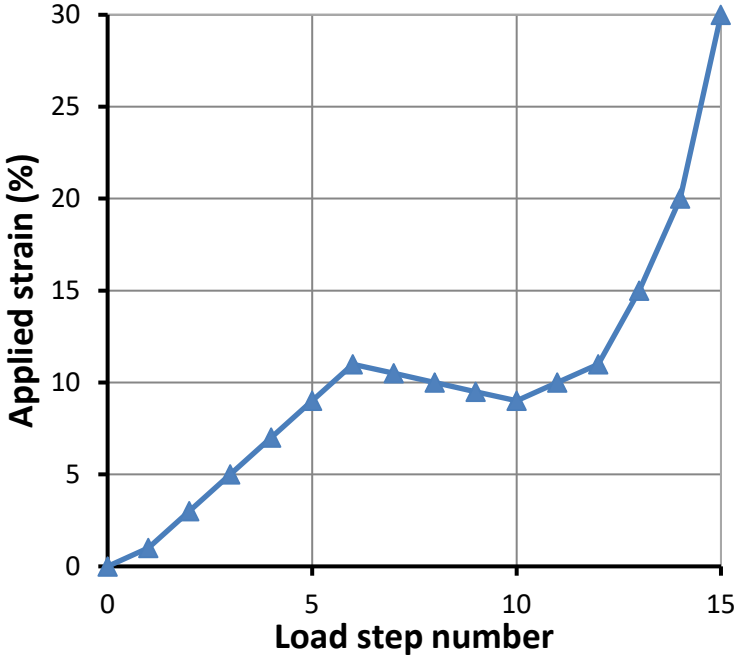

Figure 107. Applied strain versus load steps on a fictional soil (Case 5).

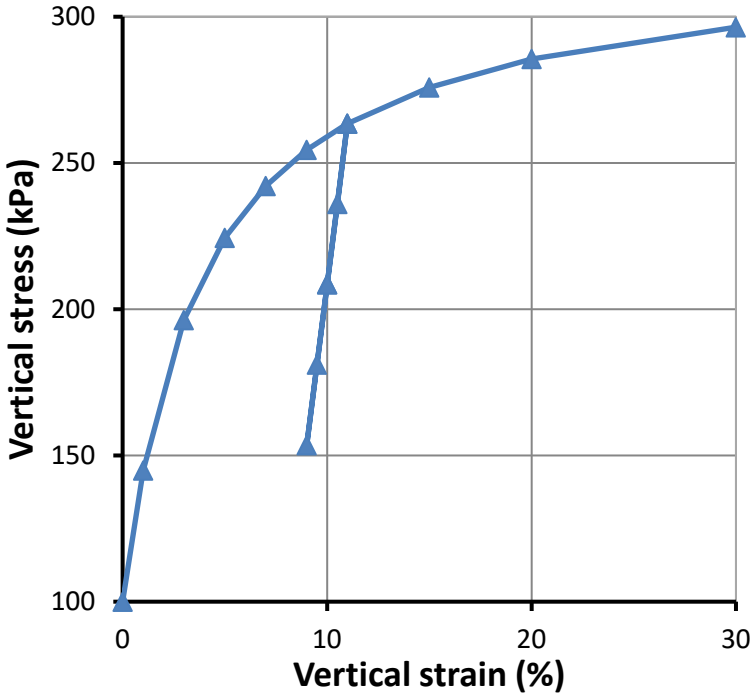

Figure 108. Stress – strain curve (Case 5).

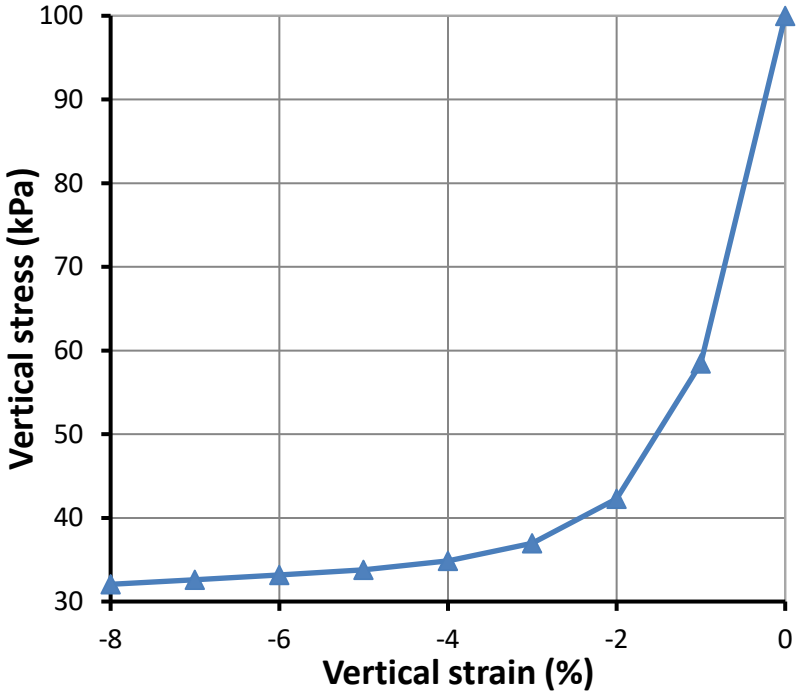

Figure 109. Stress – strain curve for an extension test on a soil specimen (Case 6).

4.2 Stresses in a Semi-Infinite Elastic Medium Under a Point Load -Boussinesq Problem

Reference: Poulos and Davis (1974)

Project: Foundations
Model: Boussinesq_PointLoad_GT

Main Factors Considered:

- Comparing the results of SVSOLID solver against closed-form solutions for a 3D stress-strain problem subjected to a point load.

4.2.1 Model Description

This problem involves the calculation of stresses and displacement in a semi-infinite mass under a point load. A 3D stress-deformation SVSOLID analysis is compared to the results of a closed-form solution.

4.2.2 Geometry and boundary conditions

Figure 110 shows a schematic of the problem where a concentrated load is applied at the ground surface. Cartesian coordinates are used to show stresses and displacements. Geometry and boundary conditions are shown in Figure 111. A 100 kN point load applied at the surface.

4.2.3 Material Properties

A summary of the material properties is provided in Table 45.

Table 45. Input material properties

Parameter	Value
Young's modulus, E	50,000 kPa
Poisson's ratio, ν	0.3

4.2.4 Results

The closed-form solution of this problem was presented by Boussinesq (1883) (Poulos and Davis, 1974). The continuum is assumed to be homogenous and behave as an isotropic elastic medium.

The closed-form solutions of stresses and vertical displacement are shown in the following equations:

$$\sigma_x = \frac{P}{2\pi}\left(\frac{3x^2z}{R^5} - (1-2\nu)\left[\frac{x^2-y^2}{Rr^2(R+z)} + \frac{y^2z}{R^3r^2}\right]\right)$$
$$\sigma_y = \frac{P}{2\pi}\left(\frac{3y^2z}{R^5} - (1-2\nu)\left[\frac{y^2-x^2}{Rr^2(R+z)} + \frac{x^2z}{R^3r^2}\right]\right) \quad [17]$$
$$\sigma_z = \frac{3P}{2\pi}\frac{z^3}{R^5}$$
$$w = \frac{P(1+\nu)}{2\pi ER}\left(2(1-\nu) + \frac{z^2}{R^2}\right)$$

where: σ_x, σ_y, σ_z are the stresses in the x, y, z directions, respectively; w is the vertical displacement; E is the Young's modulus; ν is the Poisson's ratio.

A comparison between the closed-form solution and the calculated results from SVSOLID are shown from Figure 112 to Figure 115. These figures show that SVSOLID results closely match the closed-form solutions.

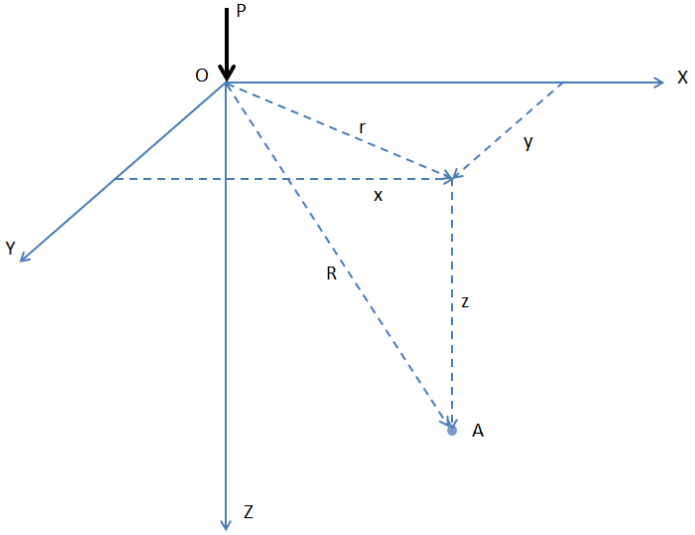

Figure 110. Schematic of the Boussinesq problem

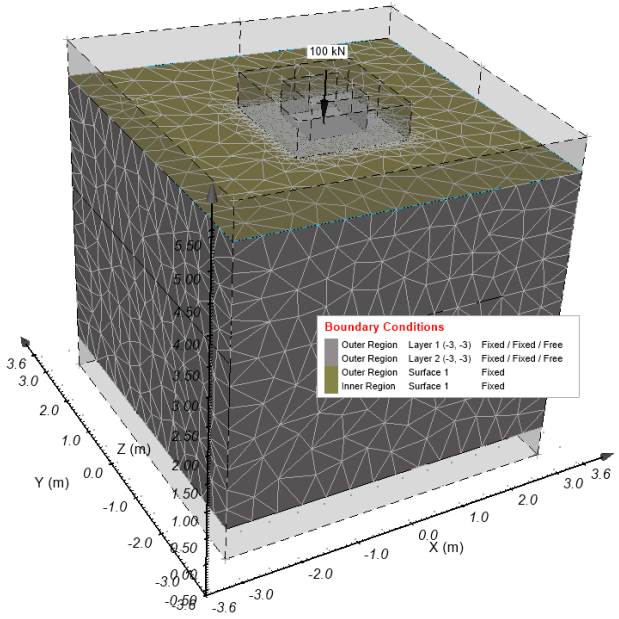

Figure 111. Geometry and boundary conditions

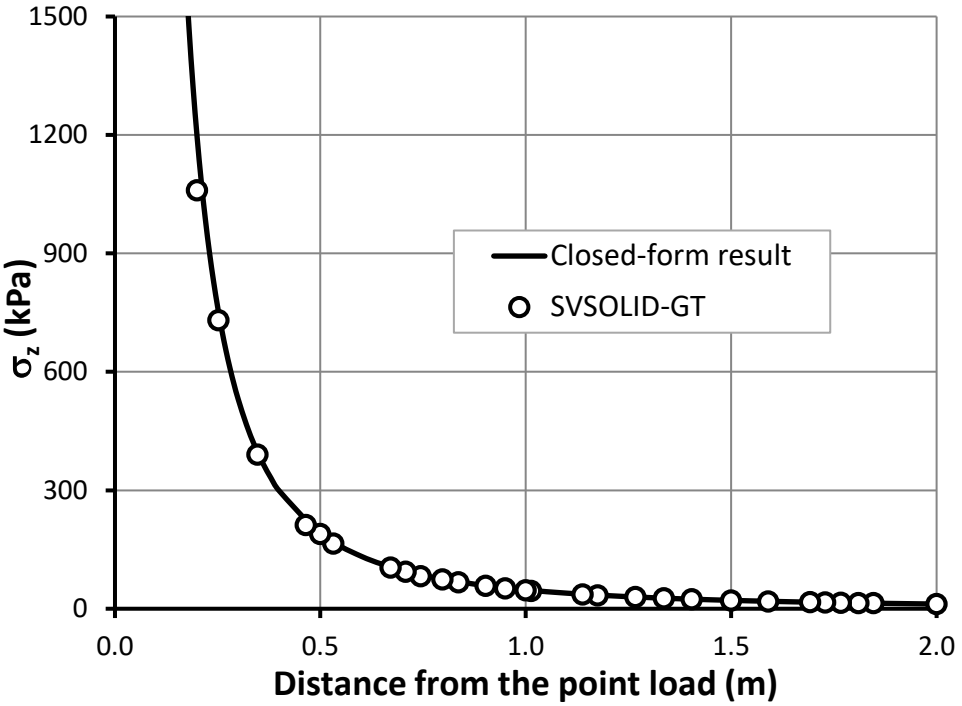

Figure 112. σ_z along the OZ axis (Figure 110)

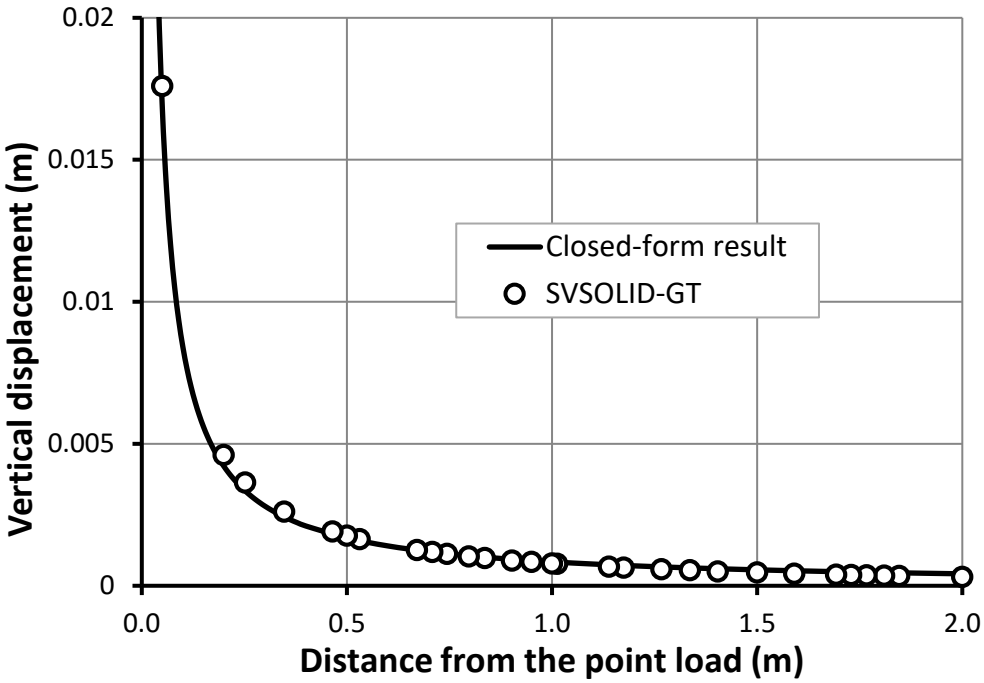

Figure 113. Vertical displacement, *w*, along the OZ axis (Figure 110)

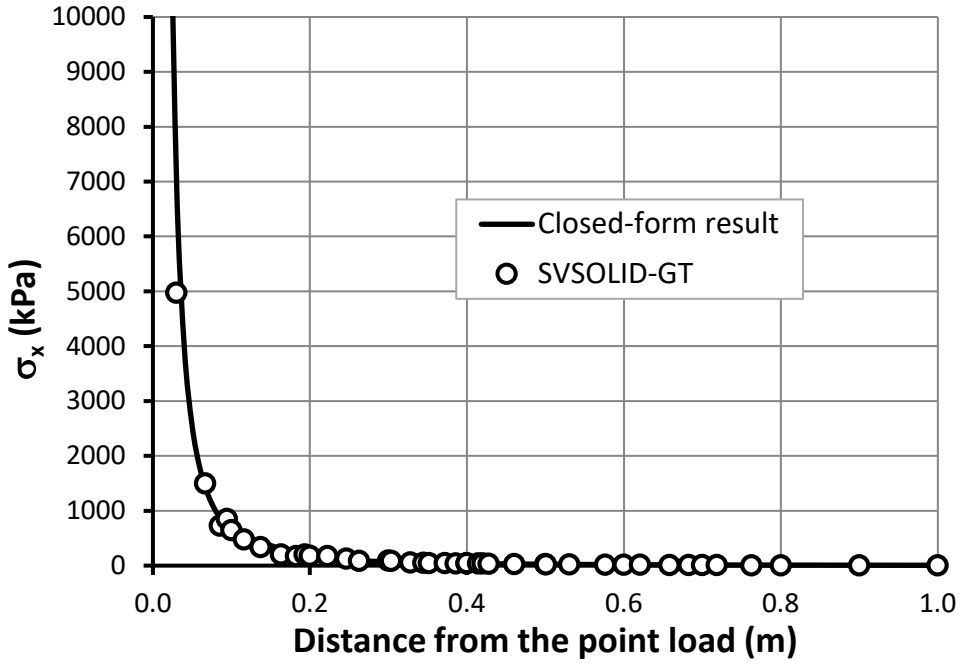

Figure 114. σ_x along the OX axis (Figure 110)

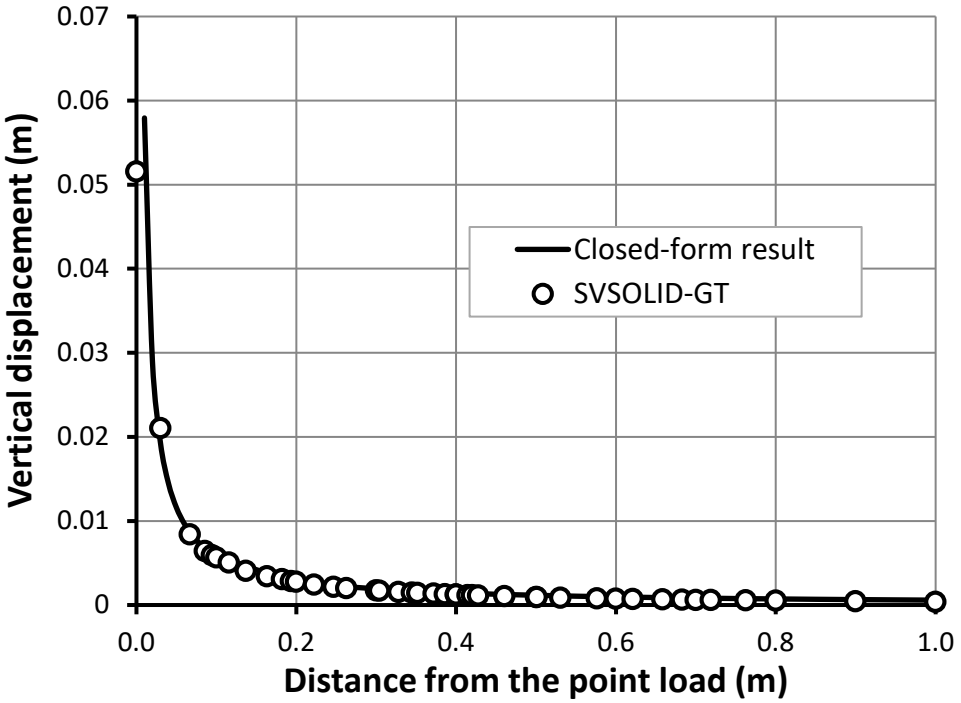

Figure 115. Vertical displacement, *w*, along the OX axis (Figure 110)

4.3 Ultimate Bearing Capacity of Circular Footing on a Homogenous Soil

Reference: Chen (2013)

Project: Foundations
Model: CircularFooting_ElasticPlastic_Case1_GT to CircularFooting_ElasticPlastic_Case4_GT

Main Factors Considered:

- Comparing the ultimate bearing capacity computed using SVSOLID against the closed-form solutions of a 3D circular footing problem.

4.3.1 Model Description

Several 3D circular footing models were created using Mohr-Coulomb material properties. Various cohesion values and friction angles were examined as part of the comparison of the closed-form solutions to the ultimate bearing capacity computed using SVSOLID.

4.3.2 Geometry and boundary conditions

Figure 116 shows the geometry and boundary conditions. The mesh region near the applied load is much denser than in the surrounding region. Only one-quarter of the geometry is modeled due to symmetry.

4.3.3 Material Properties

A summary of the material properties is provided in Table 46. The soil is assumed as weightless. The assumption does not affect the ultimate bearing capacity as the load is applied at ground surface.

Table 46. Input material properties

Parameter	Value
Young's modulus, E	20,000 kPa
Poisson's ratio, ν	0.3
Cohesion, c	1 kPa
Friction angle, ϕ	0°, 10°, 20°, 30°

4.3.4 Results

The analytical solution for ultimate bearing capacity of a circular footing. The load applied at the ground surface (without any surcharge loading) is defined as:

$$q_u = N_c\, c \qquad [\,5\,]$$

where, N_c is the bearing capacity factor and c is the cohesion of the soil. The values of N_c also depend on the friction angle of the soil as shown in Table 47.

Table 47. Bearing capacity factor, N_c

Friction angle, ϕ	0	10	20	30
N_c	5.14	8.34	14.83	30.14

A comparison between the closed-form analytical solutions and the SVSOLID results is shown from Figure 117 to Figure 120. These figures show that the results computed using SVSOLID compared closely with the closed-form results for the ultimate bearing capacity.

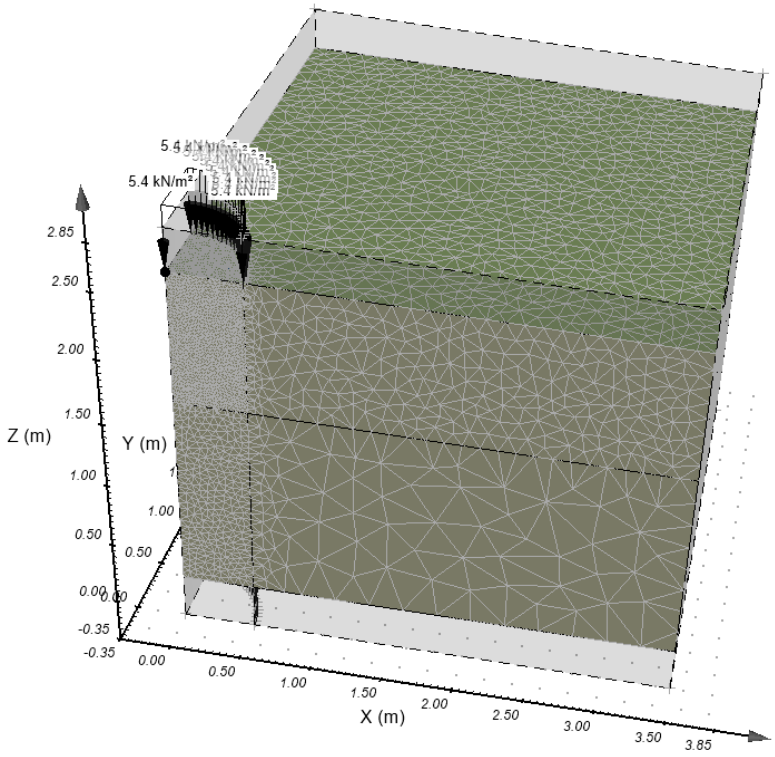

Figure 116. Geometry and boundary conditions

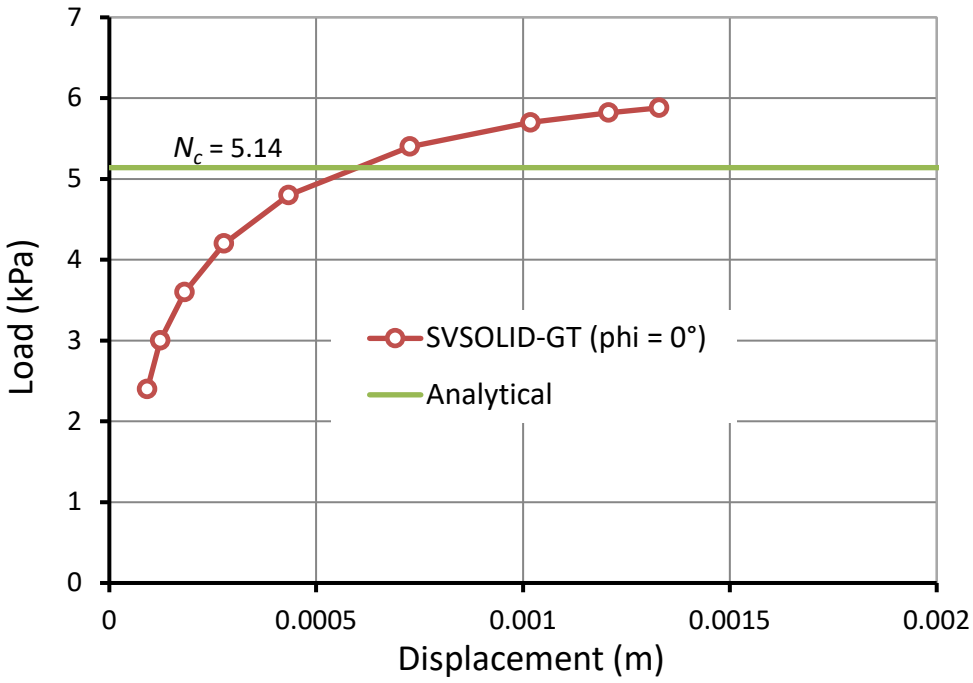

Figure 117. Load – displacement curve for ϕ = 0°

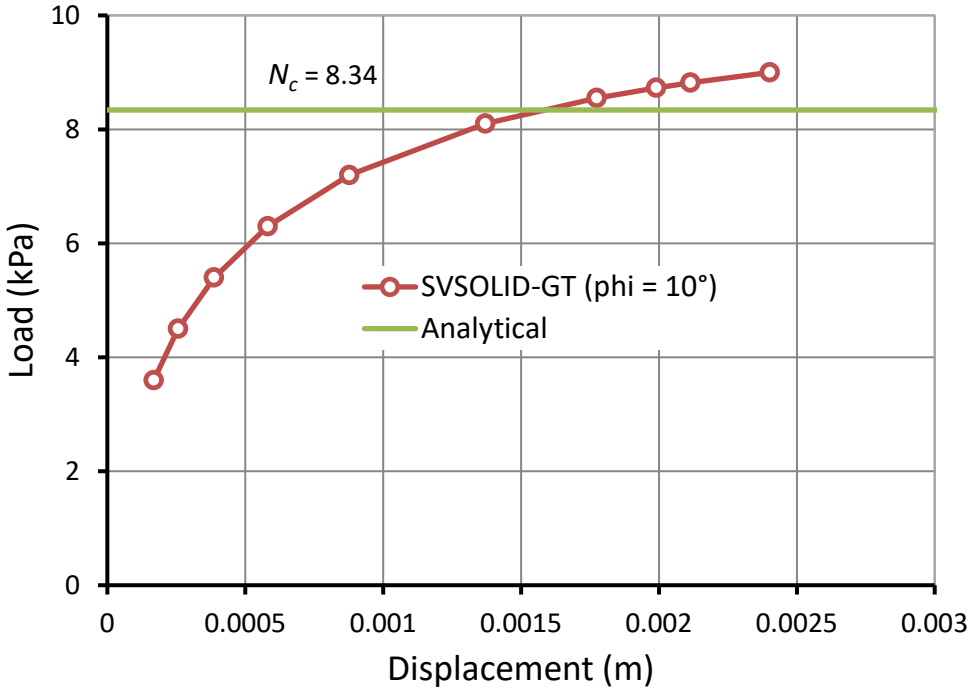

Figure 118. Load – displacement curve for ϕ = 10° and cohesion = 1 kPa

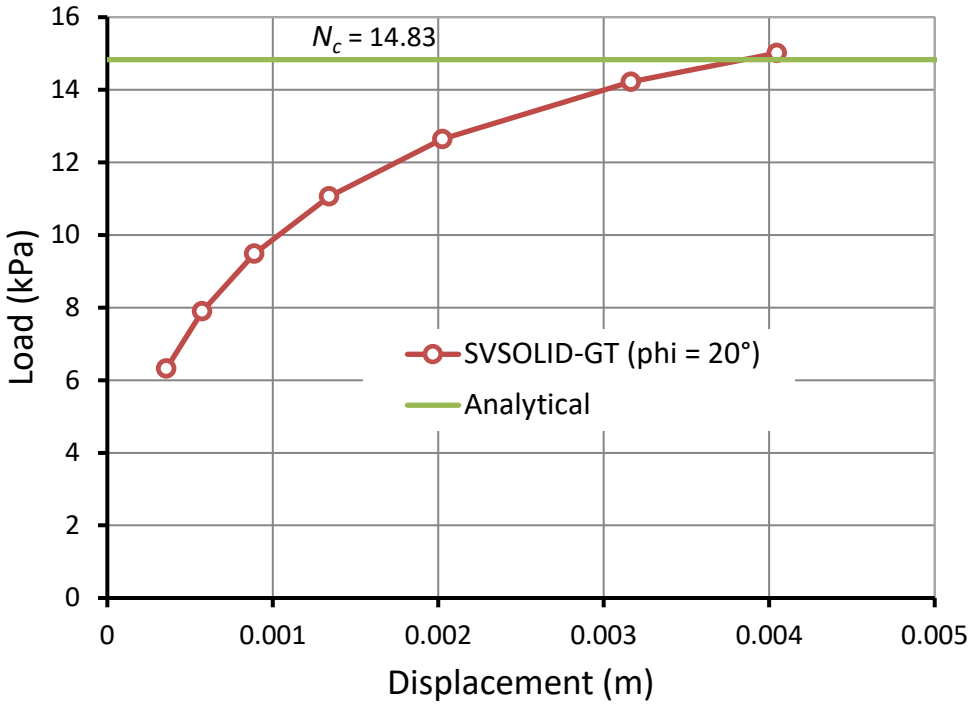

Figure 119. Load – displacement curve for ϕ = 20° and cohesion = 1 kPa

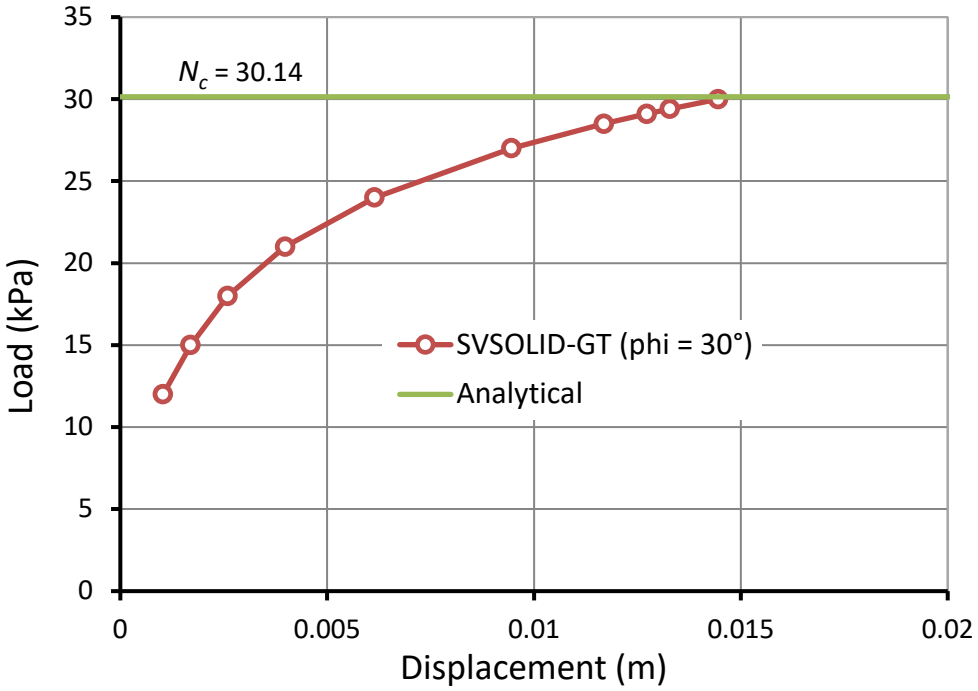

Figure 120. Load – displacement curve for ϕ = 30° and cohesion = 1 kPa

4.4 Anchor in 3D Elastic Rock Mass

Reference: Farmer (1975)

Project: Foundations
Model: 3D_Anchor_GT

Main Factors Considered:

- Comparing the results of the SVSOLID solver against the closed-form solutions of an anchor installed in 3D plane strain elastic rock mass.

4.4.1 Model Description

This problem concerns the elastic behavior of an anchor grouted in 3D elastic rock mass. The shear stress distribution along the anchor/rock interface is examined if a pull-out force of 100 kN is applied to the anchor head.

4.4.2 Geometry and boundary conditions

Figure 121 shows the geometry and boundary conditions used in this model. The model geometry has a cross-sectional area of 0.4 m x 0.4 m, and 0.6 m in height. An anchor/rock bolt is installed at the model center and 0.5 m in length from the ground surface. The displacements of the model are restricted at the bottom surface, while at the top surface z-displacement is restricted.

4.4.3 Material Properties

The anchor and rock properties are summarized in Table 48.

Table 48. Input material properties

Parameter	Value
Rock mass properties	
Young's modulus (E_R)	5.0×10^7 kPa
Poisson's ratio (ν)	0.25
Drill hole radius (R)	11 mm
Anchor properties	
Tributary area (A)	243.3 mm^2
Anchor radius (a)	8.8 mm
Young's modulus (E_a)	1.0×10^8 kPa
Bond shear stiffness (K_b)	1.4×10^7 kPa

4.4.4 Results

The shear stress developed along the anchor/grout interface is given in the following (Farmer, 1975)

$$\frac{\tau}{\sigma_o} = 0.1 \times e^{\frac{-0.2x}{a}} \quad [\ 18\ ]$$

where, τ is the shear stress along the rock bolt/grout interface, σ_0 is the applied pull-out stress, x is the distance from the head of the anchor, and a is the radius of anchor. The following assumptions were made by Farmer (1975)

- The shear modulus of grout is $G_b = 0.005\ E_a$
- The drill hole radius is $R = 1.25\ a$

The shear stiffness were determined using the following equation (St. John and Van Dillen, 1983; Dey, 2001)

$$K_b = \frac{2\pi G_b}{ln\left(1 + {}^{t}/_{a}\right)} \quad [\ 19\ ]$$

where, t = 2.2 mm is the annulus thickness and it is defined in Figure 122. The second assumption indicates he drill hole radius, R is 1.25 × 8.8 mm = 11 mm.

The shear stress along the bolt/grout interface is:

$$\tau = \frac{F_s}{2\pi a} \quad [\ 20\ ]$$

where, F_s is the shear force per unit length. Similarly, the shear stress along the rock/grout interface can be calculated using Equation [20] with R instead of a.

Figure 123 shows a comparison between the results of shear stress using Equation [18] and SVSOLID. The SVSOLID results match closely to the analytical results.

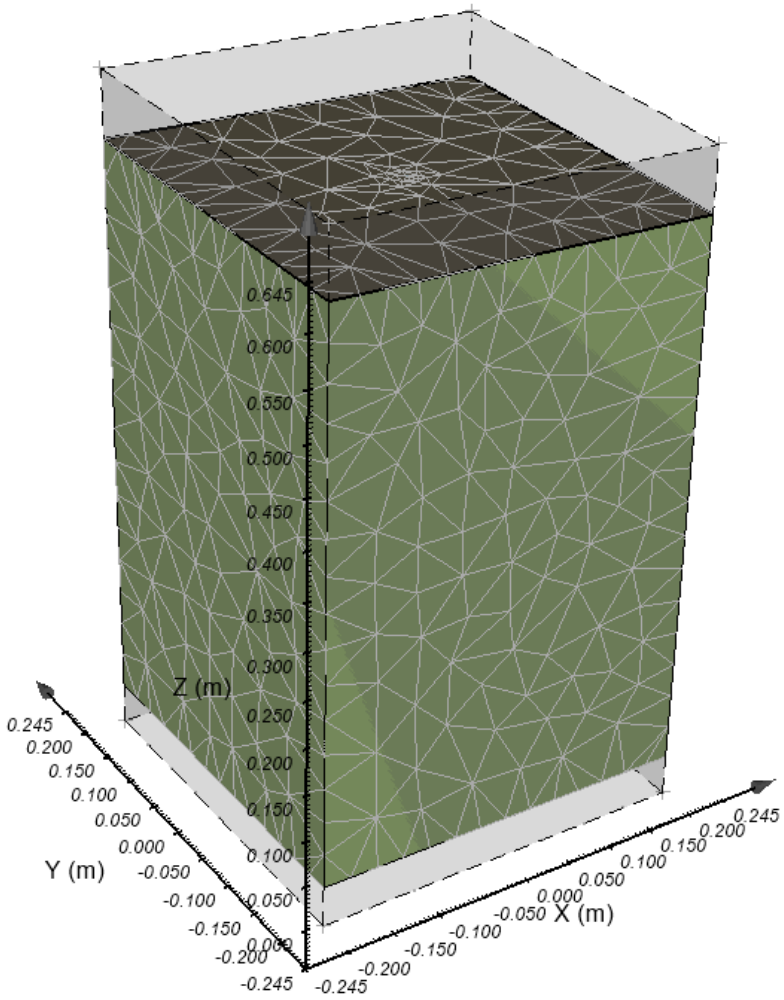

Figure 121. Geometry and boundary conditions

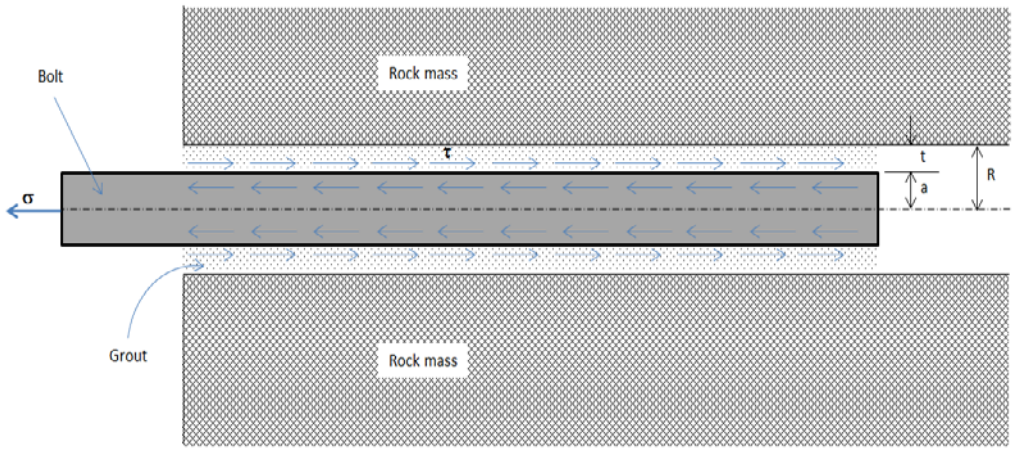

Figure 122. Schematic of rock bolt

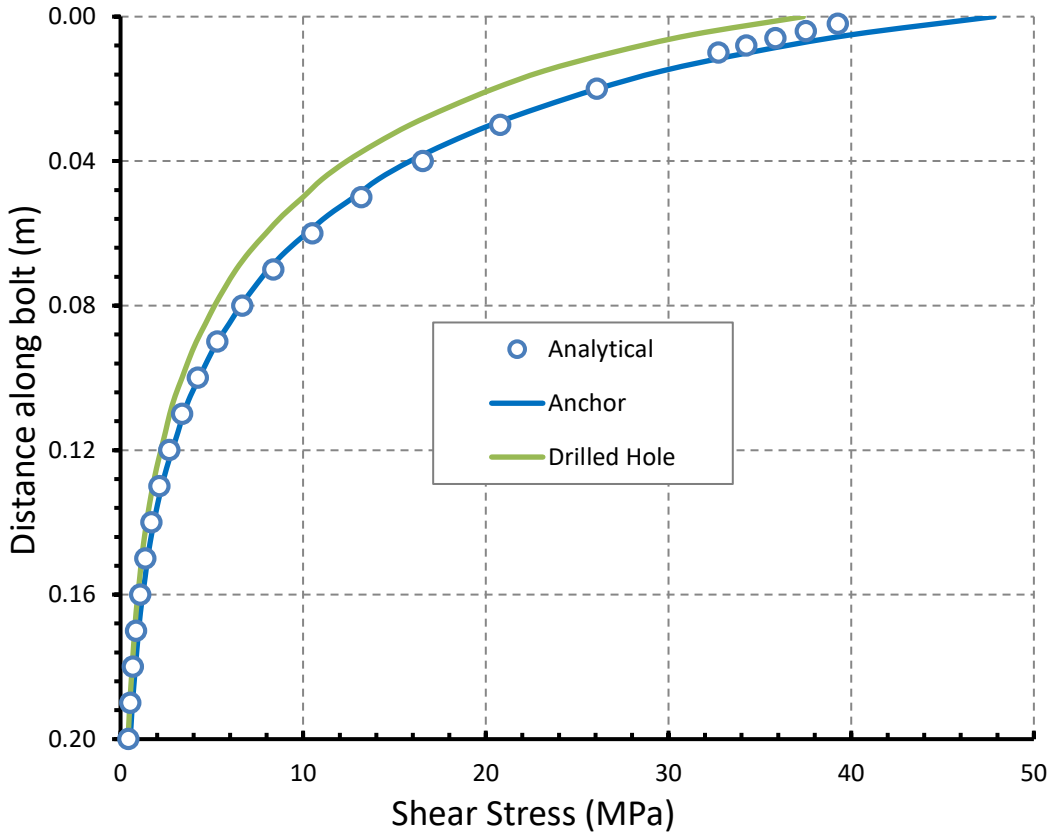

Figure 123. Shear stress along the bolt / grout (anchor) and grout / rock (drilled hole) interfaces

5 THREE-DIMENSIONAL SHEAR STRENGTH REDUCTION

This section presents 3D shear strength reduction problems solved with SVSOLID.

5.1 Homogeneous One Layer 3D Slope - SSR

Reference: Silvestri (2006)

Project: Slopes_SSR
Model: 3D_Slope_closedForm_GT

Main Factors Considered:

- Shear strength reduction factor of safety calculations
- Limit Equilibrium method (LEM) factor of safety calculations.
- 3D geometric configuration
- Limit equilibrium method (LEM) methodology to calculate the FoS

5.1.1 Model Description

The stability of a slope defined as a 3D geometry is calculated using SSR methodology. The slope is comprised on one homogeneous soil. The factor of safety (FoS) results of the SSR analysis is compared to the FoS calculated using LEM obtained using the SVSLOPE software which is part of the SOILVISION suite. Silvestri (2006) reported a FoS of 1.43 for this problem.

5.1.2 Geometry and boundary conditions

Figure 124 shows the geometry and boundary conditions in SVSOLID. Displacements are fixed in all directions on the base and along the side walls.

5.1.3 Material Properties

A summary of the material properties is provided in Table 49.

Table 49. Input material properties

Parameter	Soil
Young's modulus, E (kPa)	50,000
Poisson's ratio, ν	0.4
Cohesion, c (kPa)	0.1
Friction angle, ϕ	0.0
Unit weight, γ (kN/m^3)	1.0

5.1.4 Results

Figure 125 and Figure 126 show the total displacement contours from the SVSOLID solution. The critical slip surface determined in SVSLOPE is also shown, respectively. These figures show that the slip surfaces from both SVSOLID and SVSLOPE are similar. Table 50 shows the FoS results computed in SVSOLID and SVSLOPE.

Table 50. FoS comparison

SVSLOPE	SVSOLID	Difference (%)
1.43 (GLE*)	1.42	0.7

*GLE = General Limit Equilibrium formulation

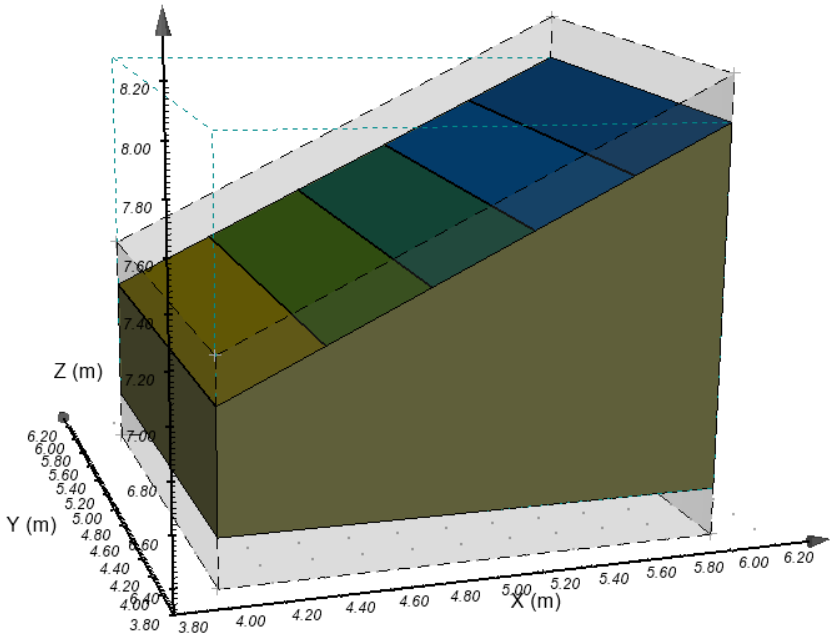

Figure 124. Geometry and boundary conditions

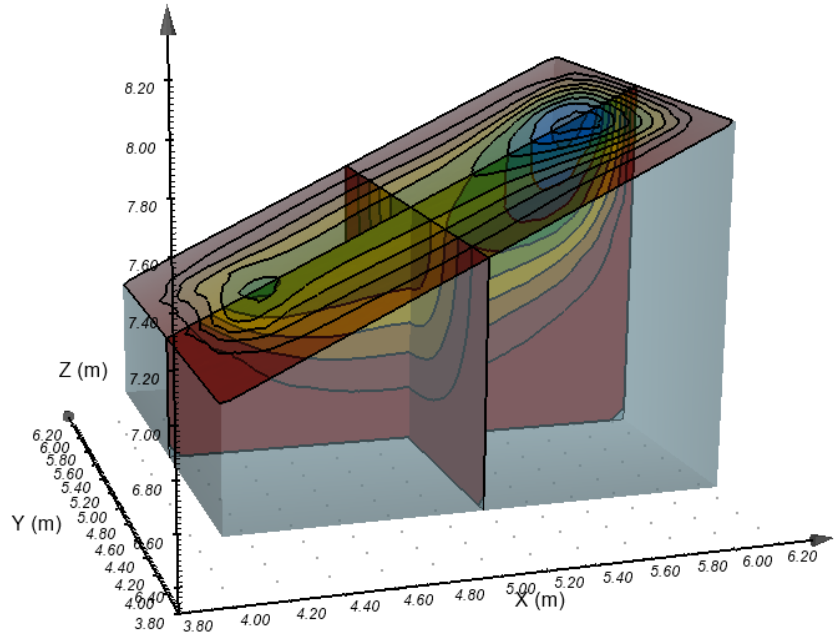

Figure 125. Total displacement contours in SVSOLID with FoS = 1.42

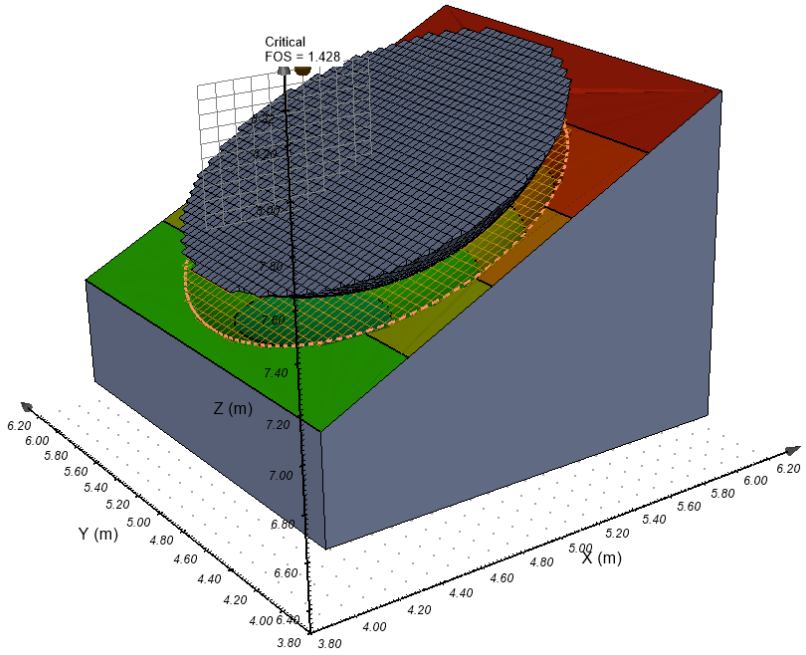

Figure 126. Critical slip surface in SVSLOPE with FoS = 1.43

5.2 Embankment Corner - SSR

Project: Slopes_SSR
Model: Embankment_Corner_SSR_GT

Main Factors Considered:

- Shear strength reduction method to calculate the factor of safety
- 3D geometric consideration for the corner of an embankment
- Limit equilibrium method (LEM) methodology to calculate the FoS

5.2.1 Model Description

A 3D SSR is performed to determine the stability of an embankment corner. The factor of safety (FoS) results from the SSR analysis is compared with the FoS determined using the limit equilibrium method (LEM) in SVSLOPE.

5.2.2 Geometry and boundary conditions

Figure 127 shows the geometry and boundary conditions in SVSOLID. Displacements are fixed in all directions at the base and the side walls.

5.2.3 Material Properties

A summary of the material properties is provided in Table 51.

Table 51. Input material properties

Parameter	Soil
Young's modulus, E (kPa)	50,000
Poisson's ratio, ν	0.4
Cohesion, c (kPa)	10
Friction angle, ϕ	22
Unit weight, γ (kN/m^3)	20

5.2.4 Results

Figure 128 and Figure 129 show the total displacement contours from the SVSOLID solution along with the critical slip surface computed in SVSLOPE, respectively. These figures show that the slip surfaces from both SVSOLID and SVSLOPE are similar. Table 52 compares the FoS results from SVSOLID and SVSLOPE.

Table 52. FoS comparison

SVSLOPE	SVSOLID	Difference (%)
1.31 (GLE*)	1.24	5.3

*GLE = General Limit Equilibrium formulation

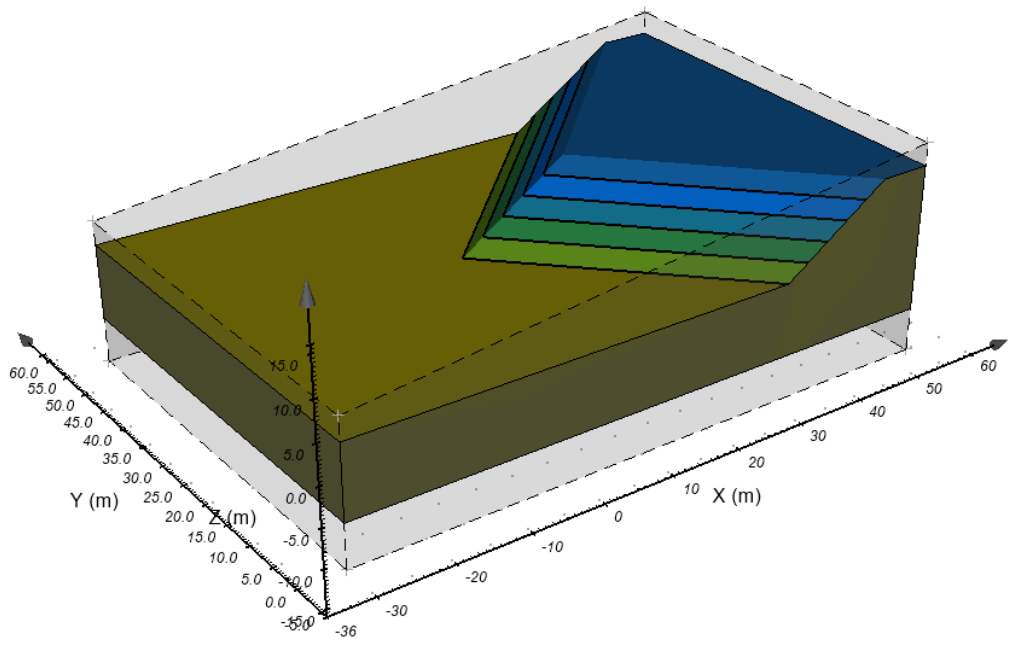

Figure 127. Geometry and boundary conditions

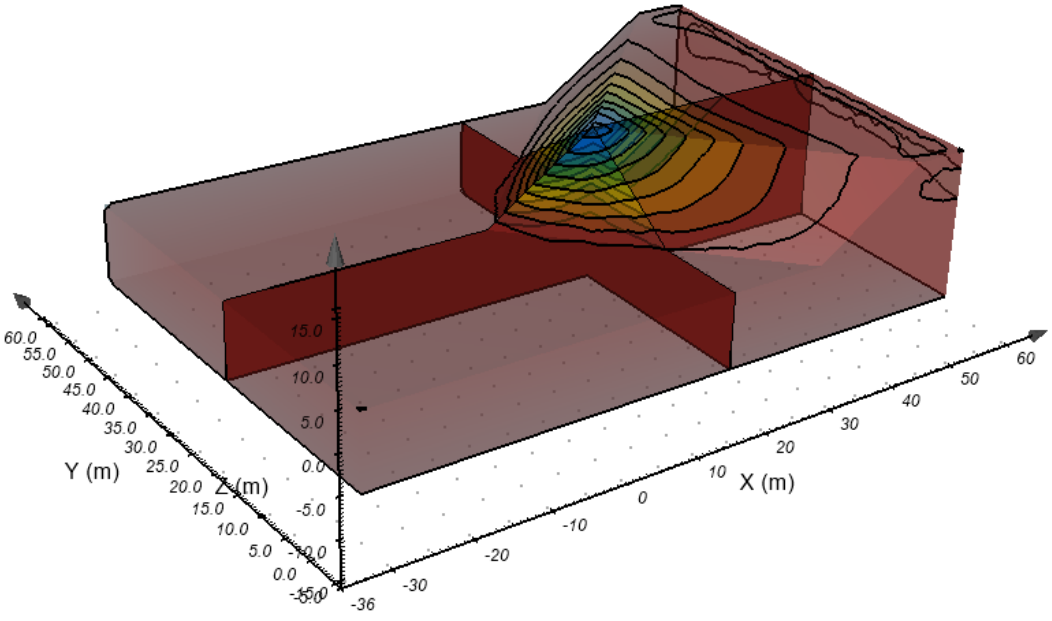

Figure 128. Total displacement contours calculated in SVSOLID yielding a FoS = 1.24

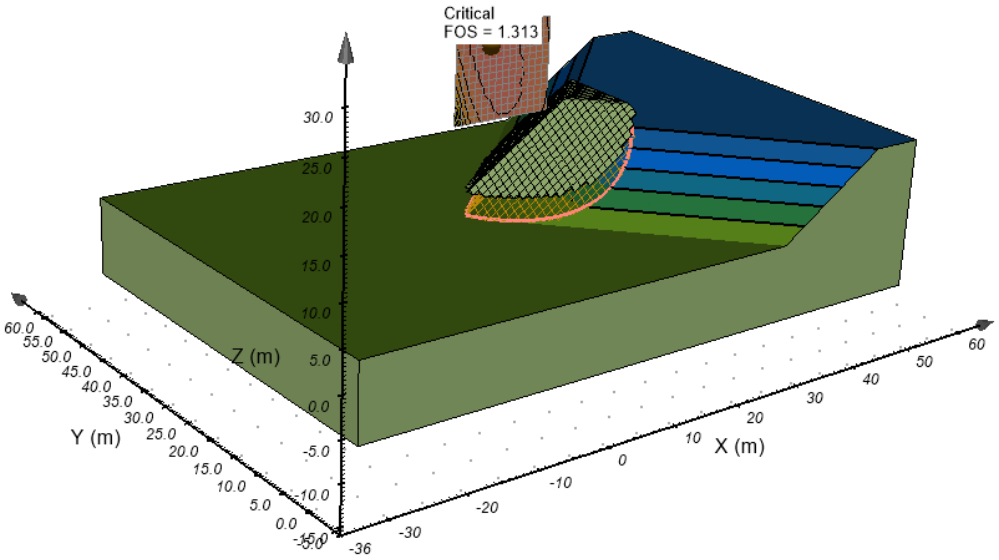

Figure 129. Critical slip surface computed in SVSLOPE where the critical FoS = 1.31

5.3 External Load on Embankment Slope - SSR

Reference: Wei et al. (2009)

Project: Slopes_SSR
Model: ExternalLoad_SSR_GT

Main Factors Considered:

- Shear strength reduction factor of safety calculations.
- Limit Equilibrium method (LEM) factor of safety calculations.
- 3D geometry which is an extension of 2D simple slope
- An external load is applied
- Limit equilibrium method (LEM) methodology to calculate the FoS

5.3.1 Model Description

A 3D slope stability analysis is performed on an embankment slope with an applied distributed load of 100 kPa on the ground surface. An analysis of this slope was reported in Wei et al., (2009). The factor of safety (FoS) results using a SSR analysis is compared with the FoS calculated from a LEM) using SVSLOPE.

5.3.2 Geometry and boundary conditions

Figure 130 shows the geometry and boundary conditions in SVSOLID. Displacements are fixed in all directions at the base and the side walls. An applied load of 100 kPa is placed on the ground surface.

5.3.3 Material Properties

A summary of the material properties is provided in Table 53.

Table 53. Input material properties

Parameter	Soil
Young's modulus, E (kPa)	50,000
Poisson's ratio, ν	0.4
Cohesion, c (kPa)	20
Friction angle, ϕ	20
Unit weight, γ (kN/m^3)	20

5.3.4 Results

Figure 131 and Figure 132 show the total displacement contours computed in SVSOLID along with the critical slip surface determined in SVSLOPE, respectively. These figures show the slip surfaces in both SVSOLID and SVSLOPE are similar. Table 54 shows the FoS results of SVSOLID and SVSLOPE.

Table 54. FoS comparison

SVSLOPE	SVSOLID	Difference (%)
1.43 (GLE*)	1.48	3.4

*GLE = General Limit Equilibrium formulation

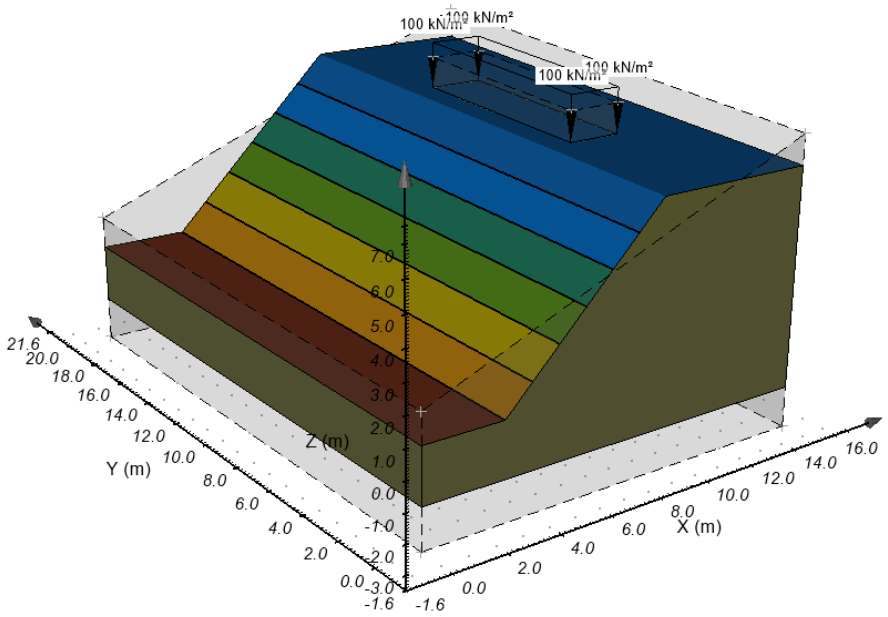

Figure 130. Geometry and boundary conditions

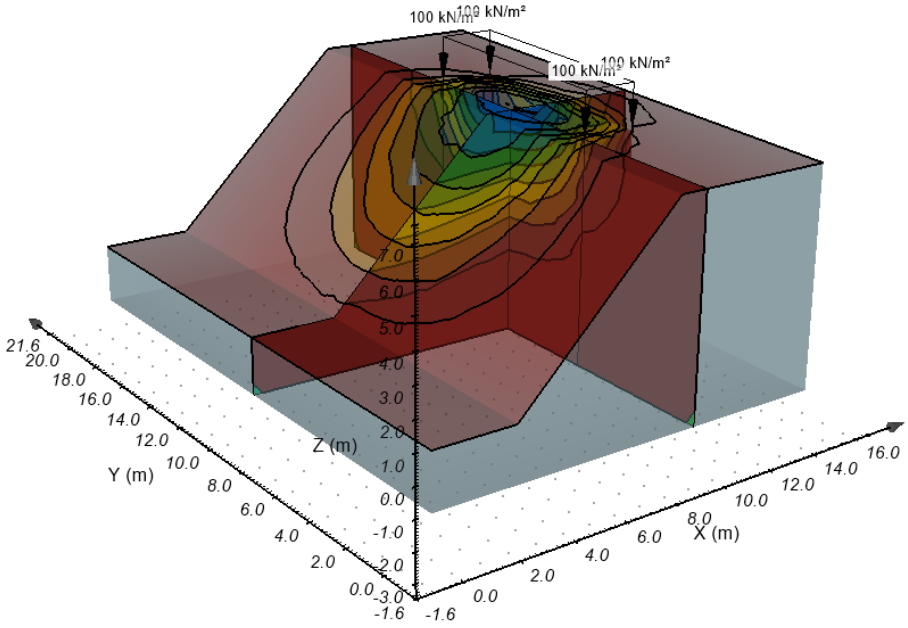

Figure 131. Total displacement contours in SVSOLID with FoS = 1.48

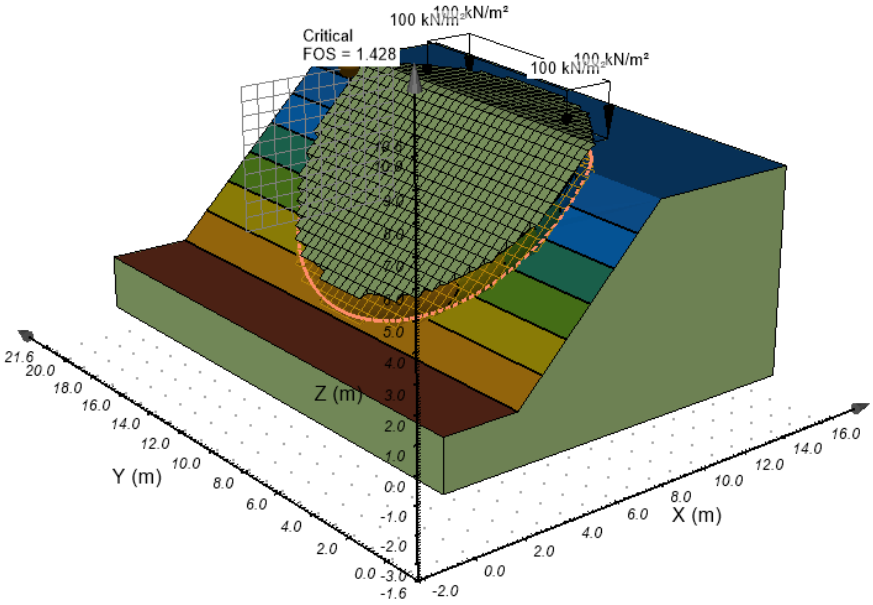

Figure 132. Critical slip surface in SVSLOPE with FoS = 1.43

5.4 Single Layer Slope - SSR

Reference: Fredlund and Krahn (1997)

Project: Slopes_SSR
Model: FredlundAndKrahn_1977_3D_Case1_SSR_GT

Main Factors Considered:

- Shear strength reduction methodology to calculate the factor of safety
- 3D geometry which is an extension of a 2D simple slope
- Limit equilibrium method (LEM) methodology to calculate the FoS

5.4.1 Model Description

The 3D geometry is extruded from a 2D slope (case 1) reported by Fredlund and Krahn (1997). The factor of safety (FoS) result from the SSR analysis is compared the FoS calculated using limit equilibrium method (LEM) in SVSLOPE.

5.4.2 Geometry and boundary conditions

Figure 133 shows the geometry and boundary conditions in SVSOLID. Displacements are fixed in all directions at the base and the side walls.

5.4.3 Material Properties

A summary of the material properties is provided in Table 55.

Table 55. Input material properties

Parameter	Soil
Young's modulus, E (psf)	50,000
Poisson's ratio, ν	0.4
Cohesion, c (psf)	600
Friction angle, ϕ	20
Unit weight, γ (lb/ft^3)	120

5.4.4 Results

Figure 134 and Figure 135 show the total displacement contours calculated in SVSOLID and the critical slip surface calculated in SVSLOPE, respectively. These figures show the slip surfaces from both the SVSOLID and SVSLOPE analysis are similar. Table 56 shows the similarity of the FoS results of SVSOLID and SVSLOPE.

Table 56. FoS comparison

SVSLOPE	SVSOLID	Difference (%)
2.22 (GLE*)	2.30	3.1

*GLE = General Limit Equilibrium

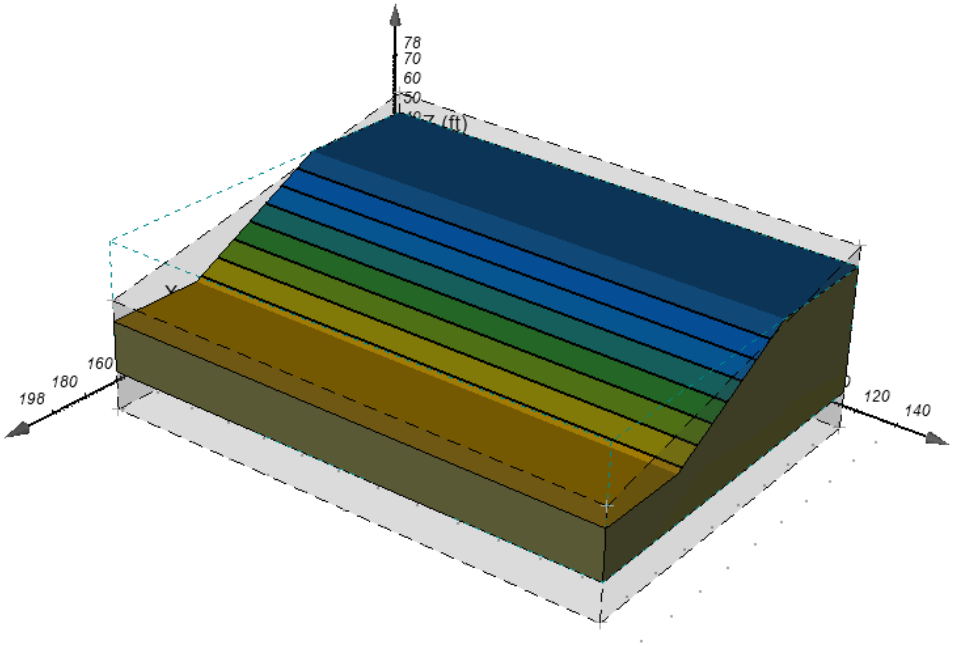

Figure 133. Geometry and boundary conditions

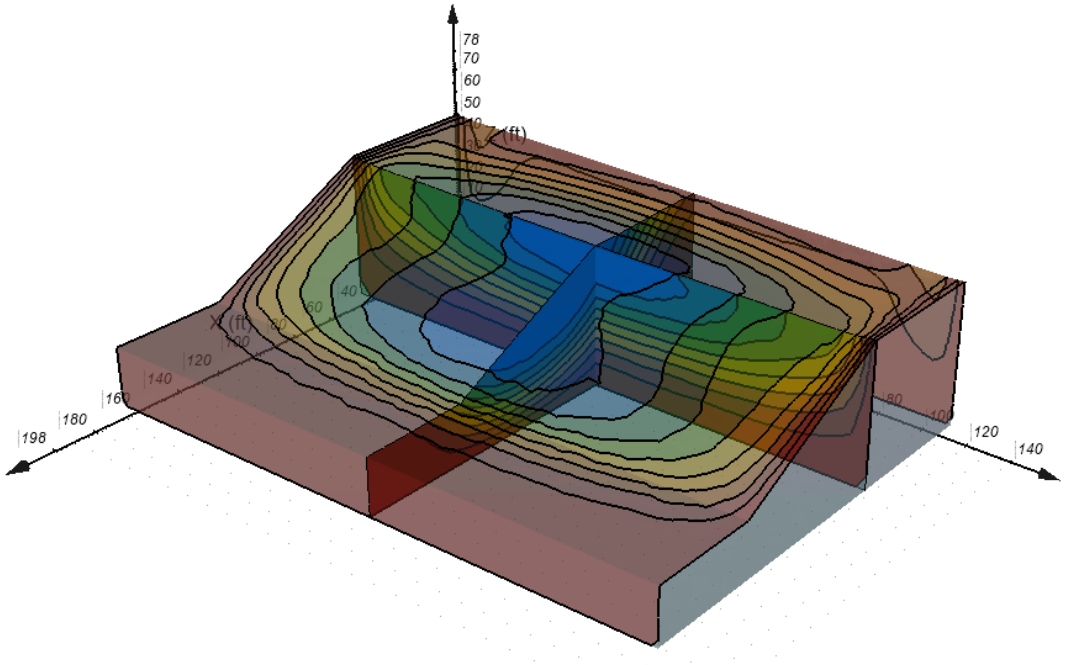

Figure 134. Total displacement contours computed in SVSOLID yielding a FoS = 2.30

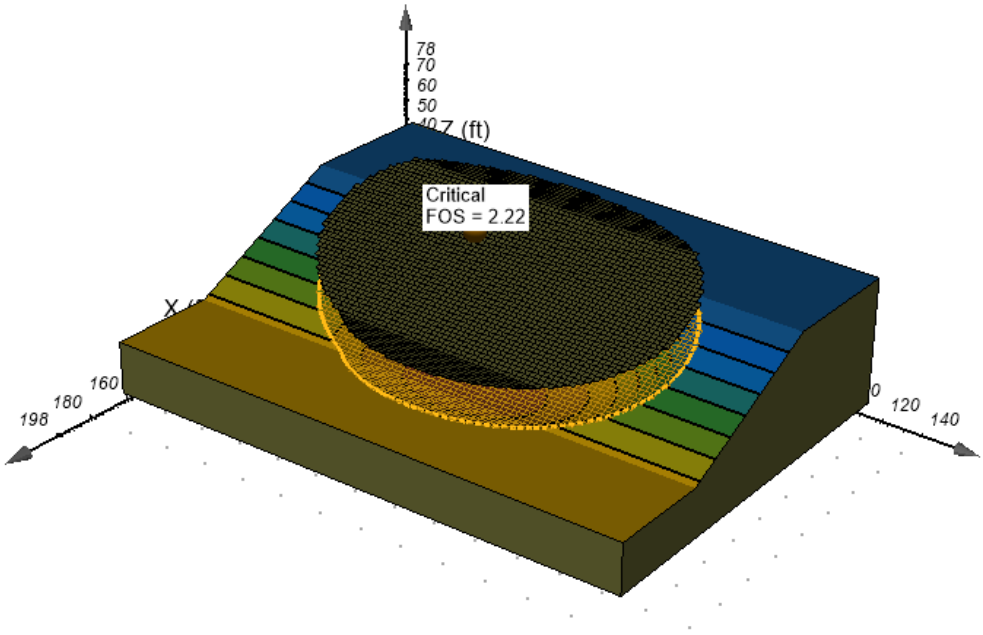

Figure 135. Critical slip surface computed in SVSLOPE yielding a FoS = 2.22

5.5 Single Layer Slope with Water Table- SSR

Reference: Fredlund and Krahn (1997)

Project: Slopes_SSR
Model: FredlundAndKrahn_1977_3D_Case5_SSR_GT

Main Factors Considered:

- Shear strength reduction factor of safety calculations.
- Limit Equilibrium method (LEM) factor of safety calculations.
- 3D geometry
- Pore-water pressure due to water table
- Limit equilibrium method (LEM) methodology to calculate the FoS

5.5.1 Model Description

This example is an extruded 3D geometry of the 2D slope (Case 5) with results reported by Fredlund and Krahn (1997). The slope has a water table. The factor of safety (FoS) result from the SSR analysis is compared to the FoS results obtained using a limit equilibrium method (LEM) in SVSLOPE.

5.5.2 Geometry and boundary conditions

Figure 136 shows the geometry and boundary conditions in SVSOLID. Displacements are fixed in all directions at the base and the side walls. Water table is daylighted at the lower edge of the slope.

5.5.3 Material Properties

A summary of the material properties is provided in Table 57.

Table 57. Input material properties

Parameter	Soil
Young's modulus, E (psf)	50,000
Poisson's ratio, ν	0.4
Cohesion, c' (psf)	600
Friction angle, ϕ'	20
Unit weight, γ (lb/ft^3)	120

5.5.4 Results

Figure 137 and Figure 138 show the total displacement contours obtained in the SVSOLID analysis and the critical slip surface obtained in SVSLOPE, respectively. These figures show the slip surfaces from the SVSOLID and SVSLOPE analyses are similar. Table 58 shows the FoS results of SVSOLID and SVSLOPE.

Table 58. FoS comparison

SVSLOPE	SVSOLID	Difference (%)
2.10 (GLE*)	2.08	1.0

*GLE = General Limit Equilibrium formulation

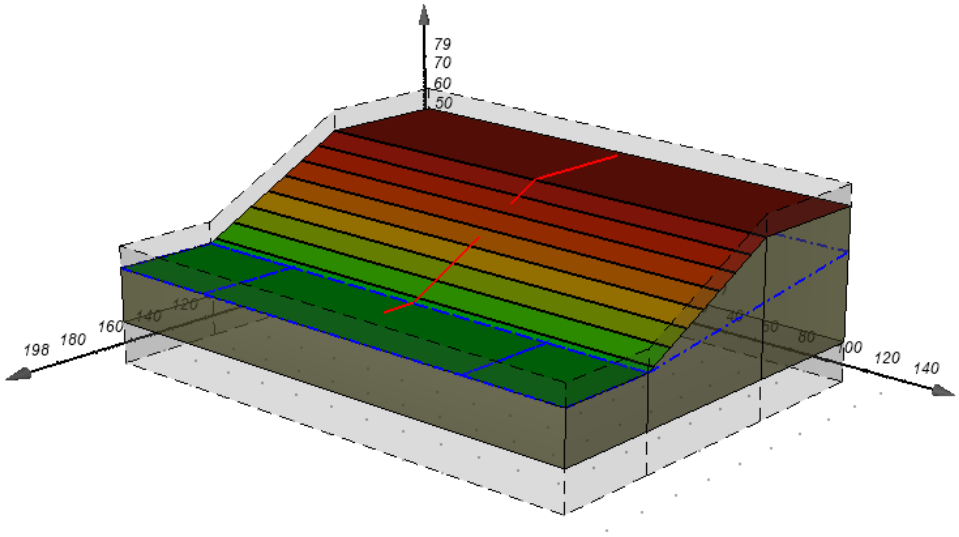

Figure 136. Geometry and boundary conditions

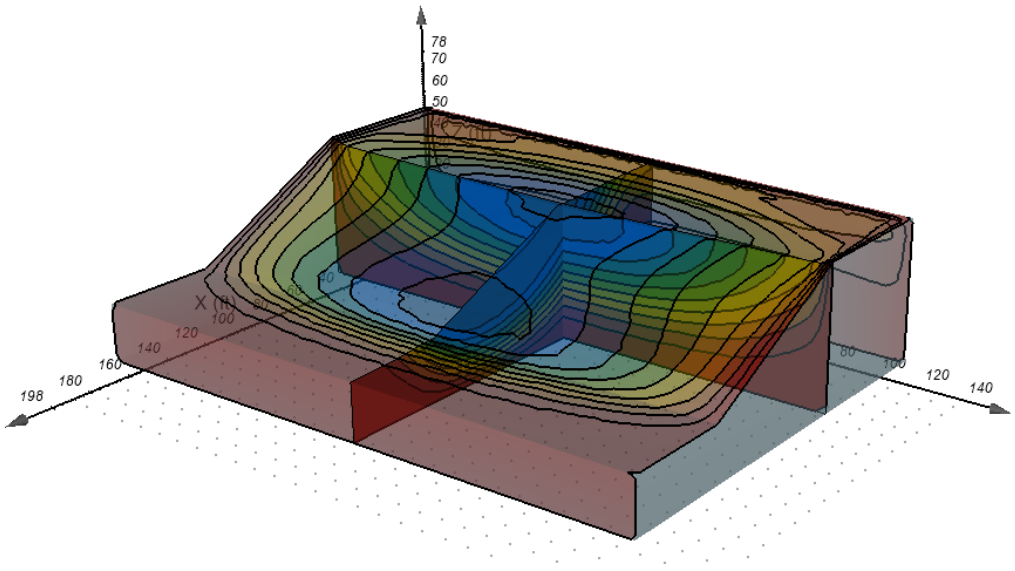

Figure 137. Total displacement contours computed in SVSOLID yielding a FoS = 2.08

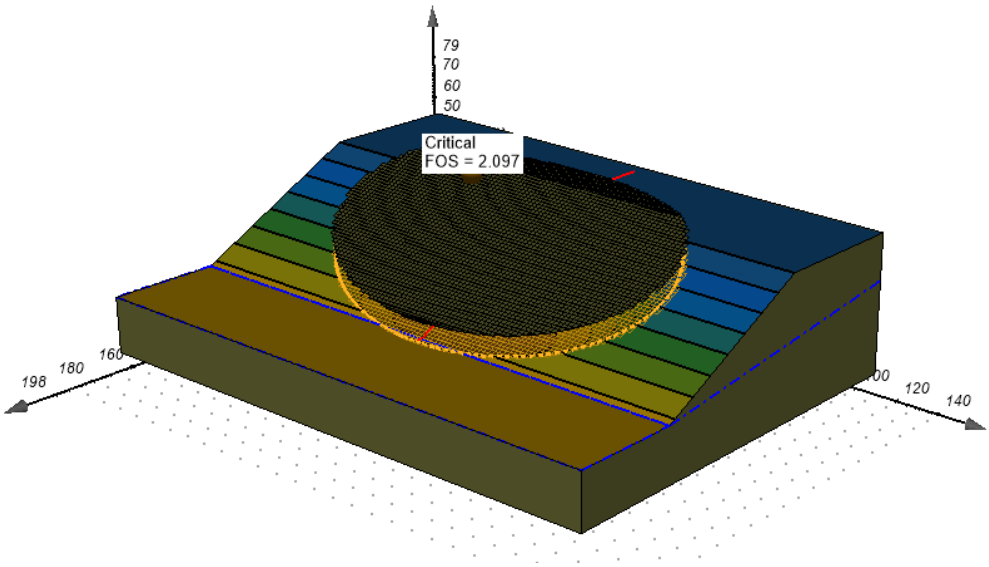

Figure 138. Critical slip surface computed in SVSLOPE yielding FoS = 2.10

5.6 An Asymmetrical Slope - SSR

Reference: Jiang (2003)

Project: Slopes_SSR
Model: Zhang_151_SSR_GT

Main Factors Considered:

- Shear strength reduction methodology to calculate the factor safety
- Limit Equilibrium method (LEM) factor of safety calculations.
- A more complex 3D geometry
- Pore-water pressure calculated from a designated water table
- Limit equilibrium method (LEM) methodology to calculate the FoS

5.6.1 Model Description

The geometry can be described as an asymmetrical slope. The anslysis of the geometry was reported in Jiang (2003). The factor of safety (FoS) results of SSR analysis is compared to the FoS results from a limit equilibrium method (LEM) using SVSLOPE.

5.6.2 Geometry and boundary conditions

Figure 139 shows the geometry and boundary conditions in SVSOLID. Displacements are fixed in all directions at the base and the side walls.

5.6.3 Material Properties

A summary of the material properties is provided in Table 59.

Table 59. Input material properties

Parameter	Soil
Young's modulus, E (kPa)	50,000
Poisson's ratio, ν	0.4
Cohesion, c' (kPa)	9.6
Friction angle, ϕ'	15
Unit weight, γ (kN/m^3)	18

5.6.4 Results

Figure 140 and Figure 141 show the total displacement contours computed in SVSOLID and the critical slip surface determined in SVSLOPE, respectively. These figures show the slip surfaces in SVSOLID and SVSLOPE are similar. Table 60 shows the FoS results determined in SVSOLID and SVSLOPE.

Table 60. FoS comparison

SVSLOPE	SVSOLID	Difference (%)
1.15 (GLE*)	1.19	3.4

*GLE = General Limit Equilibrium formulation

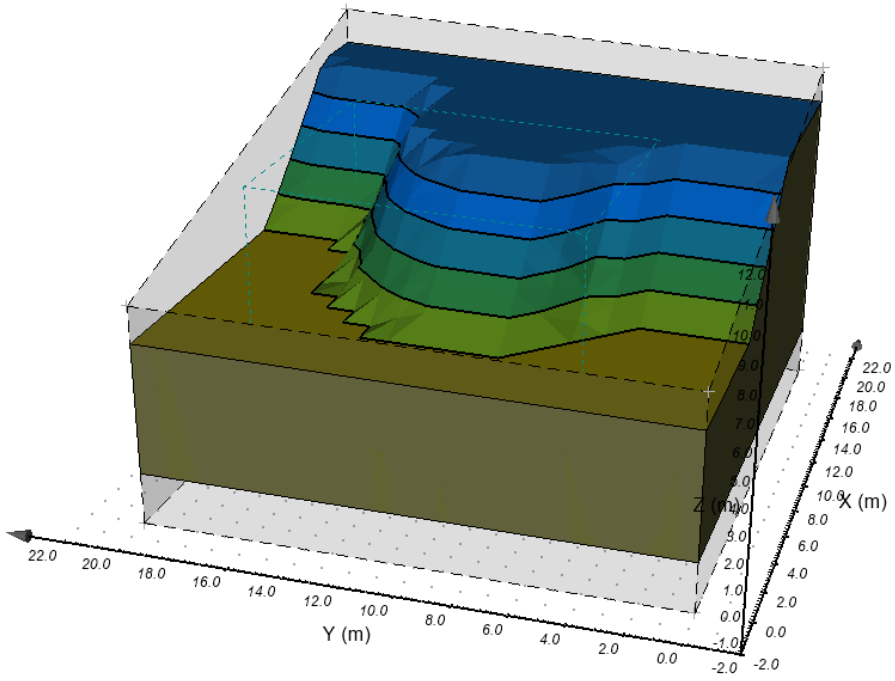

Figure 139. Geometry and boundary conditions

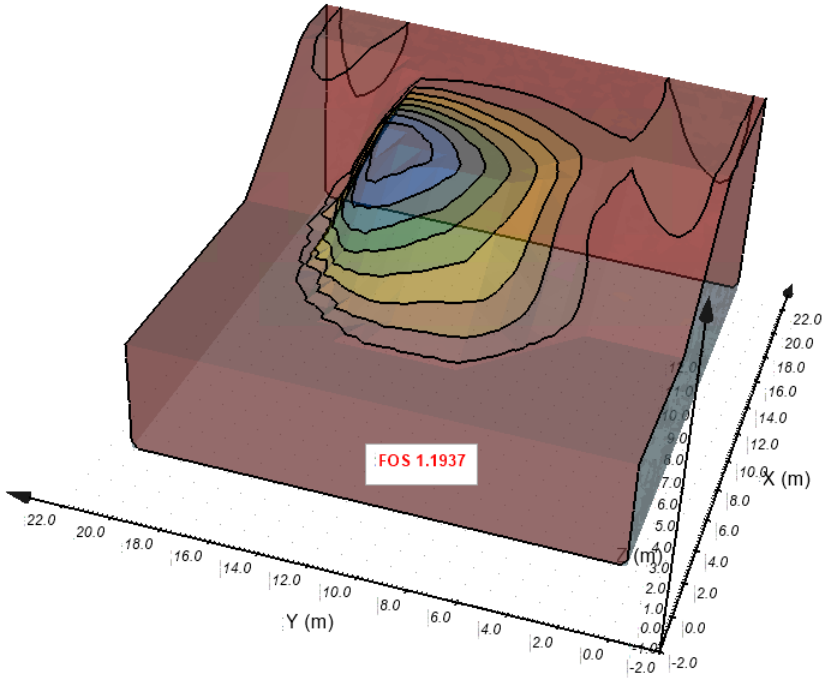

Figure 140. Total displacement contours computed in SVSOLID yielding a FoS = 1.19

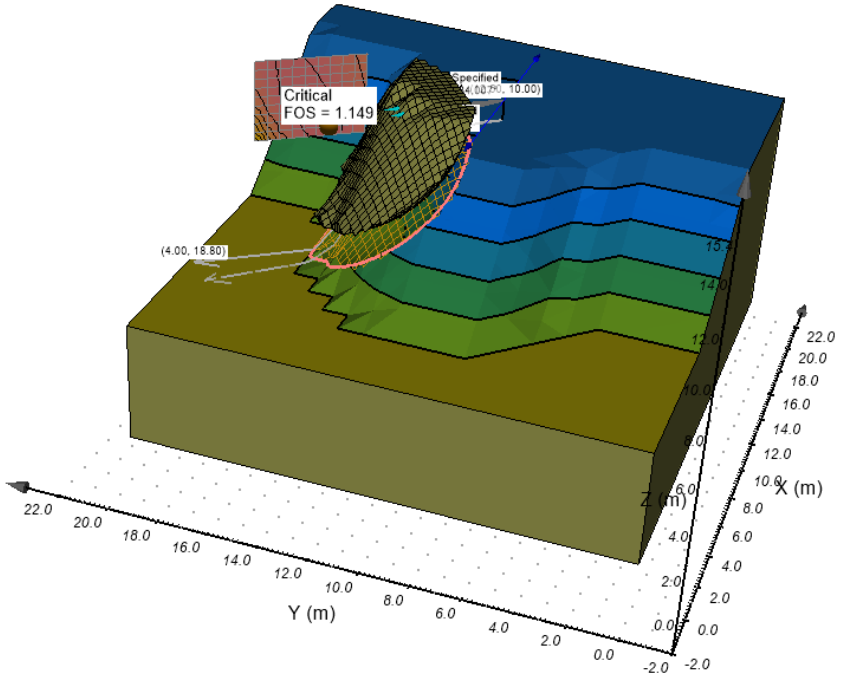

Figure 141. Critical slip surface computed in SVSLOPE yielding a FoS = 1.15

5.7 A General Asymmetrical Slope - SSR

Reference: Jiang et al. (2003)

Project: Slopes_SSR
Model: Jiang_Fig17_SSR_GT

Main Factors Considered:

- Shear strength reduction methodology for calculation of factor of safety
- Complex 3D geometry
- Pore-water pressure determined from the water table
- Limit equilibrium method (LEM) methodology to calculate the FoS

5.7.1 Model Description

The example represents a typical asymmetrical slope geometry that was reported by Jiang et al., (2003). The factor of safety (FoS) results of the SSR analysis is compared to the FoS computed using the limit equilibrium method (LEM) in SVSLOPE.

5.7.2 Geometry and boundary conditions

Figure 142 shows the geometry and boundary conditions in SVSOLID. Displacements are fixed in all directions at the base and the side walls.

5.7.3 Material Properties

A summary of the material properties is provided in Table 61.

Table 61. Input material properties

Parameter	Soil
Young's modulus, E (kPa)	50,000
Poisson's ratio, ν	0.4
Cohesion, c' (kPa)	11.7
Friction angle, ϕ'	24.7
Unit weight, γ (kN/m^3)	17.66

5.7.4 Results

Figure 143 and Figure 144 show the total displacement contours computed in SVSOLID and the critical slip surface in computed SVSLOPE, respectively. These figures show that the slip surfaces from both SVSOLID and SVSLOPE are similar. Table 62 shows a comparison of the FoS results of SVSOLID and SVSLOPE.

Table 62. FoS comparison

SVSLOPE	SVSOLID	Difference (%)
1.76 (GLE*)	1.81	2.7

*GLE = General Limit Equilibrium formulation

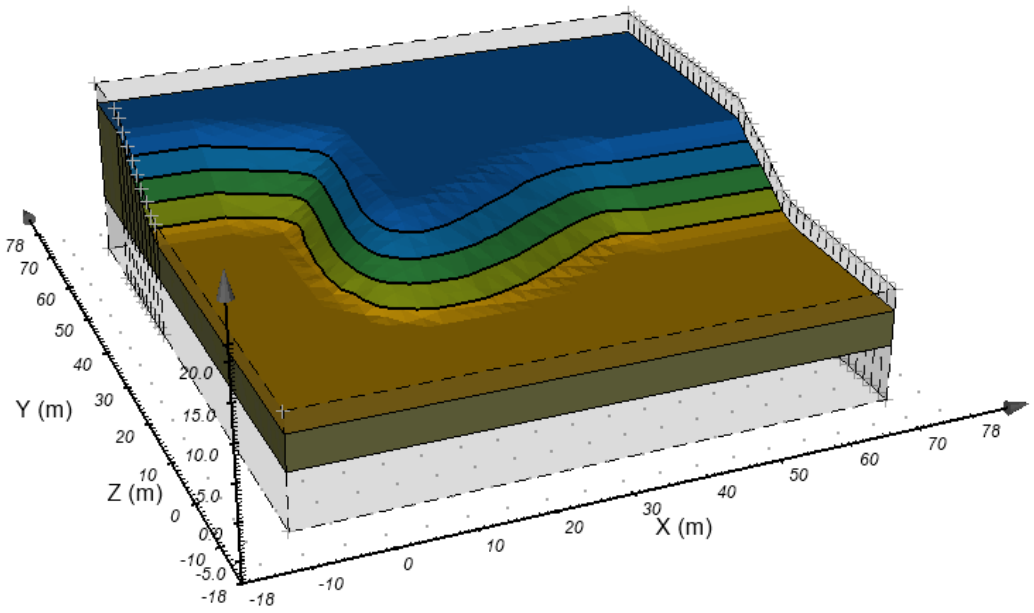

Figure 142. Geometry and boundary conditions

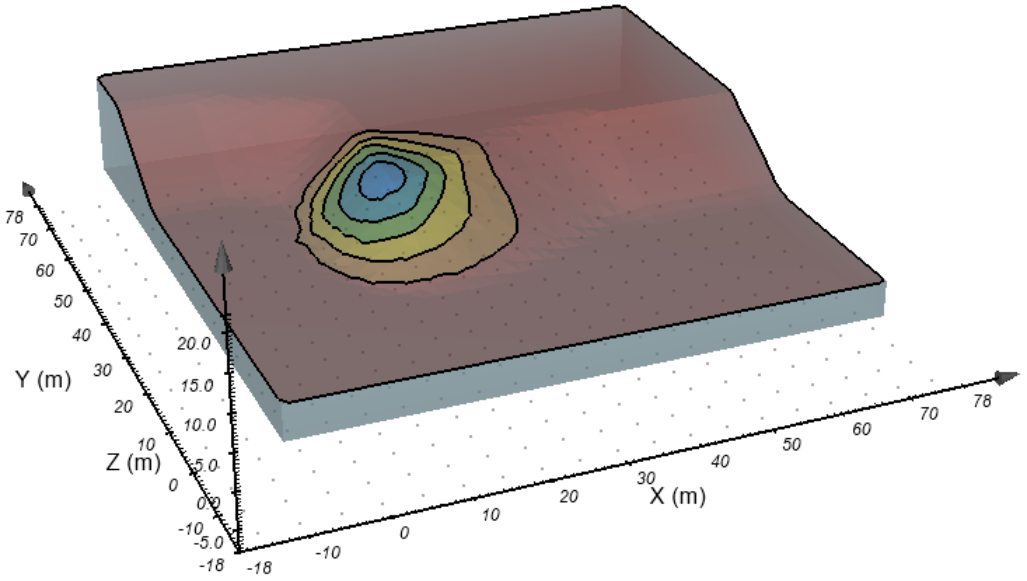

Figure 143. Total displacement contours computed in SVSOLID with a FoS = 1.81

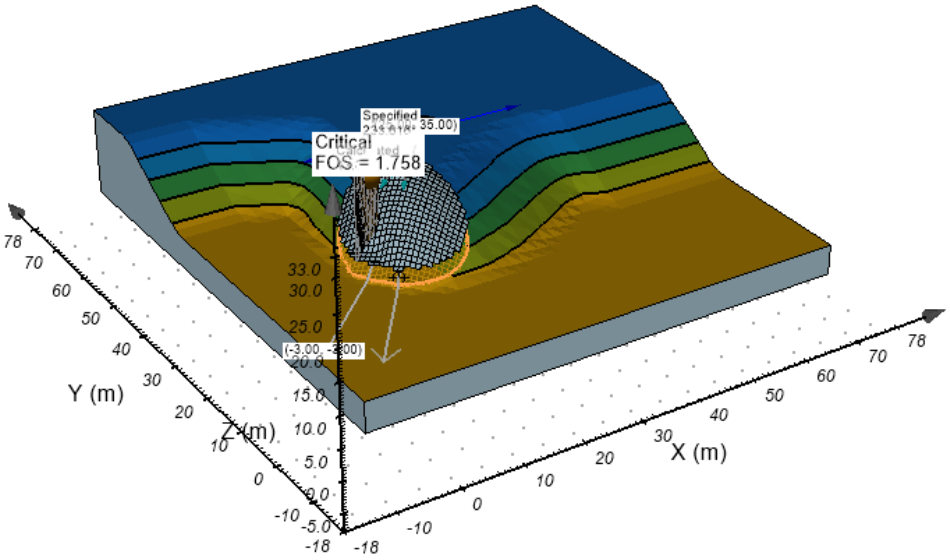

Figure 144. Critical slip surface computed in SVSLOPE with a FoS = 1.76

6 REFERENCES

Augarde, C. E., Lyamin, A. V., and Sloan, S. W. (2003). Stability of an undrained plane strain heading revisited. *Computers and Geotechnics*, 30(5), 419-430.

Brady, B.H.G., and Brown, E.T. (2004). *Rock Mechanics for Underground Mining*, Kluwer Academic Publishers, 628 p.

Chen, W. F. (Ed.) (2013). *Limit analysis and soil plasticity*. Elsevier, 638 p.

Dey, A. (2001). *Shear behaviour of fully grouted bolts under constant normal stiffness condition*. Doctoral dissertation, Faculty of Engineering, University of Wollongong

Duncan, J.M. and Chang, C.Y. (1970). Nonlinear analysis of stress and strain in soils. *Journal of Soil Mechanics & Foundations Div.*, ASCE, 96(SM5), 1629-1653.

Farmer, I. W. (1975). Stress distribution along a resin grouted rock anchor. *International Journal of Rock Mechanics and Mining Sciences & Geomechanics*. Vol. 12, No. 11, pp. 347-351.

Fredlund, D.G., and Krahn, J. (1977). Comparison of slope stability methods of analysis. *Canadian Geotechnical Journal*, 14: 429–439

Jiang, J. C., Baker, R., and Yamagami, T. (2003). The effect of strength envelope nonlinearity on slope stability computations. *Canadian Geotechnical Journal*, 40:308-325

Merifield, R. S., Sloan, S. W., & Yu, H. S. (1999). Rigorous plasticity solutions for the bearing capacity of two-layered clays. *Geotechnique*, 49(4), 471-490.

Meyerhof, G. G. (1957). The ultimate bearing capacity of foundations on slopes. *In Proceedings of the 4th international conference on soil mechanics and foundation engineering*. Vol. 1, pp. 384-386.

Poulos, H.G. and Davis, E.H. (1974). *Elastic solutions for soil and rock mechanics*. John Wiley, New York, N.Y.

Salencon, J. (1990). An introduction to the yield design theory and its applications to soil mechanics. *European journal of mechanics. A. Solids*, 9(5), 477-500.

Silvestri V. (2006). A three-dimensional slope stability problem in clay. *Canadian Geotechnical Journal*, 43(2): 224-228.

St. John, C. M., and Van Dillen, D. E. (1983). Rockbolts: A New Numerical Representation and Its Application in Tunnel Design. *In Proceedings of the 24th U.S. Symposium on Rock Mechanics*, Texas A&M University, pp. 13-26

Terzaghi, K. (1943). *Theoretical soil mechanics*. John Wiley, New York, N. Y.